
**GSI-191: SEPARATE-EFFECTS CHARACTERIZATION OF DEBRIS
TRANSPORT IN WATER**

TECHNICAL LETTER REPORT

DECEMBER 2001, REVISION 0

PREPARED BY

D. V. Rao and B. C. Letellier *

A. K. Maji, B. Marshall **

* **LOS ALAMOS NATIONAL LABORATORY**
DECISION APPLICATIONS DIVISION
PROBABILISTIC RISK ANALYSIS GROUP (D-11)

** **UNIVERSITY OF NEW MEXICO**
DEPARTMENT OF CIVIL ENGINEERING

M.L. MARSHALL, NRC PROJECT MANAGER

PREPARED FOR

U.S. NUCLEAR REGULATORY COMMISSION
OFFICE OF NUCLEAR REGULATORY RESEARCH
DIVISION OF ENGINEERING TECHNOLOGY

EXECUTIVE SUMMARY

The results of the experimental studies can be summarized as follows.

The U.S. Nuclear Regulatory Commission (NRC) Office of Regulatory Research has developed a comprehensive research program to support resolution of Generic Safety Issue (GSI)-191, which addresses the potential for debris accumulation on the pressurized water reactor (PWR) sump screen and consequent loss of emergency core cooling system (ECCS) pump net positive suction head (NPSH). Among the GSI-191 research program tasks is the experimental determination of the transport characteristics of various types of loss-of-coolant-accident (LOCA)-generated debris within a PWR containment. This report describes the results of such experiments. The data presented here focuses exclusively on debris transport on the containment floor.

The experiments described in this report measured the following properties for several types of debris.

- Terminal settling velocity in quiescent pools and in water pools in planar (lateral) motion
- Incipient tumbling velocity (i.e., the minimum fluid velocity at which an individual stationary fragment resting on the containment floor would begin to move)
- Bulk tumbling velocity (i.e., the minimum fluid velocity required to induce “bulk-scale” movement of a population of debris fragments)
- Lift-at-the-curb velocity [i.e., the minimum fluid velocity required to lift a fragment of debris over a vertical curb (typically 4 or 6 in. in height) that impedes forward motion along the floor]

In all cases, these velocities are measured in terms of the pool average flow velocity. Variations in pool velocity as a result of (for example) large-scale turbulence may cause significant variability in measured values for these threshold velocities. Experiments were performed in planar and turbulent flow conditions (and repeated several times) to evaluate and quantify the degree of data variability in such circumstances.

In addition to the transport properties listed above, experiments were performed that measured other important characteristics of post-LOCA debris behavior. Among these are

- The buoyancy characteristics of fibrous debris fragments, i.e., the rate at which low-density fiberglass insulation fragments become sufficiently saturated with water to sink into the pool as a function of temperature;
- the disintegration rate of calcium-silicate (cal-sil) insulation when submersed in hot water; and
- the extent to which the threshold velocities listed above are affected by the simultaneous presence of other types of debris (i.e., mixtures of fiber fragments and cal-sil).

TABLE OF CONTENTS

	Page
EXECUTIVE SUMMARY	I
LIST OF FIGURES.....	iii
LIST OF TABLES.....	iv
LIST OF ACRONYMS AND ABBREVIATIONS.....	v
ACKNOWLEDGEMENTS	vi
1 INTRODUCTION	1
1.1 Background: Context for the Experiments.....	1
1.2 Objectives and Scope of the Experiments.....	1
1.2.1 Test Program Objectives	1
1.2.2 Experiment Program Scope.....	3
1.3 Report Outline.....	5
2. TECHNICAL APPROACH.....	6
2.1 Test Facilities.....	6
2.2 Test Variables.....	6
2.2.1 Results of Exploratory Testing.....	6
2.2.2 Scaling Considerations	11
2.3 Test Matrix	11
3 TEST RESULTS.....	12
3.1 Low-Density Fiberglass Insulation.....	12
3.3.1 Nukon.....	12
3.1.2 Thermal-Wrap.....	13
3.1.3 Kaowool.....	14
3.2 Reflective Metallic Insulation	16
3.2.1 Aluminum RMI	16
3.2.2 Stainless-Steel RMI	16
3.3 Miscellaneous Insulation Materials.....	18
3.3.1 Cal-Sil Insulation.....	19
3.3.2 Paint Chips.....	20
3.3.3 Marinite Fire-Barrier Material.....	22
3.3.4 Silicone Foam Insulation Material.....	23
4 DISCUSSION OF RESULTS.....	25
5 REFERENCES.....	26
APPENDIX A: Test Facility Descriptions	A-1
APPENDIX B: Exploratory Test Data.....	B-1
APPENDIX C: Test Data.....	C-1
APPENDIX D: Test Procedures.....	D-1
APPENDIX E: Calibration of Test Instrumentation	E-1
APPENDIX F: Supporting CFD Calculations.....	F-1

LIST OF FIGURES

Fig. 1.1.	Role of the separate effects debris transport test data in overall GSI-191 research program ...	2
Fig. 2-1.	Photo of water flow in the large flume in Configuration A	10
Fig. 3.1.	Typical NUKON fiberglass insulation debris used in transport testing.....	12
Fig. 3.2a.	Thermal-wrap fiberglass insulation in bulk form.....	13
Fig. 3.2b.	Shredded thermal-wrap.....	14
Fig. 3.3a.	Kaowool insulation cut into 4-in. x 6-in. pieces	15
Fig. 3.3b.	Shredded Kaowool.....	15
Fig. 3.4.	Aluminum RMI.....	17
Fig. 3.5.	SS RMI cassettes (solid and slotted closure)	18
Fig. 3.6.	Calcium silicate	19
Fig. 3.7.	Paint chips.....	21
Fig. 3.8a.	Marinite fire-barrier material (dry and soaked block)	22
Fig. 3.8b.	Wet broken piece of Marinite	23
Fig. 3.9.	Silicone foam insulation material (as foamed and pieces tested).....	24
Fig. A-1.	Photograph of the small flume test apparatus	A-2
Fig. A-2.	Schematic of the small flume test apparatus	A-2
Fig. A-3.	Outlet screen in the small flume test section	A-3
Fig. A-4.	Schematic of large flume assembly	A-4
Fig. A-5.	Basic design of large flume	A-5
Fig. A-6.	Large flume apparatus	A-5
Fig. A-7.	Diagram of the large flume flow straightener	A-7
Fig. A-8.	Photograph of equipment for 'Configuration A' inlet flow conditioning.....	A-7
Fig. A-9.	Photograph of 'Configuration B' inlet flow conditioning.....	A-8
Fig. A-10.	Photograph of 'Configuration C' inlet flow conditioning	A-9
Fig. A-11.	Test section exit screen	A-9
Fig. A-12.	Test section exit screen support	A-10
Fig. A-13.	Test obstruction 'curb' in standard test section.....	A-11
Fig. A-14.	Test obstruction 'curb' in converging test section	A-11
Fig. A-15.	Large flume supply pump and overhead piping.....	A-12
Fig. A-16.	Large flume supply pump and inline flow meter.....	A-12
Fig. A-17.	Large flume flow velocity vs volumetric flow rate.....	A-13
Fig. A-18.	Plexiglas water column used in terminal settling velocity measurements	A-14
Fig. A-19.	Plastic cylinder used in dissolution tests.....	A-14
Fig. E-1.	Comparison of meter readout with actual flow measurements.....	E-1

LIST OF TABLES

Table 1-1.	List of Insulation and Fire-Barrier Materials and Sizes Included in the Test Program.....	3
Table 2-1.	Parametric Test Matrix: Transport Properties Measured as a Function of Test Variables	11
Table 3.1.	Summary of Measured Nukon Transport Properties	13
Table 3.2.	Summary of Measured Thermal-Wrap Transport Properties	14
Table 3.3.	Summary of Measured Kaowool Transport Properties.....	16
Table 3.4.	Summary of Measured Aluminum RMI Transport Properties.....	17
Table 3.5.	Summary of Measured SS RMI Transport Properties	18
Table 3.6.	Disintegration Characteristics of Cal-sil Fragments.....	20
Table 3.7.	Summary of Measured Marinite Transport Properties.....	23
Table B.1.	Terminal Velocity Measurements for 6-in. Nukon Fragments (at 80°C).....	B-1
Table B.2.	Settling Velocity at Different Temperatures (after pre-treating in 80°C water)	B-1
Table B.3(a).	Effect of Immersion of Nukon Shreds in Cal-Sil Saturated Water (6 gms/500 cc)	B-2
Table B.3(a).	Effect of Immersion of Nukon Shreds in Cal-Sil Saturated Water (6 gms/500 cc)	B-2
Table B.4(a).	Impact of Cal-Sil on Nukon Transport.....	B-3
Table B.4(b).	Paint Chips Transport Data from Small Flume Tests	B-4
Table B.5.	Variation of Floor Transport of Fiber Debris with Varying Height of Water.....	B-4
Table B.6.	Comparison of Floor Transport with Plexiglas vs Plywood.....	B-5
Table B.7(a).	Calibration of Water Balloon Velocity Measurement	B-5
Table B.7(b).	Velocity Measurements after the Placement of Diffusers	B-5
Table B.8.	Incipient Movement of Nukon and Steel RMI from 5 Separate Tests.....	B-6
Table C.1.	Nukon Settling Velocity (ft/s).....	C-1
Table C.2.	Floor Transport of Nukon	C-1
Table C.3.	Lift at Curbs – Nukon	C-2
Table C.4.	Drop Test of Nukon	C-3
Table C.5.	Thermal-Wrap Settling Velocity	C-4
Table C.6.	Floor Transport of Thermal-Wrap	C-5
Table C.7.	Lift-at-Curbs for Thermal-Wrap	C-6
Table C.8.	Drop Tests with Thermal-Wrap Debris.....	C-7
Table C.9.	Kaowool Settling Velocity.....	C-7
Table C.10.	Floor Transport of Kaowool.....	C-8
Table C.11.	Lift-at-Curbs Velocity – Kaowool.....	C-9
Table C.12.	Kaowool Drop Tests.....	C-10
Table C.13(a).	Terminal Velocity Measurements for Al-RMI Fragments	C-11
Table C.13(b).	Aluminum RMI Transport Data from Small Flume Tests (11/1999).....	C-11
Table C.14.	Drop Tests on Aluminum RMI with Inlet Flow Configuration A.....	C-11
Table C.15.	SS RMI Settling Velocity	C-12
Table C.16.	Floor Transport of SS RMI	C-13
Table C.17.	SS RMI Lift-at-Curb Velocity	C-14
Table C.18a.	SS RMI Drop Tests: Inlet Flow Conditioning Configuration B	C-15
Table C.18b.	SS RMI Drop Tests: Inlet Flow Conditioning Configuration C	C-15
Table C.19(a).	cal-sil Transport Data from Small Flume Tests (11/1999)	C-16
Table C.19(b).	Cal-sil-saturated Nukon Transport Data from Large Flume Tests.....	C-16
Table C.20.	Terminal Velocity Measurements for Epoxy Paint Chips.....	C-17
Table C.21.	Paint Chips Transport Data from Small Flume Tests (November 24, 1999)	C-18
Table C.22.	Paint Chips Transport Data from Large Flume Tests	C-18
Table C.23.	Marinite Settling Velocity.....	C-19
Table C.24.	Marinite Floor Transport.....	C-19
Table D.1.	Initial Measurement of Terminal Velocity of Aluminum RMI	D-1
Table D.2.	Initial Measurement of Terminal Velocity of cal-sil.....	D-1
Table E.1.	Flow Measurements from the Flow Meter vs Volumetric Measurements.....	E-1
Table E.2.	Calibration of Flow Meter on Small Flume	E-2

LIST OF ACRONYMS AND ABBREVIATIONS

CaI-Sil	Calcium-Silicate
CFD	Computational Fluid Dynamics
ECCS	Emergency Core Cooling System
GSI	Generic Safety Issue
LOCA	Loss-of-Coolant Accident
NPSH	Net Positive Suction Head
NRC	Nuclear Regulatory Commission
PWR	Pressurized Water Reactor
RMI	Reflective Metallic Insulation

ACKNOWLEDGEMENTS

The U.S. Nuclear Regulatory Commission (NRC) office of Nuclear Regulatory Research sponsored the work documented in this report. Mr. Michael Marshall, RES/DET, was the NRC Project Manager for this task. He provided technical direction and valuable observations during the conduct of the experimental program described herein.

The authors would also like to thank Mr. M. T. Leonard and Mr. C. J. Shaffer, for their help in organization of test results and preparation of this report. Finally, the authors would like to thank Ms. J. Lujan and Ms. M. Timmers for their assistance with editing and preparation of this document.

1 INTRODUCTION

In the event of a loss-of-coolant accident (LOCA) within the containment of a pressurized water reactor (PWR), piping thermal insulation and other materials in the vicinity of the break will be dislodged by break jet impingement. A fraction of this dislodged insulation and other materials, such as paint chips and concrete dust, will be transported to the containment floor by the steam/water flows induced by the break and the containment sprays. Some of this debris eventually may be transported to and accumulate on the suction sump screens of the emergency core cooling system (ECCS) pumps. Debris accumulation increases the differential pressure across the sump screen and, in some cases, may degrade ECCS performance to the point of failure.

The U.S. Nuclear Regulatory Commission (NRC) Office of Regulatory Research has developed a comprehensive research program to support the resolution of Generic Safety Issue (GSI)-191, which addresses the potential for debris accumulation on the PWR sump screen and consequent loss of ECCS pump net positive suction head (NPSH). Among the GSI-191 research program tasks is the experimental determination of the transport characteristics of various types of LOCA-generated debris within a PWR containment. This report describes the results of such experiments. The data presented here focus exclusively on debris transport in the water pool present on the containment floor following a LOCA.

1.1 Background: Context for the Experiments

The experimental data described in this report will be used to support a broader assessment of post-LOCA debris transport in PWR containments. In particular, the experimental program is designed to complement ongoing computational fluid dynamics (CFD) analyses of debris transport by measuring the fundamental transport properties of various types of debris fragments. Therefore, the intent of the experimental program described in this report was not to measure debris movement in a “scale model” of a PWR containment floor. Rather, the data generated in these tests are the basic physical and transport properties of debris fragments that can be applied in computational models of plant-specific accident conditions.

An illustration of the way in which the data described in this report fit into the overall GSI-191 research program is shown in Fig. 1.1. As indicated in this figure, the experiments described here are one of several sources of information that may be used to develop a CFD model to predict the extent and timing of debris transport to the recirculation sump of a PWR. Thus, results from the experiments described in this report are properly considered “separate-effects data.”

In summary, this report presents measurements of the fundamental transport properties of various types of debris that may be generated as a consequence of the destruction of insulation and other materials in a PWR containment during a postulated LOCA. No discussions are presented here on the application of these data to plant analyses.

1.2 Objectives and Scope of the Experiments

1.2.1 Test Program Objectives

The test program has three primary objectives. [Ref. 1]

1. Characterize the transportability of the debris that might result from a LOCA in a PWR in terms of threshold fluid conditions necessary to induce (a) tumbling (or sliding) of debris on the containment floor, (b) resuspension (or re-entrainment) of debris previously settled on the containment floor, (c) lifting of debris over structural impediments (e.g., debris curbs), and (d) attachment (or accumulation) of debris to vertical screen surfaces. Also, measure the settling characteristics of the debris as function of fluid conditions.
2. Evaluate the potential for destruction and/or dissolution of debris when it is subjected to high fluid turbulence and high fluid temperature simultaneously.
3. Identify the features of the containment layout and sump positioning that could affect debris transport significantly.

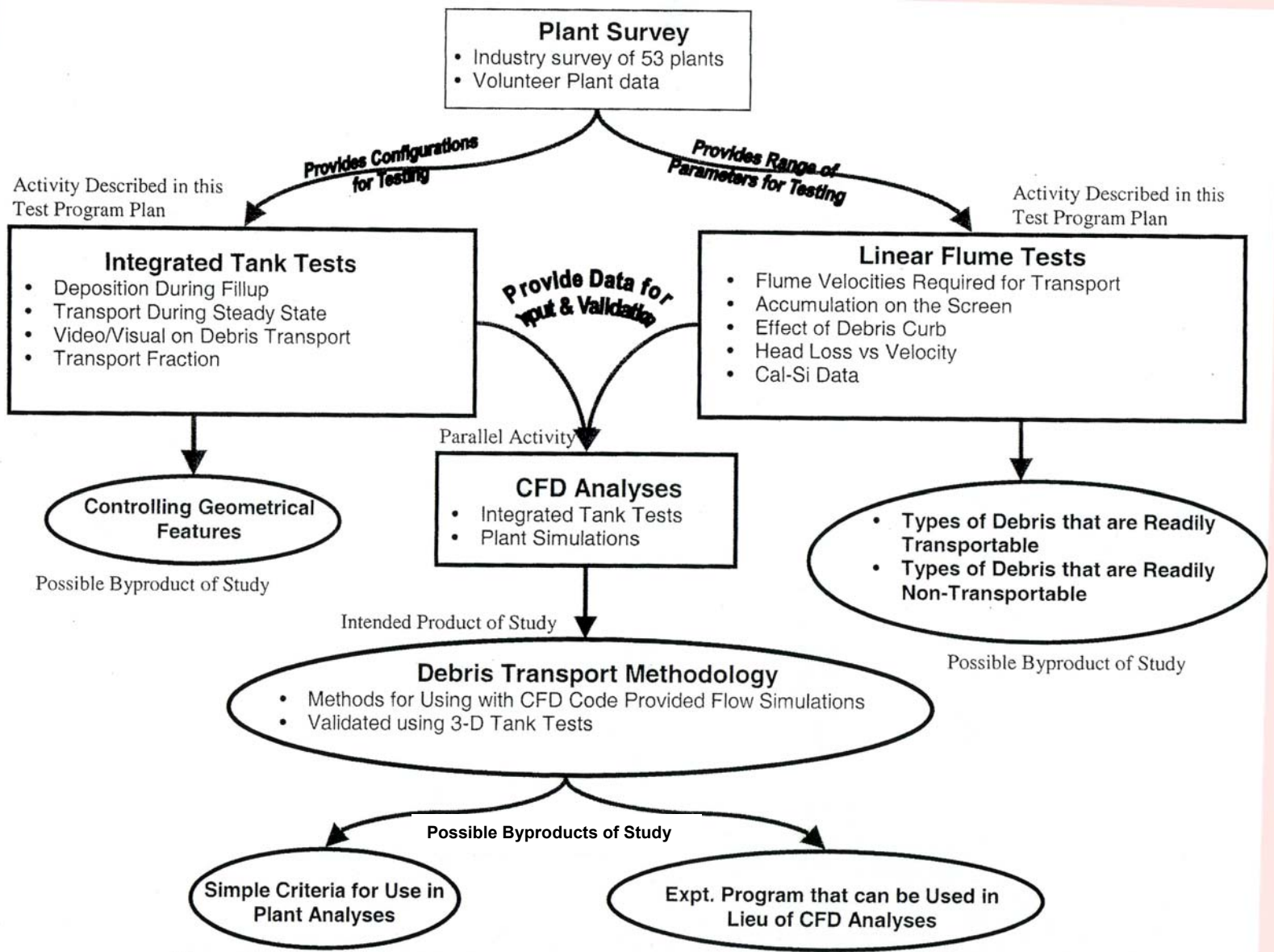


Fig. 1.1. Role of the separate-effects debris transport test data in the overall GSI-191 research program.

1.2.2 Experiment Program Scope

The number and range of parameters potentially affecting the transport of debris along the containment floor are quite extensive, for example,

- types of debris generated as a consequence of LOCA conditions in a PWR containment;
- sizes of debris fragments;
- amount and relative quantities of debris of each type;
- flow rate, pool depth, level of turbulence and temperature of the pool of water within which debris would be transported; and
- containment floor configuration (e.g., flat floor, curbs or other obstacles at the sump entrance, etc.).

The method by which this extensive list of variables was narrowed to a practical test matrix is described in Sec. 2.2. However, a brief summary of the types and sizes of debris considered in this program is presented below. Also described are the specific physical and transport properties measured in the tests.

1.2.2.1 Selection of Debris Type and Size for Testing

The type of debris generated by a LOCA in PWRs is highly plant specific as demonstrated by the industry survey of US PWRs [Ref. 2]. It may include various combinations of fibrous, particulate, or metallic thermal insulations and fire-barrier materials. Miscellaneous debris (non-LOCA debris) includes concrete dust, paint chips, dirt, and foreign materials left in the containment. The intent of the test program is to reflect this variability in the debris tested. However, from a practical point of view, it was decided to test only those insulation materials that are most prevalent in PWRs and/or most problematic. Table 1-1 provides a list of materials that meet these criteria. Some of these materials were eliminated from the test matrix because they were judged to be sufficiently similar to other (tested) materials to be treated as having similar transport properties. The insulation materials not included in the test program also are noted in Table 1-1.

The quantitative definitions of the terms “large,” “medium,” and “small” in Table 1-1 are provided in the descriptions of the test results in Sec. 3. However, in general the tests examined transport properties of fibrous debris from 6-in. patches of fiber matting (on the large end of the spectrum) to a loose collection of individual fibers (on the small end of the spectrum). The transport properties of

Table 1-1. List of Insulation and Fire-Barrier Materials and Sizes Included in the Test Program

Measured Property	Cassettes/ Blankets	Large Pieces	Medium Fragments	Small Fragments
Low-Density Fiberglass: Nukon Thermal Wrap Kaowool	Similar to Thermal Wrap below		❖	❖
	❖	❖	❖	❖
		❖	❖	❖
Temp-Mat	Not included in the study			
Mineral Wool	Not included in the study. Several types of mineral wool materials exist. Some are similar to Kaowool.			
RMI* – Aluminum (1.5 mil)	Not widely used in the PWRs, except B&W and some older designs per vendor.			❖
RMI*-Stainless Steel (2-mil)	❖	❖	❖	❖
Cal-Sil	No need for testing		❖	❖
Marinite Board (Fire Barrier)	No need. Large pieces enough	❖	❖	❖
Thermolag (Fire Barrier)	Similar to Marinite Board			
Silicone Foam (Closed Cell)	No need. Large pieces enough	❖	❖	❖
Min-K/Asbestos/Unibestos	These materials were not studied.			

❖ Indicates that material and size type are included in the test program.

* RMI = reflective metallic insulation.

GSI-191: Separate Effects Characterization of Debris Transport in Water

reflective metallic insulation (RMI) foils, both flat and crumpled, were examined over a range of sizes from approximately 2-in. x 2-in. squares to ½-in. x ½-in. flakes.

Whenever possible, debris samples were procured directly from the manufacturer. For example, low-density fiberglass used in the transport experiments was obtained from the vendor, who manufactured the base-wool following their usual methods, and then fragmented the blanket using air jets to form the debris that was used for these tests. Stainless-steel (SS) RMI was obtained in the following forms from the manufacturer.

1. Two 1-ft x 1-ft x 4-in. cassettes, one with slotted closures fabricated with 24-gage 304 SS and one with solid closures fabricated with 22-gage 304 SS.
2. 2-ft x 4-ft 24-gage, 304 SS foil sheets were cut into 2-in. square and ½-in.-square pieces. These pieces were processed by hand to make three categories of SS RMI debris: crumpled, semi-crumpled, and flat.

Photographs of the RMI foil fragments are provided in Secs. 3.2.1 and 3.2.2. Cal-sil was procured from cal-sil vendors in two basic shapes: (1) medium pieces (typically inches in length and width) and (2) small debris (simulated LOCA debris, which basically consists of approximately 1-in. chunks, attached to powdery-fibrous erosions).

1.2.2.2 Debris Physical and Transport Properties Measured

For each debris type and size listed in Table 1-1, the test program was designed to study various mechanisms (e.g., tumbling) available for its transport as a function of fluid conditions. Based on analytical formulations and literature reviews, the following properties were selected for measurement.

Physical and Settling Characteristics of the Debris. Debris characterization provides a measure of the debris being tested and thus, a practical measure for comparing results from different tests. The debris characteristics measured are (a) the physical size of the debris fragments (recorded photographically), (b) the weight of the debris fragments, and (c) the terminal velocity of a presoaked debris fragment in the water column. This series of tests is referenced as “debris characterization tests” in this report.

Debris-Settling Velocity in the Flume. Settling velocity is the velocity at which debris settles in the flume while the fragments are simultaneously subjected to horizontal flow velocity and residual turbulence. By comparing the measured settling velocity of debris fragments in a flume with the terminal velocity measured from settling column tests, insights can be drawn regarding (a) the effect of turbulence on settling and (b) the effect of turbulence and shape factor on horizontal travel distance. These tests are referenced as “drop/suspended transport tests” in this report.

Transport Distance in the Flume. Transport distance refers to the horizontal distance traveled by a piece of debris dropped at the top surface of the fluid before it touches the floor. These measurements can be used to draw insights into the flow patterns that exist in the flume and their effect on suspended debris transport. These tests also are referenced as “drop/suspended transport tests” in this report.

Tumbling Velocity. Tumbling velocity refers to the minimum fluid velocity (averaged over the flume cross section) required to induce tumbling (or sliding) of the debris fragments on the flume bottom. Two metrics were used to provide the range for tumbling velocity: (a) incipient tumbling velocity and (b) bulk tumbling velocity. The incipient tumbling velocity refers to the fluid velocity required to initiate tumbling of the smaller pieces (within a given size class) or to initiate tumbling of pieces with special shapes that provide higher drag coefficient. The bulk tumbling velocity refers to the fluid velocity required to induce “bulk-scale” movement of a given class of debris. These tests were referenced as “floor transport tests.”

Vertical Mixing Velocity.¹ Flow past a stationary fragment of debris induces an upward force commonly referred to as the lift. When the lift provided by the flow is large enough to overcome the gravitational force, debris becomes waterborne (or re-entrained). It is known that at very high fluid

¹ Final test data do not include vertical mixing velocity data because the tests showed that very high velocities would be needed to either resuspend debris or keep debris in the flowing water continuously.

velocities lift would be sufficient to vertically mix the debris to near uniformity. The intent is to measure the fluid velocity that induces vertical mixing. These tests were referenced as “mixing tests.”

Lift at the Curb Velocity. This defines the minimum fluid velocity (averaged over the flume cross section) required to lift a fragment of debris that reaches the curb via tumbling (or sliding) on the floor and transport it upward to be deposited on the screen. This series of tests is referenced as “curb tests.”

Screen Retention Velocity. This defines the minimum fluid velocity (averaged over the flume cross section) required to retain the debris fragments on the screen surface. This series of tests is referenced as “screen attachment tests.”

Dissolution and Erosion of Debris. Dissolution and erosion of debris when subjected to high temperatures and high fluid turbulence were studied. Particular emphasis was placed on dissolution of cal-sil debris in hot water.² This series of tests is referenced as “dissolution tests.”

1.2.2.3 Parameters and Conditions Simulated in the Testing

The intent of the test program is to measure the properties listed above while varying selected experimental parameters over a range that adequately reflects the post-LOCA PWR thermal and hydraulics conditions. Analyses suggested that some or many of the physical and transport properties listed above are dependent on a variety of parameters, including (1) debris size, (2) flume water depth, (3) turbulence intensity, (4) flow patterns, (5) fluid temperature, (6) simultaneous presence of combinations of debris, (7) types of obstructions and extent of congestion, and (8) height(s) of curbs. It was quickly recognized that conducting tests that would measure the above properties as function of all of these parameters would be impractical. Therefore, it was decided to carry out the test program over two primary phases: (1) an exploratory test phase and (2) a parametric test phase.

The exploratory test phase was designed to gather raw transport data on select types of insulation and identify test parameters that strongly influence transport properties. Conversely, the exploratory tests provided a basis for eliminating test conditions from the parametric test matrix that would have little effect on results. Therefore, the objective of the exploratory tests was to provide data that support minimization of the size and complexity of the parametric test matrix.

The results of the exploratory tests are described in qualitative terms in Sec. 2.2.1 of this report. A complete listing of exploratory test results is provided in Appendix B.

1.3 Report Outline

Section 2 of this report outlines the overall technical approach to the experimental program. This includes information regarding the test facilities used to conduct the experiments and the test variables considered in the experiments (including a summary of the exploratory test performed to narrow the field of variables). Section 3 summarizes the results of the final parametric experiments. A discussion of the results and observations from the exploratory and parametric tests is provided in Sec. 4.

Additional information regarding the construction, dimensions, and operation of the test facilities is provided in Appendix A. Data collected from the exploratory tests described in Sec. 2.2.1 are tabulated in Appendix B. Raw test data from the final parametric experiments are listed in Appendix C. Appendix D describes the test procedures used to perform the various experiments. Appendix E provides the instrument calibration results for the flow meters used to monitor volumetric flow into the flumes. Finally, Appendix F summarizes results of CFD simulations carried out to draw insights into the flow patterns that existed in the flume when the testing was carried out.

² No attempt was made to simulate the PWR sump water chemical environment in these tests (e.g., concentration of boric acid, pH control additives, etc.)

2 TECHNICAL APPROACH

2.1 Test Facilities

All tests were performed at the University of New Mexico (UNM) Civil Engineering Department Hydraulics Laboratory. The three individual test facilities located at the Laboratory are described below.

Small Flume Test Facility

UNM maintains a small flume (10 ft long, 1 ft wide, and 1.5 ft deep) for instruction and research at the University related to open-channel flow. The small flume is capable of testing insulation fragments at transport velocities typical of those anticipated on a PWR containment floor during ECCS recirculation cooling, but the water depth is limited to a maximum of 1 ft. Therefore, this flume is used in the current test program only to examine the behavior of smaller debris (e.g., fiber fragments) and for particulate debris (e.g., cal-sil). The flume was also used extensively in the exploratory phase of the test program as described in Sec. 2.2.1.

Large Flume Test Facility

UNM has built a large flume (20 ft long, 4 ft high, and 3 ft wide) for the specific purpose of studying debris transport in water. The large flume provided the capability for testing insulation transport under a wider range of flow conditions than could be achieved in the small flume. This facility was used to develop most of the data contained in this report.

Variations in the test facility configuration were used to examine the effect of turbulence levels on the debris transportability. In the base-case tests, a series of entrance flow diffusers were used to dampen and straighten the flow before it entered the test section. This configuration, referred to as Configuration A, allowed for simulation of debris transport under conditions that are typical of remote sumps (where break-induced turbulence does not affect local flow patterns). In Configurations B and C, the diffuser was removed, and strong eddies dominated the flow. These configurations were used to quantify the effect of flow turbulence on particle movement. The difference between Configurations B and C was the method of introducing water into the flume inlet. In Configuration B, an outlet of 10 in. was located approximately 2 ft above the water surface, i.e., free-fall entry. In Configuration C, the inlet pipe was reduced to 6 in. at the exit, and the pipe exit was located 1 ft from the flume floor.

Settling Column

UNM built a settling column, which provides a good hydrostatic environment for measuring debris fragment terminal velocity. The settling column is a transparent column of water 34 in. high and 10 in. in diameter.

Drawings, photographs, and additional details on the operating conditions of each of these test facilities are provided in Appendix A.

2.2 Test Variables

A review of existing literature suggests that some or many of the transport properties selected for study would be dependent on a variety of parameters, including (1) debris size, (2) flume water depth, (3) turbulence intensity, (4) flow patterns, (5) fluid temperature, (6) simultaneous presence of combinations of debris, (7) types of obstructions and extent of congestion, and (8) height(s) of curbs. It was quickly recognized that conducting tests that would measure the above properties as function of all of the parameters listed above would be impractical. Therefore, it was decided to carry out an exploratory test program to identify important parameters for study and also to better design the final phase of testing. The issues addressed during the exploratory testing program are as follows.

1. Examine the effect of water temperature, as it relates to (a) the terminal velocity and (b) the dissolution and saturation characteristics of the debris.

2. Examine if transport of a particular debris type is influenced by the presence of other debris type(s) in the flume at the same time.
3. Examine the effect of flume water height as an experimental parameter.
4. Explore the importance of floor roughness, curb height, and obstructions and the need to test various curb heights and geometric layouts.
5. Examine the flow patterns established by flow straighteners and diffusers to ensure that the resulting flow is planar. Compare the results from the present program with results from previous investigators to confirm that the setup used in the present study produces similar results under similar test conditions.
6. Examine the repeatability of the test data.
7. Examine if the vertical mixing velocity is a required measurement.³

2.2.1 Results of Exploratory Testing

A detailed listing of the data collected in the exploratory tests is provided in Appendix B. The significant results of these tests are summarized below.

2.2.1.1 Effect of Temperature

Post-LOCA water temperature is approximately 80°C, which is significantly different from the ambient temperature proposed for use in the test program. It can be postulated that water temperature could affect debris settling characteristics because density and viscosity are temperature-dependent. Further, the saturation rates of debris may be temperature-dependent because surface tension varies with temperature. This set of experiments provided data to quantify these effects, as described below.

Saturation of Debris in Hot Water. When fibrous debris was introduced to water at ambient temperature, it was observed to float on the surface for more than 24 h. Even when shredded fiber fragments were forcibly immersed in ambient-temperature water for 24 h, they subsequently would rise up to the surface when released. However, if the fiber shreds were immersed in hot water (80°C) for as little as 2 min, they readily sank and remained submerged. In the aftermath of a LOCA, the temperature of water in a PWR recirculation sump is likely to be closer to 80°C than to ambient (~20°C). Consequently, all fibrous debris used in subsequent tests (i.e., the remaining exploratory tests and subsequent parametric tests) was immersed in 70°C water for at least 10 min.

The 10-min immersion time was derived from measurements of the terminal velocity of 6-in. fragments of fiber insulation after being submerged in 80°C water for 5 min and for 30 min. The results demonstrated that immersion in hot water for longer than 5 min has no effect on terminal velocity.⁴

Effect of Water Temperature and Debris Fragment Size on Terminal Velocity. Terminal velocity measurements were made to determine whether the changes in water temperature (after initial debris saturation) would affect terminal velocity. These measurements were made on 6-in. and 1-in. pieces of fiber debris. After the debris fragments were saturated in 80°C water, they were placed just under the surface of a column of water at 22°C and (separately) of a column of water at 80°C. The time required for the debris to travel from 10 in. to 30 in. below the top surface was measured⁵.

The resulting terminal velocities are nearly identical, indicating that settling of fiber and other heavier debris is governed by Newton's Law. Therefore, all further testing could be carried out at room temperature without significantly affecting debris-settling rates.

2.2.1.2 Simultaneous Presence of Different Insulations

Most operating PWRs use a variety of materials to insulate the primary piping. This raises the possibility that debris composed of several different materials may be present in the sump. One must then ask whether the transport properties of a particular type of debris are strongly influenced by interactions with other types of debris. Of particular interest is whether the transport of fiber fragments

³ Final test data do not include vertical mixing velocity data because the tests showed that very high velocities would be needed to either resuspend debris or keep debris in the flowing water continuously.

⁴ Measured results are listed in Table B-1 in Appendix B.

⁵ Measured results are listed in Tables B-2(a) and -2(b) in Appendix B.

would be influenced by the presence of cal-sil suspensions in the flume water and if floor transport of RMI fragments or paint chips is influenced by the presence of fibrous shreds. A series of tests was designed to examine these interactions.

Effect of Cal-Sil Concentration in Water on the Terminal Velocity. The first series of tests was designed to evaluate the influence of cal-sil (dissolved in hot water) on the terminal velocity of fiber fragments. Small pieces of fiber insulation of two slightly different sizes (1-in. pieces weighing 0.06–0.08 g and 1½-in. pieces, weighing 0.16–0.18 g) were soaked for 5 min. in 80°C water, which was saturated with cal-sil (6 grams of cal-sil in 500 cm³ water). The saturated debris fragments were subsequently placed in the settling column, which was filled with clean water at 22°C. Terminal velocities were measured based on the time required to travel from 15 in. to 30 in. below the water surface.⁶ These results suggest that the presence of cal-sil particulate (in suspension) does not have a significant effect on the settling characteristics of fibrous debris.

Exploratory tests also were conducted to examine the effect of cal-sil (dissolved in hot water) on aluminum RMI pieces. Small (2-in. x 2-in.) pieces of RMI were soaked in water saturated (3 g in 500 cm³) with cal-sil for 30 min and then dropped into clear water to see if the cal-sil inhibited or enhanced the velocity of the falling RMI pieces.⁷ Results again showed that the presence of cal-sil has a negligible effect on debris settling velocity.

Effect of Other Debris on the Tumbling Velocity. Two exploratory tests were conducted to determine whether tumbling velocity (and other transport properties) would be affected by the simultaneous presence of different materials in the flume water. The first tests examined whether saturation of fibrous debris with cal-sil would affect fibrous debris transport properties. In these tests, several nearly identical shreds of fiber insulation were selected. Half of them were immersed in cal-sil saturated water for 10 min and the rest were submerged in clean water. They then were dropped into the large flume with a preset water velocity. The time taken for each shred of insulation to settle and the horizontal distance traveled during that time were measured.⁸ The qualitative behavior of debris movement along the floor of the flume also was noted. The results clearly establish that treatment of fiber debris in cal-sil-saturated water has a negligible effect on transport characteristics.

A second set of exploratory tests was carried out in the small flume to determine whether the simultaneous presence of fiber and paint chips alter the transport properties of either debris. The small flume was selected primarily to take advantage of the better visibility offered by the water clarity. These tests⁹ showed that the fiber debris fragments and paint chips exhibit distinct transport properties and do not interact with each other in a significant way. The fiber was observed to tumble down the floor of the flume at lower velocities, leaving the paint chips behind.

2.2.1.3 Effect of Water Height in the Flume

The height of the water on the containment floor can change significantly with time. Therefore, the effect of water (or flume) height on transport properties was examined by comparing transport properties measured with different depths of water. The tests were conducted in the small flume (with 3 in. of water) and in the large flume (with 8-12 in. and 24 in. of water). The data¹⁰ suggest that the height of water above the debris does not introduce sufficient variation in the test results to warrant its inclusion as a test variable. Therefore, the parametric tests in the large flume were all conducted with a water depth of 18 in.

2.2.1.4 Effect of Floor Roughness on Floor Transport

The floor of the large flume has a plexiglass surface, which is considered sufficiently similar to the smooth, painted floor surfaces of power plants to allow meaningful transport properties to be measured.

⁶ Measurements are listed in Table B-3(a) in Appendix B. A second series of tests was conducted using the same procedure except a lower concentration of cal-sil was used (3 g per 500 cm³ of water instead of 6 g). The results were the same as those reported in Table B-3(a), within statistical variations in the test data.

⁷ Measurements are listed in Table B-3(b) in Appendix B.

⁸ Measurements are listed in Table B-4(a) in Appendix B.

⁹ Measurements are listed in Table B-4(b) in Appendix B.

¹⁰ Measurements are listed in Table B-5 in Appendix B.

Nevertheless, exploratory tests were carried out to determine the effect (if any) of surface roughness on transport properties. The range of surface roughness examined was intended to span the possible range of PWR floor surface conditions. Engineering judgment suggests that the roughest floor surface would be uncoated concrete, which is closer in roughness to that of treated plywood than to that of plexiglass. Therefore, a plywood surface was placed at the bottom of the large flume, and the transport properties of fiber debris and SS RMI were measured (i.e., incipient and bulk tumbling velocity). The results¹¹ show that changing the floor surface did not have any statistically significant effect on the transport properties of either material.

2.2.1.5 Determination of Flow Uniformity in Large Flume

As discussed in Sec. 2.1, the large flume is designed to simulate a wide spectrum of flow patterns, from planar (or uniform) flow to nonplanar (or turbulent) flow. The latter is characterized by large-scale eddies. Water enters one end of the large flume through a vertical supply pipe that is suspended several feet above the floor of the flume. Water from the supply pipe is discharged into a diffuser box at the entrance of the flume. Water exiting the diffuser box enters a short mixing region (4 ft long) before it flows into the flow straightener and ultimately into the active section of the flume. These features of the flume were designed to minimize the nonplanar component of the entry flow while at the same time provide the flexibility to intentionally induce nonplanar flow fields in some tests (this can be done by removing the flow straighteners and/or diffuser).

Exploratory experiments were conducted here to confirm that the flow straighteners perform their intended function and that any residual nonplanar component (if any) has an insignificant effect on debris transport.

Figure 2-1 is a photograph of the entrance portion of the large flume (in cross section) because of the presence of flow straighteners/diffusers between the diffuser box (at the far right) and the active section of the flume (far left). A few tests also were conducted in which visual observations of flow conditions were enhanced by injecting liquid dyes and by watching small tracer particles and air bubbles. All these observations attest to the fact that flow patterns are planar.

First-order insights into flow patterns also can be gained by measuring the local flow velocities in the flume at different horizontal and vertical points. Calibrated tracer balloons were used to gain these insights.¹² The tracer balloons were colored water balloons with a sufficient number of lead shots (1/32 in. in diameter) added to make them neutrally buoyant. These balloons were sufficiently large and light that no observable slip existed between the balloons and the bulk water flow (which can be easily established by dye injection). These balloons were first calibrated in the small flume¹³ to determine if they were measuring the velocity accurately.

Velocity was measured with balloons dropped 6 in. downstream of the flow straightener and allowed to travel 4 ft.¹⁴ It was observed that the flow is quite uniform through the height of the flume, and the average velocity is very close to the velocity near to the floor of the flume. The velocity at the top surface is still somewhat higher than the average velocity.

¹¹ The measurements are listed in Table B-6 in Appendix B.

¹² The initial plan was to use small turbine-type flow meters that are typically used in hydrology laboratories (also called Pigmy meters) to perform these local velocity measurements. Even though the manufacturer's data sheets suggest that these flow meters would work accurately at water velocities as low as 0.1 ft/s, our experiments revealed otherwise. In spite of using several such Pigmy meters, including brand new ones and ones that were greased and refurbished, they proved to be unreliable at the low water velocities (<0.5 ft/s) that were of present interest.

¹³ The small flume has the following features that facilitate this calibration: (a) it is equipped with an accurate bulk flow meter and (b) on numerous occasions in the past, the flow patterns were characterized to ensure that uniform flow exists across the length of the flume. Measurements from the balloon calibration tests are listed in Table B-7(a) in Appendix B.

¹⁴ The measurements are listed in Table B-7(b) in Appendix B.



Fig. 2-1. Photo of water flow in the large flume in Configuration A.

2.2.1.6 Repeatability of Floor Transport Data

To develop a sense of variability in test measurements, the incipient tumbling velocity of fiber and SS RMI debris was measured on five consecutive days with different samples.¹⁵ Incipient motion of fiber was found to occur at 0.11 to 0.12 ft/s. Similarly, the incipient motion of SS RMI was found to occur at 0.23 to 0.25 ft/s except in the 5th experiment, when a single piece moved a couple of inches at a velocity of 0.12 ft/s. The velocity had to be raised to 0.19 ft/s before the same piece moved another 10 in. To limit the effects of debris orientation or minor perturbations in flow conditions¹⁶ on measurements, “incipient motion” was defined as movement of at least 6 in. within 1–2 min of an increment of the flow velocity.

2.2.1.7 Comparison with Data from Previous Investigators

Prior investigators developed transport data for select types of debris in preselected shapes. For example, buoyancy properties and incipient tumbling velocity were measured by Brocard for fiberglass insulation debris of various sizes [Ref. 3]. He observed that fiberglass insulation “readily absorbs water, particularly hot water, and sinks rapidly (from 20 to 30 s in 120°F water).” This observation is consistent with the water saturation tests described above (Sec. 2.2.1.1).

Brocard also report incipient tumbling velocities for individual shreds (loosely connected fibers) as follows.

<u>Sample size</u>	<u>Incipient Tumbling Velocity (ft/s) [Ref. 3]</u>
Individual shreds	0.2

¹⁵ Measurements are listed in Table B-8 in Appendix B.

¹⁶ Either one of these could have caused the unusual behavior of the one piece of RMI foil.

GSI-191: Separate Effects Characterization of Debris Transport in Water

This value is slightly higher than those observed in the exploratory test phase (and confirmed later in the parametric tests). Incipient motion of small fiberglass shreds was detected in the UNM apparatus at velocities ranging from 0.07 ft/s to 0.17 for small shreds, depending on the specific type of fiberglass insulation tested and local flow conditions (see Sec. 3.1).

This comparison establishes that the experimental setup and procedures used in the present test program produce results that are sufficiently similar to those developed in previous test programs to allow meaningful comparisons to be made.

2.2.2 Scaling Considerations

The emphasis of the test program described in this report is to measure transport properties of LOCA-generated debris fragments, not to perform scaled tests that will determine the quantity of debris that might transport to a screen in a particular plant. Therefore, geometric scaling (i.e., flume vis-à-vis PWR containment floor) is not of direct relevance to this study. The scaling concerns are related to parameters that influence debris transport and capturing their range adequately in the planned experiments. These parameters are

1. debris size/shape,
2. water temperature (affects fluid viscosity/density),
3. flow velocity, and
4. flow patterns.

The experiments used fragments of actual insulation materials that were fabricated to closely resemble anticipated debris. Exploratory tests and analytical formulations have led to the conclusions that the effect of water temperature on transport is negligible and that transport is according to Newton's law (or turbulent regime). Hence, the use of ambient-temperature water in the testing is acceptable, provided that the Reynolds number values in the present flume fall in the turbulent regime. The water velocities were selected such that the Reynolds numbers are sufficiently large to ensure turbulent transport. Finally, present experiments made no attempt to exactly simulate the flow patterns anticipated in a PWR. Instead, it varied flow patterns over a fairly representative range and studied the effect they would have on debris transport.

2.3 Test Matrix

The measurements and observations made in the exploratory testing described above provided a technical basis for reducing the number and range of variables over which transport properties need to be measured. In consultation with members of the US NRC's expert panel that developed Phenomena Identification and Ranking Tables (PIRTs) for PWR debris transport in dry ambient conditions [Ref. 4], a final test matrix for parametric testing was developed as shown in Table 2-1.

Table 2-1. Parametric Test Matrix: Transport Properties Measured as a Function of Test Variables.

<i>Measured Property</i>	Test Variables						
	Debris Size	Water Temp.	Flume Average Velocity	Flume Water Depth	Fluid Entry Condition	Flume Cross-Section	Debris Curb Height
<i>Size (weight)</i>	❖						
<i>Shape (dimensions)</i>	❖						
<i>Terminal Velocity</i>	❖	❖		❖			
<i>Settling in turbulent pools</i>	❖		❖	❖	❖	❖	
<i>Transport distance</i>	❖		❖	❖	❖	❖	
<i>Tumbling</i>	❖		❖	❖	❖	❖	❖
<i>Vertical Mixing</i>	❖		❖				
<i>Lift at the Curb</i>	❖		❖	❖	❖	❖	❖
<i>Screen Retention</i>	❖		❖		❖		
<i>Dissolution/Destruction*</i>	❖	❖					

* The effect of turbulence was explored. Turbulence was simulated with a stirrer.

3 TEST RESULTS

This section presents results of the parametric test phase. The procedures used to perform these tests are described in Appendix D. The calibration of the major instrumentation used to collect data is described in Appendix E. Data collected from the various tests are presented according to the insulation type studied.

Low-density fiberglass	Sec. 3.1
RMI	Sec. 3.2
Miscellaneous Debris Materials (cal-sil, paint chips, fire-barrier material, silicone foam)	Sec. 3.3

3.1 Low-Density Fiberglass Insulation

3.1.1 Nukon

Nukon is a low-density fiberglass material used as insulation in several of the operating PWRs. The material used in the transport experiments was provided by the vendor, who manufactured the base-wool following their usual methods and then fragmented the blanket using air jets to form the debris that was supplied to UNM. Visually the debris resembles size classes 3 and 4, as described in the NUREG/CR-6224 (Fig. 3.1). Some large (4-in. and 6-in.) pieces of Nukon also were tested for settling velocity to demonstrate the effect of the size of the material. Settling velocity tests, incipient motion tests, and lift tests were conducted in accordance with the test procedures described in Appendix D. For each of the tests, the samples used were soaked in 80°C water for at least 10 min. The amount of Nukon used for the incipient motion tests and the lift tests are about 3.0 g (a handful) and representative of the sample shown in Fig. 3.1.

A summary of the measured Nukon transport properties is given in Table 3.1. Actual measurements made during these tests are tabulated in Appendix C.



Fig. 3.1. Typical Nukon fiberglass insulation debris used in transport testing.

Table 3.1. Summary of Measured Nukon Transport Properties.

Fragment Size:	6-in.	4-in.	1-in.
Settling Velocity (ft/s)	0.41	0.40	0.15
<hr/>			
Inlet Flow Conditioning:	Configuration A	Configuration B	Configuration C
Incipient Tumbling Velocity (ft/s)	0.12	0.07	0.06
Bulk Tumbling Velocity (ft/s)	0.16	0.09	0.10
Lift-at-the-Curb Velocity (ft/s)			
2-in. curb	0.25	0.25	0.22
6-in. curb	0.34	0.25	0.28

3.1.2 Thermal-Wrap

This fiberglass material is similar to the Nukon insulation discussed in the previous section, and the test results are largely similar. Thermal wrap comes in 2-ft x 4-ft blanket form that is approximately 4-in. thick (Fig. 3.2a). These blankets initially were cut into 4-in. by 6-in. pieces with scissors. These smaller pieces subsequently were shredded with a leaf shredder to produce the material shown in Fig. 3.2b.

Some large (4-in. x 6-in.) pieces also were tested to demonstrate the effect of the size of the material. Settling velocity tests, incipient motion tests, and lift tests were conducted with the procedures described in Appendix D. For each of the tests, the samples used were soaked in 80°C water for at least 10 min. The blanket comes apart during handling after soaking.

Five additional pillows (1 ft x 1 ft x 4 in.) of the thermal-wrap insulation were obtained. The pillows were tested for terminal velocity after soaking them in water for 24 h. The terminal velocity of the five pillows was determined to be 0.25 to 0.54 ft/s.

A summary of the measured thermal-wrap transport properties is given in Table 3.2. Actual measurements made during these tests are tabulated in Appendix C.



Fig. 3.2a. Thermal-wrap fiberglass insulation in bulk form.



Fig. 3.2b. Shredded thermal-wrap.

Table 3.2. Summary of Measured Thermal-Wrap Transport Properties.

	Fragment Size:		1x1-in. pieces		2x2.5-in. pieces	
	Settling Velocity (ft/s)		0.16		0.13	
Inlet Flow Conditioning:	Configuration A		Configuration B		Configuration C	
	shredded debris	4 in. x 6 in. pieces	shredded debris	4 in. x 6 in. pieces	shredded debris	4 in. x 6 in. pieces
Incipient Tumbling Velocity (ft/s)	0.16	0.12	0.07	0.19	0.10	0.17
Bulk Tumbling Velocity (ft/s)	0.19	0.16	0.11	0.23	0.11	0.20
Lift-at-the-Curb Velocity (ft/s)						
2-in. curb	0.25	0.25	0.25	0.28	0.22	0.22
6-in. curb	0.28	0.30	0.25	0.25	0.30	0.30

3.1.3 Kaowool

Kaowool insulation was obtained from Radiant Energy Shield (RES) samples in 4-ft x 3-ft pieces. The white Kaowool (1-½-in. nominal thickness) is enclosed inside the fireblanket. The white Kaowool from these blankets was cut initially into 4-in. by 6-in. pieces with scissors (Fig. 3.3a). These smaller pieces then were shredded with a leaf shredder to produce the debris shown in Fig. 3.3b. For each of the tests, the samples used were soaked in 80°C water for at least 10 min.

Some large (4-in. x 6-in.) pieces (Fig. 3.8a) also were tested to demonstrate the effect of the size of the material. Settling velocity tests, incipient motion tests, and lift tests were conducted according to the procedures described in Appendix D. A summary of measured Kaowool transport properties is given in Table 3.3. Actual measurements made during these tests are tabulated in Appendix C.



Fig. 3.3a. Kaowool insulation cut into 4-in. x 6-in. pieces.

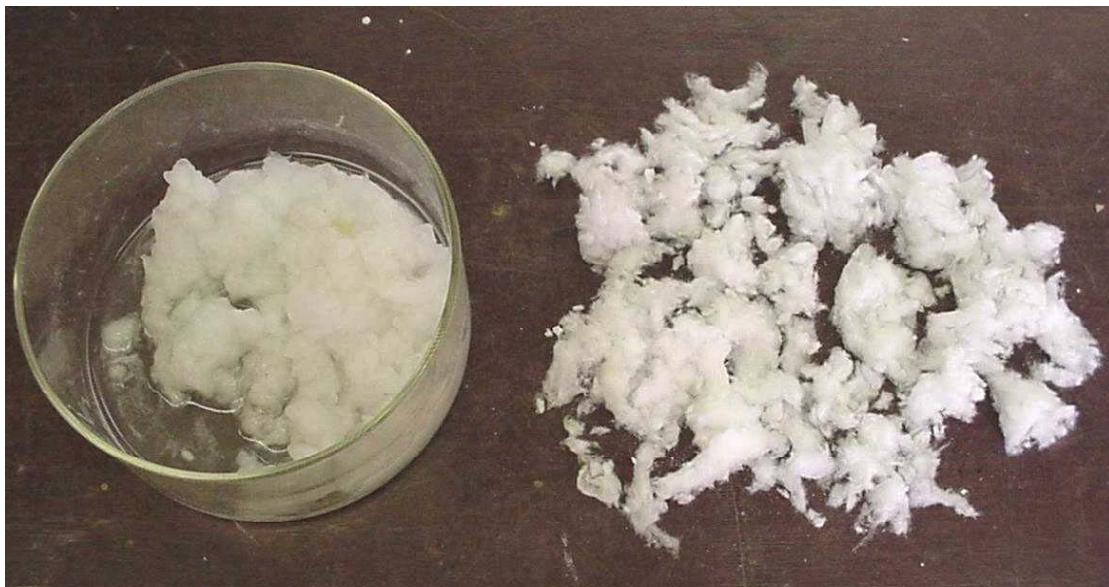


Fig. 3.3b. Shredded Kaowool.

Table 3.3. Summary of Measured Kaowool Transport Properties.

	Fragment Size:		Shredded pieces			
Settling Velocity (ft/s)	4 in. x 6 in. pieces		0.21			
Inlet Flow Conditioning:	Configuration A		Configuration B		Configuration C	
	shredded fragments	4 in. x 6 in. pieces	shredded fragments	4 in. x 6 in. pieces	shredded fragments	4 in. x 6 in. pieces
Incipient Tumbling Velocity (ft/s)	0.16	0.12	0.09	0.25	0.17	0.17
Bulk Tumbling Velocity (ft/s)	0.19	0.16	*	0.25	0.20	0.22
Lift-at-the-Curb Velocity (ft/s)						
2-in. curb	0.30	0.25	0.25	0.28	0.28	0.30
6-in. curb	0.41	0.47	0.25	0.25	0.32	0.39

*Not established in the tests

3.2 Reflective Metallic Insulation

As indicated earlier, the transport properties of two types of RMI were examined: aluminum RMI and SS RMI. The results of the measurements for each of these materials are summarized in the next two sections.

3.2.1 Aluminum RMI

Aluminum RMI was obtained from an insulation vendor in small fragments (1/2-in. and 2-in. square pieces). The thickness of these fragments was confirmed on site to be approximately 1.5-mil. The vendor subjected the pieces to air jets to produce crumpled samples. To distinguish their transport properties, the aluminum RMI was categorized into crumpled, semi-crumpled, and flat. The photo in Fig. 3.4 shows the resulting range of sizes for this type of debris.

The settling data suggest that crumpled and semi-crumpled pieces settle slowly compared with flat pieces of RMI, which is expected because the crumpling naturally provides more projected area for flow resistance. A similar trend is also evident for tumbling, where tumbling occurred at lower velocity for crumpled pieces as compared with flat pieces.

A summary of measured aluminum RMI transport properties is given in Table 3.4. Actual measurements made during these tests are tabulated in Appendix C.

3.2.2 Stainless-Steel RMI

SS RMI cassettes (Fig. 3.5) were dropped into the flume with 18 in. of water. The slotted cassette took 5 min to take in water and sink. The cassette with solid closures took longer to absorb water (13 min) and sink. No floor transport was observed at a velocity of 0.5 ft./s, and some floor transport (dragging along the floor) was observed at 1.0 ft./s. No intermediate velocities were used for further exploration of this form of SS RMI.

The steel debris (foil fragments) were not immersed in hot water before testing because it did not resist sinking in water nor release air bubbles that might reside in the creases of the crumpled pieces. The test results reported below were from tests conducted according to the procedures discussed in Appendix D. A summary of test results is given in Table 3.5. Actual measurements made during these tests are tabulated in Appendix C.



Fig. 3.4. Aluminum RMI.

Table 3.4. Summary of Measured Aluminum RMI Transport Properties.

Fragment Size:	Mixture of flat, crumpled, & semi-crumpled foils (2-in. square)
Settling Velocity (ft/s)	0.11
Inlet Flow Conditioning:	Configuration A
Incipient Tumbling Velocity (ft/s)	0.20
Bulk Tumbling Velocity (ft/s)	0.30
Lift-at-the-Curb Velocity (ft/s)	*

*Not measured in these tests



Fig. 3.5. SS RMI cassettes (solid and slotted closure).

Table 3.5. Summary of Measured SS RMI Transport Properties.

Fragment Size:	Crumpled or semi-crumpled foils (1/2-in. square)		Crumpled or semi-crumpled foils (2-in. square)		Crumpled or semi-crumpled foils (2-in. square)	
Settling Velocity (ft/s)	0.37		0.48			
Inlet Flow Conditioning:	Configuration A		Configuration B		Configuration C	
	½ in. x ½ in.	2 in. x 2 in.	½ in. x ½ in.	2 in. x 2 in.	½ in. x ½ in.	2 in. x 2 in.
Incipient Tumbling Velocity (ft/s)	0.28	0.28	0.41	0.28	0.20	0.20
Bulk Tumbling Velocity (ft/s)	0.30	0.30	0.41	0.37	0.22	0.22
Lift-at-the-Curb Velocity (ft/s)	0.84	0.84	0.30	0.30	none	1.0
2-in. curb	none	none	0.30	0.30	none	none
6-in. curb						

3.3 Miscellaneous Insulation Materials

Although low-density fiberglass and RMI are the most prevalent materials used to insulate piping in a PWR containment, other materials may contribute to post-LOCA debris. These include cal-sil (widely used to insulate steam generators and other special components), paint chips (from erosion of coated surfaces), fire-barrier materials (such as Marinite), and silicone foam insulation. The basic transport properties of these materials also were examined in this test program, although not necessarily over the same range of conditions used for fiberglass and RMI. The results of tests performed for cal-sil, paint chips, Marinite fire-barrier, and silicone foam are described in this section.

3.3.1 Cal-Sil Insulation

Representative samples of the debris used in these experiments are shown in Fig. 3.6. Because the major emphasis of the cal-sil tests was to collect data on the disintegration and transport characteristics of smaller debris, very few tests were conducted using the larger pieces.

Disintegration Characteristics of Cal-Sil

Several pieces of cal-sil samples weighing approximately 10 g (± 0.2 g) each were selected from the debris provided by the vendor. They were separated into three batches of five samples and were dropped into three different water baths maintained (1) at ambient temperature (approximately 20°C), (2) at elevated temperature (approximately 80°C), and (3) at elevated temperature with occasional stirring of water. The debris fragments were subjected to these conditions for 20 min, after which the water was drained and the residual debris samples were dried and weighed.

Table 3.6 lists the measured weight of the samples at the end of each test. In ambient-temperature water, approximately 20% of the cal-sil detached from the original sample and went into suspension. Although not explicitly shown here, stirring the water bath appeared to have very little effect on fragment disintegration in this case. At this temperature, particles and loosely bound strands of fiber were observed to detach and go into suspension; particles bound to larger masses of fiber tended to remain intact.

Fragment disintegration increased with water temperature; within 20 min, approximately 50% of the fragment mass was liberated as a suspension in hot water. As shown in the last column in Table 3.1, occasional stirring further enhanced fragment disintegration. At the elevated temperature (and particularly with stirring), the web of fiber that initially bound the material together expanded and disintegrated more readily than at ambient conditions.



Fig. 3.6. Calcium silicate.

**Table 3.6. Disintegration Characteristics of Cal-Sil Fragments.
(Initial Weight of Each Cal-Sil Fragment is 10 g)**

Trial No	Weight of Cal-Sil Retained as Fragment (gm)		
	Ambient Water	80°C Water	80°C Water + Stirring
1	8.7	5.23	2.25
2	7.5	4.70	3.1
3	8.3	6.05	2.4
4	8.16	5.0	2.2
5	8.4	6.0	1.9
Average	8.2	5.4	2.4

Tumbling Velocity of Cal-Sil

Five pieces of cal-sil insulation were added to the flume floor at a water velocity of approximately 0.05 ft/s. Because ambient (~20°C) water was used, significant disintegration was not observed and the pieces remained intact during the transport tests. The water velocity was increased gradually until tumbling or sliding of the fragments was first noted (approximately 0.25 ft/s). At this velocity, referred to as incipient tumbling velocity, smaller fragments (attached to the bigger chunks by fine fibers) started to detach and move toward the screen. These smaller pieces ultimately reached and adhered to the screen, but the larger chunks remained intact with no significant movement. Further increase in the flow velocity eventually caused movement of all the cal-sil fragments, irrespective of their shape. This velocity, the bulk tumbling velocity, is approximately 0.35 ft/s. Actual transport data obtained for cal-sil fragments are tabulated in Appendix C.

Simultaneous Cal-Sil and Fiber Transport

Additional testing was performed to further examine the influence of cal-sil on fiber debris transport properties (recall that exploratory testing suggested fiber fragments saturated in cal-sil particulate, absorbed from suspension, had a negligible effect on transport properties.) To confirm this observation, 20 g of cal-sil was added to 500 cm³ of water and heated for 20 min to near boiling. The cal-sil was fully dissolved with only few visible small chunks left behind. Dry Nukon fragments then were added, and the water was heated further for about 10 min. Visually, one could see that cal-sil particles adhered to the Nukon fragments. These fragments then were dropped at the flume top surface (drop tests). The time required for the debris to reach the floor and the horizontal distance traveled during that time were measured at two different flume velocities. Measurements from these confirmatory tests are tabulated in Appendix C.

The resulting settling velocities were compared with those obtained from experiments with Nukon fiber in clean water (Sec. 3.1.1). The results confirmed that cal-sil does not significantly affect Nukon debris settling or lateral transport characteristics.

3.3.2 Paint Chips

Epoxy-based paint chips¹⁷ ranging in size from 1 in. x ½ in. to 1/8 in. x 1/8 in. were manufactured for testing (Fig. 3.7). These chips had a median thickness of approximately 15 mil.

¹⁷ The paint chip samples used in the transport tests may not be prototypic of those generated during a LOCA. The effects of aging, and numerous other factors that influence paint chips' shape, size, and configuration were not taken into account when manufacturing the chips used in these tests.



Fig. 3.7. Paint chips.

The tumbling velocity for these chips was measured in the small and large flumes and for two different flow conditions (i.e., inlet configurations in the large flume). However, because water clarity was superior in the small flume, it was the primary apparatus used for the paint-chip transport study. A few tests were conducted in the large flume, including some tests to capture the effect of large-scale turbulent eddies on paint chip transport.

The measurements made during these tests are tabulated in Appendix C. The major results can be summarized as follows.

Drop tests in the large flume with Configuration A (planar flow) indicated that at a flow velocity of 0.4 ft/s, the paint chips added at the top surface would settle out with a median settling velocity of 0.16 ft/s. This value compares very well with the median velocity of 0.15 ft/s measured using the settling column.

In the small flume, incipient tumbling velocity for paint chips (where slight movement was first observed) was found to be approximately 0.4 ft/s. Bulk motion occurred only when the flow velocities reached or exceeded 0.45 ft/s. At a flow velocity of 0.5 ft/s, movement is almost instantaneous, and the paint chips are capable of being transported several feet. One could also see that the debris is intermittently lifted off the floor and resettles.

The effects of turbulent flow patterns on settling and transport properties were examined in the large flume. With inlet flow conditioning, Configuration A (planar flow) tumbling measurements again indicated incipient tumbling occurs at approximately 0.4 ft/s, and bulk tumbling occurs at a flow velocity of approximately 0.45 ft/s. These values are almost identical to the values measured using the small flume and reconfirmed the influence of flume water height to be negligible.

GSI-191: Separate Effects Characterization of Debris Transport in Water

However, introducing large-scale turbulence influenced transport significantly. By changing to inlet flow [Configuration B (i.e., free-fall with no diffuser)], the debris incipient tumbling velocity reduced to approximately 0.31 ft/s. Bulk movement occurred at a slightly lower velocity with turbulence present at 0.4 ft/s as opposed to 0.45 ft/s with planar flow.

Lift-at-the-curb velocity measurements also were carried out in the large flume using a 2-in.-high curb. The water height was maintained between 18 and 19 in. At a water velocity of approximately 0.5 ft/s, debris started to lift off the floor and deposit on the screen. Not all pieces lifted over the curb, but those that were curled up and thus provided higher projected surface area made it past the curb at these velocities.

Finally, additional tests were conducted to further examine the influence of paint chips on fiber debris transport properties and vice versa (recall that exploratory testing suggested that the two debris materials did not interact and fiber fragments departed the flume floor leaving the paint chips behind.) To confirm this observation, tests were again performed in which both debris types were introduced to the large flume. The results again clearly showed that fiber fragments tumbled out at lower velocities, leaving the paint chips behind. Incipient tumbling velocities for the fiber fragments were consistent with those observed in the fiber-only tests described in Sec. 3.1.1. The paint chips departed only when the flow velocity was increased to approximately 0.4 ft/s.

3.3.3 Marinite Fire-Barrier Material

The Marinite Fire-Barrier debris comes in the form of solid blocks (rectangular and curved pieces) (Fig. 3.8a). Simply dropped in water, the material readily sinks to the bottom. Pieces of Marinite (1/2 in. thick) were submerged in boiling water (100°C) for 30 min. As a result, the material became soft with a rubbery texture on the exposed surface. This rubbery material remains intact (does not disintegrate). A very small amount of a milky whitish substance is released when the wet material is rubbed. A small amount (pieces smaller than 1/4 in.) of the soft rubbery material (Fig. 3.8b) could be pulled from the soft wet surface. These small pieces also sink readily.

Considering the amount of plastic deformation needed to pull these small rubbery pieces apart, the disintegration of Marinite into smaller fragments as a result of turbulence was judged to be highly unlikely. Nevertheless, the transport properties of the softened material were measured. The test data are tabulated in Appendix C. A summary of the measurements is given in Table 3.7.



Fig. 3.8a. Marinite fire-barrier material (dry and soaked block).

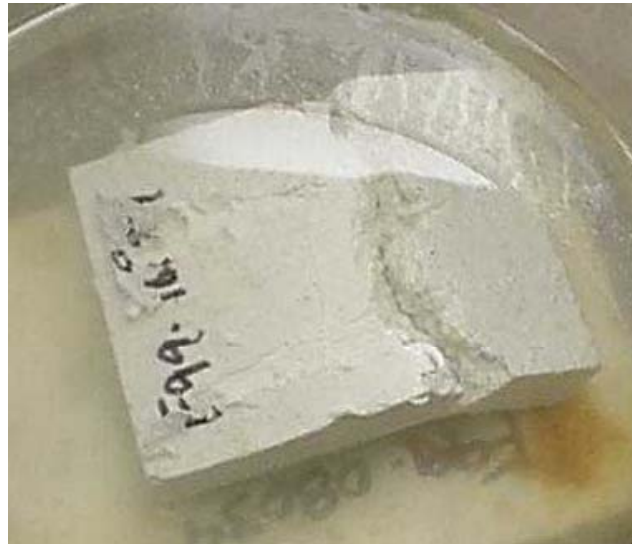


Fig. 3.8b. Wet broken piece of Marinite.

Table 3.7. Summary of Measured Marinite Transport Properties.

Inlet Flow Conditioning:	4-in x 4-in curved sample	4-in x 4-in flat sample	1-in x 1-in flat sample
Settling Velocity (ft/s)	0.45	0.56	0.59
Incipient Tumbling Velocity (ft/s)	0.77	*	0.77
Bulk Tumbling Velocity (ft/s)	0.99	*	0.79

*Motion not observed at velocities up to 0.99 ft/s

3.3.4 Silicone Foam Insulation Material

Silicone foam was obtained after it had been mixed and foamed in 5-gal. buckets by the supplier. As shown in Fig. 3.9, irregular pieces (roughly 2 in. on one side) were cut from these buckets and subjected to the following tests.

1. The foam was forcefully immersed (with weights on top) in 80°C water for over 10 min.
2. The foam was forcefully immersed in boiling water for 15 min, squeezed under water to force out air bubbles, and resubmerged.
3. The same foam samples subsequently were kept submerged in room-temperature water for 3 days.

After all of this processing, the foam continues to float readily.

Pieces of the foam were dropped in the flume with water velocity at 1.0 ft/s. The pieces floated on the surface, were carried downstream to the screen, and remained afloat.



Fig. 3.9. Silicone foam insulation material (as foamed and pieces tested).

4 DISCUSSION OF RESULTS

The test results described in this report reveal key transport properties of LOCA-generated debris in various forms and material types. These properties include settling velocity in quiescent pools as well as in flowing pools in planar flow; incipient, and bulk tumbling velocities, and the velocity required to lift debris over short obstacles, such as a 4- or 6-in. curb on the containment floor.

The trends in the many measurements described here are consistent with intuition. For example, the flow velocity required to lift debris fragments over a curb is generally higher than that needed to initiate debris motion and usually higher than that required to sustain motion after the fragment begins to move. Settling velocity for debris fragments that are roughly symmetrical in shape (e.g., clumps of fiber fragments) is unaffected by the lateral flow of water; that is, measurements made in a stationary settling column are consistent with those made in an operating flume regardless of flow conditions. Similar results were observed for nonsymmetric fragments, such as RMI foils and paint chips, *provided* the flow conditions in the flume were planar (i.e., inlet flow Configuration A). However, when large-scale turbulence was introduced, the settling velocity (and incipient tumbling velocity) reduced significantly for the nonsymmetric fragments.

For some types of debris, an obvious trend between “bulk tumbling’ velocity” and “lift-at-the-curb” velocity was difficult to discern. For fiber fragments, the difference between these two velocities was found to be as little as 0 and as much as a factor of 3, depending on the specific material involved and the degree of large-scale turbulence in the flume. For SS RMI debris, lifting crumpled or semi-crumpled foils over a 4- or 6-in. curb appeared to occur randomly; i.e., there was no discernable correlation to flow velocity. In some cases, foils jumped the curb at velocity equal to the bulk tumbling velocity. In other cases, foils remained captured at the bottom of the curb at significantly higher velocities.

Measurements of many debris transport parameters were repeated during many experiments to gain a quantitative understanding of data variability (or alternatively measurement repeatability). In planar flow conditions, variability was relatively small; for example, incipient flow velocity was generally found to vary by $\pm 10\%$. Data variability was considerably larger in turbulent flow conditions, but this was expected. In such conditions, fluid velocities in the immediate proximity of debris fragments can differ substantially from the average flume water velocity (which is the velocity measured in these experiments). As a result, the actual velocity required to initiate fragment motion or to sustain bulk fragment motion can appear to span a wide range when in fact this variability is most likely a result of variations in fluid velocity within the flume.

Finally, it is important to repeat a statement made in the introduction of this report regarding the objectives of these experiments. That is, the intent of the experimental program described in this report was not to measure debris movement in a “scale model” of a PWR containment floor. Rather, the data generated in these tests are basic physical and transport properties of debris fragments that can be applied in computational models of plant-specific accident conditions.

5 REFERENCES

1. D. V. Rao et al., "PWR Sump Debris Transport Test Program Plan," Draft Report, Los Alamos National Laboratory, Rev. 0.
2. D. V. Rao et al., "GSI-191: Summary and Analysis of US Pressurized Water Reactor Recirculation Sump Performance," Los Alamos National Laboratory Technical Letter Report LA-UR-4083, Rev. 1 (August 2001).
3. D. N. Brocard, "Buoyancy, Transport, and Head Loss of Fibrous Reactor Insulation," Alden Research Laboratory/US NRC report NUREG/CR-2982, SAND82-7205 (July 1983).
4. B. E. Boyack et al., "PWR Debris Transport in Dry Ambient Containments—Phenomena Identification and Ranking Tables (PIRTs)," Los Alamos National Laboratory report LA-UR-99-3371, Rev. 2 (December 14, 1999).

APPENDIX A TEST FACILITY DESCRIPTIONS

The Civil Engineering Department conducted the debris transport tests described in this report at the UNM Open-Channel Hydrology Laboratory. The Hydrology Laboratory has long constructed and operated open-channel flumes and scaled models of spillways, rivers, and confluences. Typical models include open-channel structures (e.g., spillways and confluences), submerged structures (e.g., reservoir outlets), sediment transport (e.g., mobile particles tumbling along the channel floor), and pressurized conduits (e.g., pipe systems).

At the start of the test program, the hydrology laboratory provided most of the infrastructure necessary to carry out this test program, including (1) several operating flumes, (2) facilities for particle characterization/sieving, (3) a large sump and (4) a 2200-gal./min centrifugal pump. The existing facilities were modified, and additional apparatus was built to collect data on debris transportability as function of debris type/size, flow patterns, floor type, and flume velocity. The test facilities provided also were sufficient to acquire data related to the destruction and transport of cal-sil insulation fragments.

A.1 Small-Flume Test Apparatus

UNM operates a small-flume test apparatus located in the UNM Civil Engineering Hydrology Laboratory to perform sediment transport testing and other basic transport studies. The dimensions of the small flume were 1 ft wide, 1.5 ft deep, and 10 ft long. A photograph of the small flume is shown in Fig. A-1, and the flume is shown schematically in Fig. A-2. The small flume was capable of testing insulation debris transport at transport velocities typical of those expected on the containment floor during the recirculation phase of ECCS operation; however, the depth of water is limited to 1 ft maximum.

Selected hardware and instrumentation modifications were made to the small flume, and it was widely used in the exploratory testing phase (1) to establish the importance of flume water height on debris transport and (2) to develop test procedures that were ultimately used in the large flume. The primary advantages of the small flume are that (1) it provided uniform, calm, and well-characterized flow throughout its length; (2) the debris were more visible because of the narrowness of its test section than was the wider large flume (which is especially important when the debris is small and or fragile; and (3) it was relatively easy to clean fine debris that could not be filtered effectively from the flume and its sump (e.g., cal-sil dust). Because of these advantages, the small flume was used exclusively to study the transport of cal-sil, cal-sil and Nukon fibrous debris mixtures, paint chips, and small crumpled RMI fragments. Comparison of small flume test data with the large flume test data also added a measure of quality assurance to the overall test data.

The flume had two pumps with a combined flow capacity of approximately 100 gal./min. Water was pumped from a small collection volume underneath the flume into the flume entrance and then drained back into the collection volume at the flume exit. Front and rear control gates were used to control flow height and velocity through the flume test section. The slope of the flume could also be varied. The flume was equipped with 40-GPM flow meters that accurately measured total volumetric flow.¹⁸ The average flume velocity was derived from the volumetric flow measurements. Conventional flow visualization/measurement techniques were used to confirm that calm, uniform, and straight flow patterns existed through out the flume length. At high flume velocities, the existing instrumentation ensured that the flow fields were sufficiently uniform.

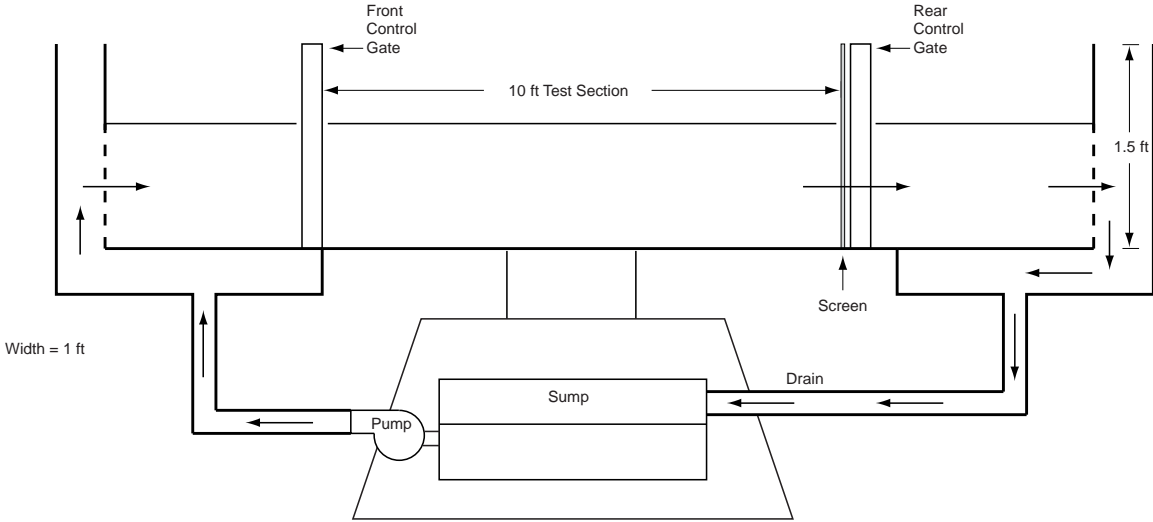
A screen located at the outlet end of the flume test section was used to catch debris. The screen was constructed of #4 wire mesh screen (~1/4-in. square openings). The screen is shown in Fig. A-3. Head losses caused by debris accumulation on the screen could be measured. A steel gate (1/16 in. thick) was constructed at the downstream end to control the outflow of water. This gate is operated manually by a 1/2-in.-diam screw. The sides were sealed with caulk. This rear control gate, along with the gates at the upstream end, allowed both the velocity and the height to be controlled independently.

¹⁸ Although the flume was equipped with 'Pigmy' type turbine flow meters to measure local flow velocities in the test section at various elevations, the meters were found to be inadequate for the flow velocities of present interest.

**GSI-191: Separate Effects Characterization
of Debris Transport in Water**



Fig. A-1. Photograph of the small flume test apparatus.



Small Flume - Side View

Not to scale

Fig. A-2. Schematic of the small flume test apparatus.



Fig. A-3. Outlet screen in the small flume test section.

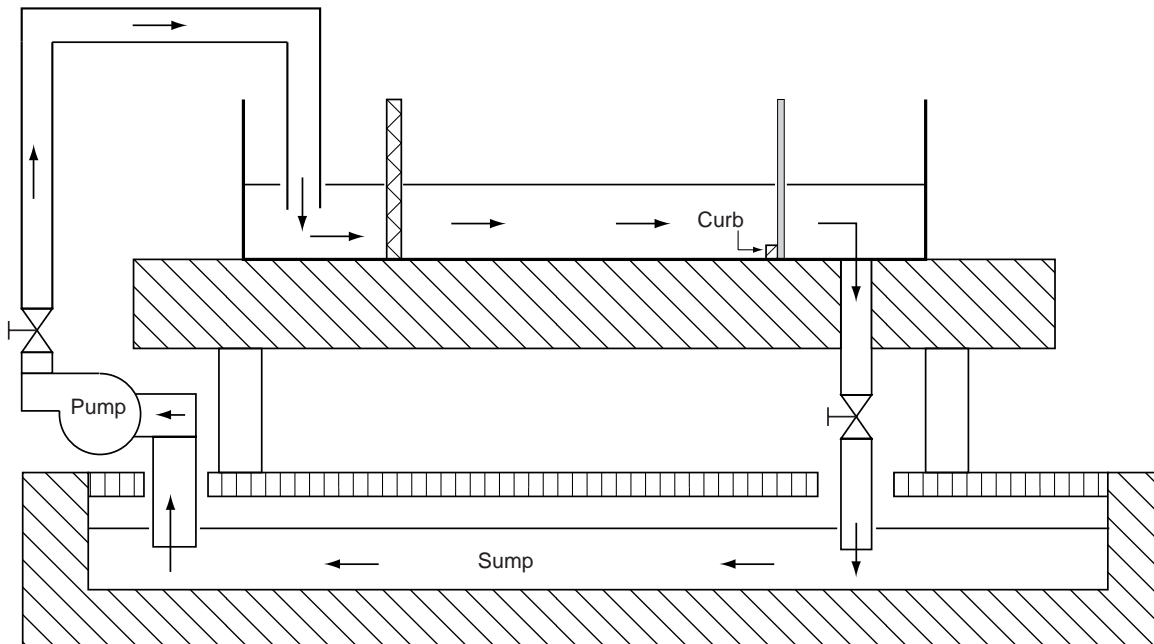
A.2 Large-Flume Test Apparatus

Most of the debris transport tests were conducted in the large flume. The large flume was not designed to provide test data directly scalable to plant applications but instead was designed to serve as a test rig for simulating a variety of different flow conditions and to study the effect of these flow conditions on debris transport, i.e., suitable for conducting separate-effects testing. The design requirements of the large-flume apparatus were as follows.

- The pumping loop was to have sufficient capacity and control to collect debris transport data over a linear velocity range of 0.05 ft/s to 1.5 ft/s.
- The flume was to be sufficiently wide to accommodate large-scale debris transport without wall effects.
- The top surface had to be a free surface to accurately simulate containment sump flow.
- The flume geometry and physical features had to provide the experimenter with the capability of simulating the variety of flow patterns required by the experimental program.
- The flume geometry was to provide the flexibility to place an obstruction in the flow path (e.g., curbs) and to vary cross-sectional flow area (converging or diverging cross sections).

An extensive effort was devoted to understanding types of flow patterns established in the flume for different operating conditions. Also, CFD analyses were undertaken to gain further insights (see Appendix F).

Water was pumped from a sump and injected into the flume at the inlet end. Water drained from the flume at the outlet end. The drained water accumulated in the sump, where it was available for pumping back into the flume again. A schematic of the large flume is shown in Fig. A.4. The inlet water was conditioned at the flume inlet to remove unwanted turbulence and to create a uniform flow through the flume test section. An outlet screen was placed across the flume in front of the drain to catch debris. The test section was modified in selected tests to change the channel geometry and/or to place obstacles in the flow stream. These aspects are discussed in the following sections.



Not to scale

Fig. A-4. Schematic of large-flume assembly.

Large-Flume Construction.

The large flume was constructed to sit atop an 8-ft by 50-ft steel tilting table with an articulated center 2.5 ft above the floor; the table is the centerpiece of the UNM Open-Channel Hydraulics Laboratory. Adjustable hydraulic jacks capable of varying the table's slope from 0 to 10% were used to level the flume. The tilting table sits above a 2-ft by 2-ft recirculation channel and a 360-ft³ sump.

The basic design of the large flume is shown in Fig. A-5. The flume consists of an open-top box 20 ft long, 3 ft wide, and 4 ft high. The water inlet and flow conditioning occur in the first 6 ft of the flume; the last 4 ft of the flume were reserved for the screen and outlet drain. This left 10 ft of the flume available for testing.

The flume was constructed with 1/2-in.-thick Plexiglas on the sides and treated plywood on the bottom and ends. An epoxy-coated inner liner of Plexiglas 1/16 in. thick was placed on the bottom plywood floor. The epoxy coating was applied to the floor Plexiglas to obtain a surface roughness comparable to epoxy-coated PWR floors.¹⁹ The wall and floor sections were held together with a sturdy steel "Unistrut" frame.

The large flume rested on two sturdy 6-in. by 6-in. aluminum I-beams and was constructed on the UNM tilting table for accurate leveling. The flume was designed with sufficient structural strength such that it could be moved as required to accommodate other experiments. The large flume partially filled with water flowing at 0.15 ft/s is shown in Fig. A-6.

¹⁹ As discussed in Sec. 2.2.1.2, this design feature had an insignificant effect on debris transportability for the types and sizes of debris tested in this program.

GSI-191: Separate Effects Characterization of Debris Transport in Water

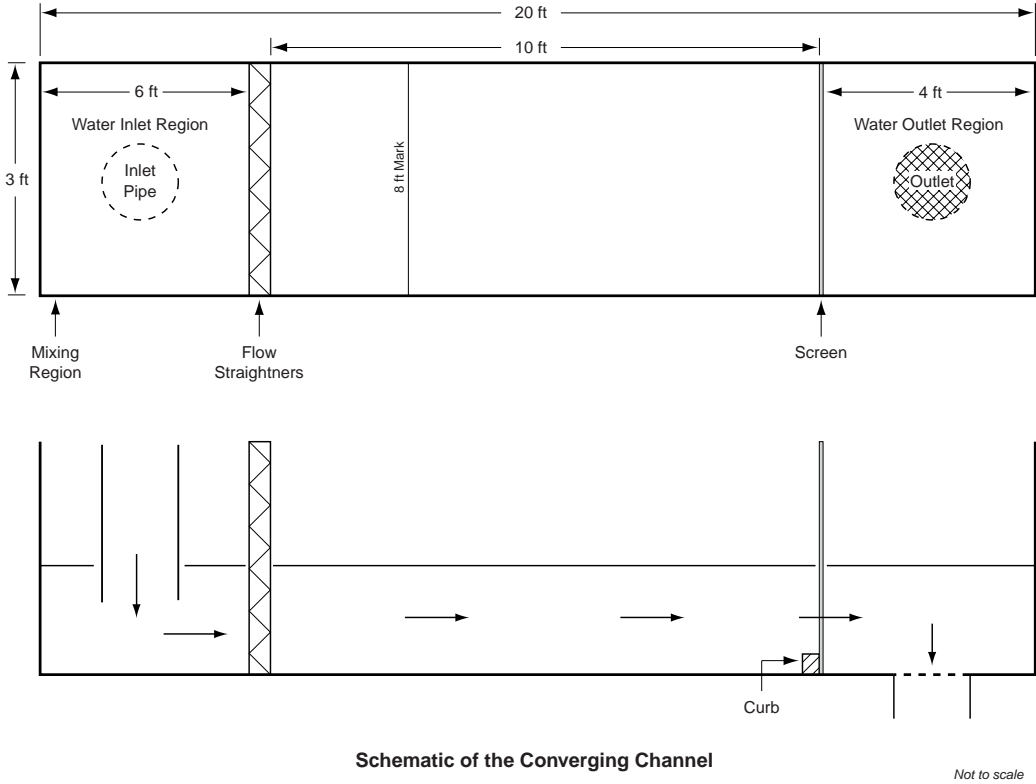


Fig. A-5. Basic design of large flume.



Fig. A-6. Large-flume apparatus.

Large-Flume Inlet Flow Conditioning

One goal of the large flume testing was to explore the effect of large-scale fluid turbulence on the transport of debris. To achieve this goal, three distinct configurations were used to introduce water to the flume. The configurations produced a wide range of flow conditions along the flume spanning the range of highly turbulent to nearly laminar conditions.

Tests were conducted using three inlet flow configurations, each of which produced a different flow pattern in the flume. These were:

- Configuration A: Diffused Flow Entry
- Configuration B: Free-Fall Flow Entry
- Configuration C: Immersed Pipe Flow Entry

Configuration A provided flow conditioning more appropriate to a quiescent region of the containment floor pool, whereas Configurations B and C provided two somewhat different flow conditions appropriate to more turbulent regions of the containment pool. Each of these configurations is described below.

Configuration A: Diffused Flow Entry. In a significant number of tests conducted as part of this study, it was necessary to create a uniform flow downstream of the flow straightener. Injecting water into the flume inlet section from a pipe created strong turbulence and nonuniform flow. The method selected to condition the inlet flow consisted of a series of damping pads followed by a flow straightener. The damping pads were actually synthetic air-conditioning humidifier pads held in place by #4 wire mesh attached to wooden frames. A dampening section consisted of a total of five wooden frames holding four humidifier pads in between them.

A sheet-metal flow straightener section followed the turbulence dampening pads. The flow straightener further straightened the flow. The straightener is shown schematically in Fig. A-7. The dimensions of the straightener assembly were 3 ft by 4 ft to fit within the flume cross section and 1 ft thick. The flow conditioner section is shown in Fig. A-8.

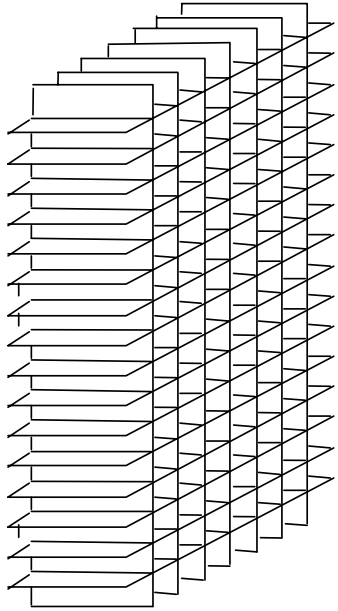
As discussed in Sec. 3, considerable flow visualization/characterization testing was done before the hardware configurations described above were selected. Conventional techniques such as dye injection and tracer particle tracking were used to visually establish that flow patterns were straight and that no visible eddies existed in the test section. In addition, local flow velocities were measured at several horizontal and vertical locations to ensure that flow entering the test section was straight and that no unusual flow patterns existed. These measurements relied on “neutrally buoyant water balloons” at low flow rates and “Pigmy” type turbine flow meters at the higher flow rates through the flume.

In addition, CFD modeling of the flume flow patterns also was undertaken to further ensure that flow patterns were as intended. The modeling details of the CFD simulations are presented in Appendix F. These models also confirmed that the flow patterns expected for this configuration were uniform.

Configuration B: Free-Fall Flow Entry. Conditioning Configuration B was designed to create three-dimensional flow patterns and to study the effect such flow patterns could have on the transport of debris. To facilitate this, the diffuser pads were removed from the apparatus. Water was allowed to free fall from the pipe exit located approximately 2 ft above the water surface. Water then flowed through the metal-frame straighteners before it entered the test section where debris would be located. This configuration is shown in Fig. A-9.

During both the design and subsequent testing, extensive flow visualization and flow measurement techniques were used to characterize the flow patterns created as a result of this configuration. All of these measurements suggested that a fast-moving water layer existed at the bottom and further that the flow field was dominated by large-scale eddies. The locations and extents of these eddies appeared to shift closer to the sump as flow rate was increased. Qualitatively, at least, it could be stated that the flow patterns were in agreement with those predicted by the CFD analyses.

**GSI-191: Separate Effects Characterization
of Debris Transport in Water**



Flow Straightener
Sheet Metal
15 pieces, 4'x1'
11 pieces, 3'x1'
6" slots 3" c/c

Fig. A-7. Diagram of the large-flume flow straightener.



Fig. A-8. Photograph of equipment for 'Configuration A' inlet flow conditioning.



Fig. A-9. Photograph of “Configuration B” inlet flow conditioning.

Configuration C: Immersed Pipe Flow Entry. The effect of inlet conditioning on debris transport characteristics also was examined using Configuration C. As in Configuration B, the flow-dampening pads were removed. However, in Configuration C, the inlet pipe was also extended so that the pipe exit was 1 ft from the flume floor. In addition, the diameter of the pipe exit was reduced from 10 in. to 6 in. The apparatus for Configuration C is shown in Fig. A-10.

Large-Flume Outlet Screening

A screen filtered the water flow leaving the large flume test section. The geometrical scaling of the screen should take into consideration the following factors:²⁰ (a) the screen should be smooth enough that the screen attachment velocity measured is representative of PWR plant conditions and (b) the screen sufficiently dampens the flow so that downstream geometrical configuration (e.g., drain design) does not significantly influence upstream flow patterns

This screen was constructed from commercially available screening material. The weave of this screen created diamond-shaped cells that were approximately ¼ in. wide by 1/8 in. high. This screen is shown in Fig. A-11. The screen was supported by a section of standard-use grating located directly behind the screen as shown in Fig. A-12. A secondary, fine-mesh screen covered the drain port to capture fine debris passing through the test section screen.

The head-loss pressure drop measurements across the screen arrangement at varying flow rates and curb arrangements showed that the head losses approximated those observed for the volunteer plant (e.g., 3 in. water at 0.75 ft/s).

²⁰ Note that features of the screen (e.g., clearance size) are immaterial to the experiments being conducted in this testing. Screen facial roughness is somewhat important because it influences debris detachment velocity. From that point of view, the screen selected resembles PWR screens very closely in that it offers a smooth surface with no observable dimples or other such geometrical features that may induce friction. The CFD simulations also indicated that the dampening provided by the screen arrangement was somewhat important for establishing prototypical flow patterns when curbs are present.



Fig. A-10. Photograph of 'Configuration C' inlet flow conditioning.

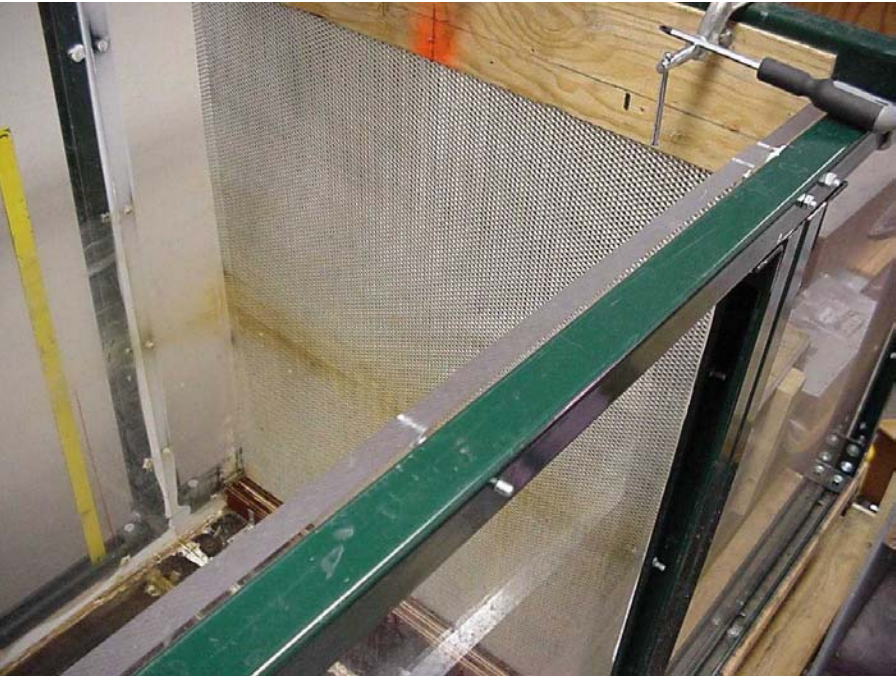


Fig. A-11. Test section exit screen.



Fig. A-12. Test section exit screen support.

Large-Flume Alternate Test Cross-Sections.

In selected tests, the test section of the large flume was modified to examine local transport phenomena. For example, obstructions were attached to the floor of some tests to block the transport of debris. Floor obstructions in the form of “curbs” were attached to the flume floor in selected tests to simulate curbs found in some PWRs. These curbs were placed just in front of the screen, were about 2 in. thick, and were either 2 in. or 6 in. high. Figure A-13 shows a typical curb in the standard test section, and Fig. A-14 shows a curb in the converging test section.

Large-Flume Pumping and Flow Control.

A variable speed (frequency) centrifugal pump capable of 2200 gal./min pumped water from the sump to overhead piping to the test apparatus. Water from the test apparatus drained back into the sump, which was located below the laboratory main floor. The piping to and from the pump was nominally 10 in. in diameter. The distribution piping consisted of sections of 10-in., 8-in., and/or 6-in. pipe, depending on test requirements. The pump and sections of the overhead piping are shown in Fig. A-15. An auxiliary 10-hp pump was also available to supply an auxiliary flow via a 4-in. flexible pipe.

The water flow through the flume was regulated primarily by motor-frequency adjustment. The overhead piping included a 10-in. butterfly valve that could be used to make finer adjustments to the flow. The drainage 12-in. pipe had a 12-in. butterfly valve that was used to regulate the water height in the flume. Thus, the apparatus allowed for independent variation of both the test section velocity and the water depth at any given flow rate.

The pumping system included an in-line flow meter located downstream of the pump in a 10-in. section of pipe. The accuracy of the in-line flow meter was verified for flows ranging from 100 to 600 gal./min by comparing meter readings with flow rates determined from flume filling times. The in-line meter is shown in Fig. A-16.

Calibration tests were conducted to determine the required pump flow needed to achieve a desired flume velocity at a specified water depth. The average flow velocity as a function of pump flow rate and flume height is shown in Fig. A-17 for two flume heights.



Fig. A-13. Test obstruction "curb" in standard test section.



Fig. A-14. Test obstruction "curb" in converging test section.



Fig. A-15. Large flume supply pump and overhead piping.



Fig. A-16. Large flume supply pump and in-line flow meter.

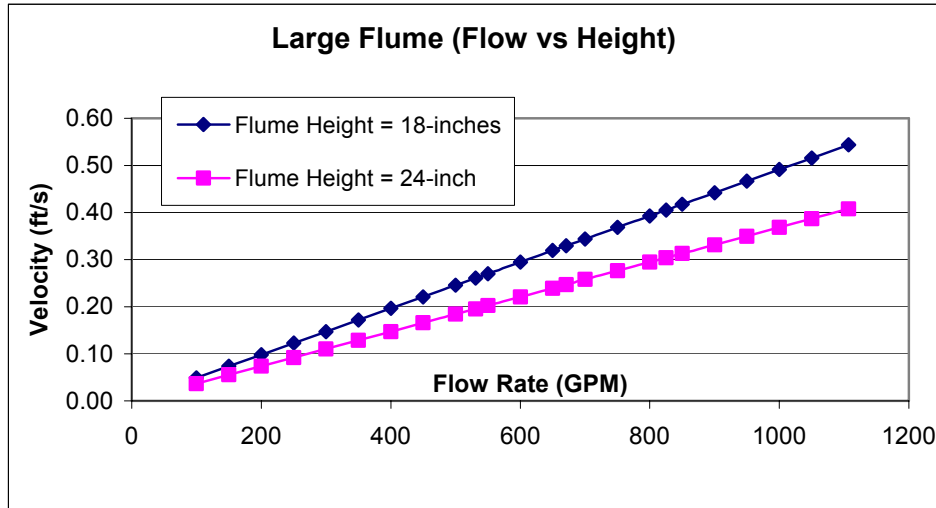


Fig. A-17. Large flume flow velocity vs volumetric flow rate.

A.3 Still-Water Test Apparatus

Tests of selected debris behavior in still water were conducted to augment the flume debris transport tests. These tests included the measurement of the terminal settling velocity in still water and the dissolution behavior of cal-sil insulation material. The effect of cal-sil in the water on the settling velocity of other debris also was investigated with this apparatus. Specifically, the test apparatus was designed to provide insights into the following aspects of debris transportability:

- How long does it take for the fibrous shreds to become fully saturated with water? Is that affected by water temperature?
- Do cal-sil, Marinite, or other such particulate insulations disintegrate in water? If so, how long does it take for the fragments to become dissolved in water? Is that affected by water temperature and/or turbulence?
- What is the terminal velocity of each debris type and size being tested in the flume? Does temperature or the height of water affect that?

This apparatus was used extensively during the exploratory phase (1) to evaluate the need for conducting transport testing at elevated temperatures and (2) to develop procedures for pretreating the insulation debris. During the parametric testing phase, the test apparatus was used primarily for debris characterization.

Settling Column

The terminal settling velocity measurements were performed by dropping pieces of pretreated²¹ debris of various types in a column of water and then timing their fall through a prescribed distance (10 to 30 in. below the water surface). The water column shown in Fig. A-18 was constructed of Plexiglas and was 10 in. in diameter and 34 in. in height. As confirmed by exploratory testing, the height of the settling column was sufficient to ensure that terminal velocity is reached before debris reaches the bottom half of the test apparatus.

A graduated metal tape was attached to the outside of the column. A small water heater adjacent to the water column was available to supply 80°C water to the column. Water can be removed from an outlet at the bottom of the cylinder. A stopwatch accurate to 0.01 s was used (note that human reflexes limited the accuracy to about 0.2 s).

²¹ The results of exploratory testing were used to develop the procedures used to pretreat the debris (e.g., duration and temperature of presoaking the debris). Refer to Sec. 2.2.1 for additional information.



Fig. A-18. Plexiglas water column used in terminal settling velocity measurements.

Dissolution Test Apparatus

The dissolution behavior of cal-sil, Marinite, and silicone foam insulation fragments in water was investigated by dropping precharacterized (mass and size measured) pieces into a large plastic cylinder (approximately 2 ft in diameter and 1.5 ft in height) filled with water to a height of 1 ft. Cal-sil that did not disintegrate into the water settled into the tray placed in the bottom of the cylinder. This apparatus is shown on Fig. A-19. Samples were weighed on scales accurate to 0.01 g.



Fig. A-19. Plastic cylinder used in dissolution tests.

**APPENDIX B
EXPLORATORY TEST DATA**

Table B.1. Terminal Velocity Measurements for 6-in. Nukon Fragments (at 80°C).

	Submergence Time: 5 min	Submergence Time: 30 min
Sample #1	0.41	0.33
Sample #2	0.41	0.41
Sample #3	0.33	0.41
Sample #4	0.41	0.41
Sample #5	0.41	0.41

Table B.2. Settling Velocity at Different Temperatures (After Pretreating in 80°C Water).

(a) 1-in. pieces

	80°C water	22°C water
Sample #1	0.14	0.13
Sample #2	0.16	0.16
Sample #3	0.13	0.15
Sample #4	0.15	0.16
Sample #5	0.15	0.14

(b) 6-in. pieces

	80°C water	22°C water
Sample #1	0.41	0.41
Sample #2	0.41	0.33
Sample #3	0.41	0.41
Sample #4	0.41	0.41
Sample #5	0.41	0.41

**GSI-191: Separate Effects Characterization
of Debris Transport in Water**

Table B.3(a). Effect of Immersion of Nukon Shreds in Cal-Sil Saturated Water (6 g/500 cm³).
Shred Size: 0.06–0.08 g pieces

Test	Measured Settling Velocity of Nukon Shreds (ft/s)		
	No Cal-Sil	6 gms Cal-Sil/500 cc	3 gms Cal-Sil/500 cc
1	0.13	0.17	0.12
2	0.16	0.15	0.16
3	0.15	0.11	0.18
4	0.16	0.15	0.17
5	0.14	0.16	0.16

Shred Size: 0.16–0.18 g pieces

Test	Measured Settling Velocity of Nukon Shreds (ft/s)		
	No Cal-Sil	6 gms Cal-Sil/500 cc	3 gms Cal-Sil/500 cc
1		0.18	0.23
2		0.20	0.21
3		0.19	0.15
4		0.14	0.23
5		0.17	0.17

Table B.3(b). Effect of Immersion of Aluminum RMI in Cal-Sil Saturated Water.

Test	Measured Settling Velocity (ft/s)	
	No Cal-Sil	With Cal-Sil
1	0.14	0.14
2	0.15	0.13
3	0.14	0.15
4	0.08	0.10
5	0.09	0.09
6	0.08	0.13
7	0.10	0.13
8	0.10	0.19
9	0.12	0.09
Average	0.11	0.12

**GSI-191: Separate Effects Characterization
of Debris Transport in Water**

Table B.4(a). Impact of Cal-Sil on Nukon Transport.
(Performed in the Large Flume)

Debris Type	Q (gal/min)	Height (in.)	Velocity (ft/s)	Observation			
Nukon treated in cal-sil	1000 (1000-1025 gpm) 49 Hz	24	0.40	<i>Debris rolled on the floor and reached the screen. They moved over the weir.</i>			
				Drop Test #	<u>Horz. Dist.</u>	<u>Time (s)</u>	<u>V_{set} (ft/s)</u>
				1	53"	16.2	0.13
				2	57"	15.9	0.13
				3	43"	12	0.17
				4	47"	14.2	0.15
5	57"	15.4	0.14				
Nukon in clean water	1000	24	0.40	<i>All pieces rolled to the screen. None got over the weir.</i>			
				Drop Test #	<u>Horz. Dist.</u>	<u>Time (s)</u>	<u>V_{set} (ft/s)</u>
				1	40"	11.7	0.18
				2	61"	18.7	0.11
				3	67"	15.1	0.13
				4	71"	16.3	0.13
5	51"	14.9	0.14				
Nukon treated in cal-sil	500 (490-515 gpm) 41 Hz	24	0.20	<i>All pieces rolled to the screen. None got over the weir.</i>			
				Drop Test #	<u>Horz. Dist.</u>	<u>Time (s)</u>	<u>V_{set} (ft/s)</u>
				1	27"	12.6	0.16
				2	34"	15.6	0.13
				3	28"	15.6	0.13
				4	26"	12.7	0.15
5	27"	13.5	0.15				
Nukon in clean water	500 (490-515 gpm) 41 Hz	24	0.20	<i>Debris rolled on the floor and reached the screen. They moved over the weir.</i>			
				Drop Test #	<u>Horz. Dist.</u>	<u>Time (s)</u>	<u>V_{set} (ft/s)</u>
				1	20"	12.5	0.17
				2	28"	14.2	0.15
				3	26"	12	0.17
				4	31"	13	0.16
5	32"	15.4	0.14				

**GSI-191: Separate Effects Characterization
of Debris Transport in Water**

Table B.4(b). Paint Chips Transport Data from Small Flume Tests.
Chips used ranged from 1/8 in. to 1 in. with few larger than 1 in.
Between 20 and 25 chips or 50 ml in volume were placed on the flume floor.

Run	Debris Types	Flume Velocity (ft/s)	Observation
1	Paint-Chips	0.10	No Movement
2		0.15	No Movement
3		0.20	No Movement
4		0.25	No Movement
5		0.30	Slight movement of particles
6		0.35	Still No movement (flutter)
7		0.40	1 Piece Moved
8		0.45	All Pieces started to move
9		0.50	All pieces moved immediately to screen.
Test Repeat			
10	Paint + Nukon	0.05	No transport/Movement
		0.10	Some fluttering (Nukon fines move)
		0.15	≈10% Nukon transport/No paint movement
		0.20	≈50-75% Nukon transport/ No paint movement
		0.25	100% Nukon transport/No paint movement
		0.45	Paint-chips move slowly; may go to screen
		0.50	All pieces reached screen instantaneously.

Table B.5. Variation of Floor Transport of Fiber Debris with Varying Height of Water.

Average Velocity (ft/s)	Small Flume 3 in. water height	Large flume 8 in.-12 in. water height	Large flume 18 in. water height
0.05	No transport	No transport	No transport
0.10	10% transport	No transport	No transport
0.15	50% transport	50%transport	50% transport
0.20	70% transport	80% transport	100% transport
0.25	95% transport	100% transport	

Table B.6. Comparison of Floor Transport with Plexiglas vs Plywood.

Avg. Velocity (ft/s)	Nukon On Plexiglas	Nukon On Plywood	Steel RMI On Plexiglas	Steel RMI On Plywood
0.10	No transport	No transport		
0.11	No transport	10% transport		
0.12	50% transport	10% transport		
0.16	80% transport	50% transport		
0.19	100% transport	100% transport	No transport	No transport
0.25			10% transport	25% transport
0.28			20% transport	25% transport
0.30			60% transport	50% transport
0.37			100% transport	100% transport

Table B.7(a). Calibration of Water Balloon Velocity Measurements.

Velocity of Balloon (ft/s)	Average velocity from Q (ft/s)
0.13	0.15
0.22	0.21
0.19	0.20

Table B.7(b). Velocity Measurements after the Placement of Diffusers.

Location	V (ft/s)	V (ft/s)
Top Surface	0.50	0.57
Middle	0.44	0.50
Bottom	0.41	0.48
$V_{avg}(Q)$	0.42	0.54

**GSI-191: Separate Effects Characterization
of Debris Transport in Water**

Table B.8. Incipient Movement of Nukon and Steel RMI from 5 Separate Tests.

Test #1			
Flow Rate (gpm)	Velocity (ft/s)	SS RMI	Nukon
146	0.07	No movement	No movement
184	0.09	No movement	No movement
217	0.11	No movement	No movement
250	0.12	No movement	Slight movement
325	0.16	No movement	
391	0.19	No movement	
464	0.23	No movement	
509	0.25	Slight movement	

Test #2			
Flow Rate (gpm)	Velocity (ft/s)	SS RMI	Nukon
217	0.11	No movement	No movement
250	0.12	No movement	Slight movement
325	0.16	No movement	
391	0.19	No movement	
464	0.23	1 out of 3 pieces moved 2–4 in. over 5 min	

Test #3			
Flow Rate (gpm)	Velocity (ft/s)	SS RMI	Nukon
217	0.11	No movement	~3% moved when settling pipe was removed. Not to screen.
250	0.12	No movement	Small pieces and loose clumps move
325	0.16	No movement	
391	0.19	No movement	
464	0.23	Slight movement	
509	0.25	Movement	

Test #4			
Flow Rate (gpm)	Velocity (ft/s)	SS RMI	Nukon
217	0.11	No Movement	No Movement
250	0.12	No Movement	~5% moves
391	0.19	No Movement	~80% moves
464	0.23	Both pieces moved 2–4 in. over 5 min.	
509	0.25	Moved nearly to screen in 5 min.	

Test #5			
Flow Rate (gpm)	Velocity (ft/s)	SS RMI	Nukon
217	0.11	No Movement	No Movement
250	0.12	1/2 of pieces moved ~2 in	<5% moves
391	0.19	The same piece that moved at 391 gpm went another 8–10 in.	All Nukon travels to screen
464	0.23	No Movement	
509	0.25	No Movement	
573	0.28	The same piece that moved at 391 gpm went another ~5 in.	
612	0.30	All begins to move	

APPENDIX C TEST DATA

C.1 Low-Density Fiberglass

C.1.1 Nukon Test Measurements

Settling velocity measurements made for three sizes (1 in., 4 in., and 6 in.) of fragments of Nukon fiber are listed in Table C.1. The average settling velocity obtained for each size was calculated.

Incipient and bulk tumbling velocities were measured in the large flume with all three methods of inlet flow conditioning. Results are listed in Table C.2. Velocities required to lift Nukon fragments above a 2-in. and a 6-in. curb also were measured as shown in Table C.3.

Drop tests were conducted according to the procedure described in Appendix D. Results are shown in Table C.4 for each method of inlet flow conditioning. The horizontal distance measured for Configuration A is compared with the theoretical distance (i.e., average flow velocity times the time-of-fall).

Table C.1. Nukon Settling Velocity (ft/s).

	6 in. pieces	4 in. pieces	1 in. pieces
Sample #1	0.41	0.41	0.13
Sample #2	0.41	0.33	0.16
Sample #3	0.41	0.41	0.15
Sample #4	0.41	0.41	0.16
Sample #5	0.41	0.41	0.14
Ave. vel (ft/s)	0.41	0.40	0.15

Table C.2. Floor Transport of Nukon.

Inlet Flow Conditioning: Configuration A

Type of Insulation	Velocity (ft/s)	Observation
Nukon	0.11	No movement
Nukon	0.12	10–50% moves in different tests
Nukon	0.16	80% moves
Nukon	0.19	100% moves

Inlet Flow Conditioning: Configuration B

Type of Insulation	Velocity (ft/s)	Observation
Nukon	0.06	No movement
Nukon	0.07	50% moves
Nukon	0.09	100% moves
Nukon	0.11	No further testing

Inlet Flow Conditioning: Configuration C

Type of Insulation	Velocity (ft/s)	Observation
Nukon	0.06	0–10% movement in different tests
Nukon	0.07	10–20% moves in different tests
Nukon	0.10	80% moves
Nukon	0.11	100% moves

Table C.3. Lift at Curbs – Nukon.

Inlet Flow Conditioning: Configuration A

Type of Insulation	Velocity (ft/s)	2 in. Curb	6 in. Curb
Nukon	0.22	Stayed at the curb	Stayed at the curb
Nukon	0.25	Some jumped over	Stayed at the curb
Nukon	0.28	No further testing	<5% jumped over (very small pieces)
Nukon	0.34	No further testing	20–30% over curb
Nukon	0.37	No further testing	100% over curb

Inlet Flow Conditioning: Configuration B

Type of Insulation	Velocity (ft/s)	2 in. Curb	6 in. Curb
Nukon	0.19	Stayed at the curb	Stayed at the curb
Nukon	0.25	Small pieces jumped over Most moved upstream	Small pieces jumped over Most moved upstream
Nukon	0.28	No further testing	No further testing

Inlet Flow Conditioning: Configuration C

Type of Insulation	Velocity (ft/s)	2 in. Curb	6 in. Curb
Nukon	0.19	Stayed at the curb	Stayed at the curb
Nukon	0.22	Small pieces jumped over	Stayed at the curb
Nukon	0.25	No further testing	Stayed at the curb
Nukon	0.28	No further testing	Small pieces jumped over

**GSI-191: Separate Effects Characterization
of Debris Transport in Water**

Table C.4. Drop Test of Nukon.

Inlet flow conditioning: Configuration A

Q (gal/min)	Velocity (ft/s)	Water Height (in.)	Horizontal Distance (in.)	Time (s)	Theoretical Distance (in.)
490	0.23	19	19.0	8.1	22.3
			19.0	N/A*	N/A
			18.5	7.5	20.7
			18.0	8.2	22.6
			18.0	N/A	N/A
			19.0	6.8	18.8
531	0.24	19.75	20.75	8.9	25.6
			20.0	8.3	23.9
679	0.33	18	23.75	6.8	26.9
			21.5	7.0	27.7
			24.0	9.0	35.6
			27.0	8.0	31.7
			20.0	5.9	23.4
820	0.37	19.5	36.0	5.7	25.3
			60	8.8	39.1
			41	6.9	30.6
			22	7.5	7.5
			20	6.8	6.8
			15	5.5	5.5
1107	49	19.25	35	8.2	8.2
			37	8.0	8.0
			36	8.2	8.2

Inlet flow conditioning: Configuration B

	Trial 1		Trial 2		Trial 3		Trial 4		Trial 5	
Vel. (ft/s)	Time (s)	Dist. (in.)								
0.15	11	15	6	29	8	26	5	20	6	18
0.22	25	34	5	23	5	16	10	10	6	26
0.27	11	35	7	33	7	29	7	16	18	40
0.36	9	31	7	15	5	28	8	45	13	12
0.42	13	58	11	26	15	34	9	40	5	1

Inlet flow conditioning: Configuration C

	Trial 1		Trial 2		Trial 3		Trial 4		Trial 5	
Vel. (ft/s)	Time (s)	Dist. (in.)								
0.31	6.8	35	12.1	75	10.9	78	36.3	*	10.6	79
0.33	5.1	31	11.6	55	19.5	*	7.1	29	13.7	71
0.45	13.1	40	20	*	10.4	55	15.9	*	12.5	*
0.54	13.3	*	17.6	*	4.2	21	12.1	28	18.5	82
0.57	4.8	29	11.8	*	13.8	*	6.4	40	14.4	*

* Measurement not taken.

C.1.2 Thermal-Wrap Test Measurements

Results of the settling velocity tests are presented in Table C.5 for two characteristic sizes of shredded Thermal-Wrap fragments (1 in. x 1 in. and 2 in. x 2.5 in.). Two sizes (or clumps) of shredded fibers were examined to determine the extent to which settling velocity is sensitive to this variable. The average settling velocity obtained for each size is calculated.

Incipient and bulk tumbling velocities were measured in the large flume with all three methods of inlet flow conditioning. Results are listed in Table C.6. Velocities required to lift Thermal-Wrap fragments above a 2-in. and a 6-in. curb also were measured as shown in Table C.7.

Drop test results are shown in Table C.8 for Configurations B and C of inlet flow conditioning. Tests were not performed for Configuration A.

Table C.5. Thermal-Wrap Settling Velocity.

Thermal Wrap (1 in. x 1 in. clumps)			Thermal Wrap 2 in. x 2.5 in. (clumps)		
No.	18 in.	0 in.	No.	18 in.	0 in.
1	NA	13.47	1	5.97	14.59
2	6.78	14.37	2	7.91	17.19
3	7.06	17.56	3	7.72	19.88
4	6.97	15.78	4	NA	23.41
5	4.91	12.56	5	6.97	11.25
6	6.84	19.22	6	11.04	26.06
7	6.53	16.12	7	5.88	12.69
8	5.6	17.36	8	10.56	29.37
9	NA	NA	9	9.37	28.16
10	NA	NA	10	NA	16.65
Ave. Velocity (ft/s) =		0.16	Ave. Velocity (ft/s) =		0.13

(The terminal velocity of the five 1 ft x 1 ft x 4 in. pillows was determined to be 0.25 to 0.54 ft/s.)

Table C.6. Floor Transport of Thermal-Wrap.

Inlet flow conditioning: Configuration A

Type of Insulation	Velocity (ft/s)	Observation
Thermal-wrap fragments	0.11	No movement
Thermal-wrap 4 in. x 6 in.	0.11	No movement
Thermal-wrap fragments	0.12	No movement
Thermal-wrap 4 in. x 6 in.	0.12	50% moves
Thermal-wrap fragments	0.16	Some movement
Thermal-wrap 4 in. x 6 in.	0.16	50% moves
Thermal-wrap fragments	0.19	100% moves
Thermal-wrap 4 in. x 6 in.	0.19	100% moves

Inlet flow conditioning: Configuration B

Type of Insulation	Velocity (ft/s)	Observation
Thermal-wrap fragments	0.06	No movement
Thermal-wrap 4 in. x 6 in.	0.06	No movement
Thermal-wrap fragments	0.07	Some movement
Thermal-wrap 4 in. x 6 in.	0.07	No movement
Thermal-wrap fragments	0.11	100% moves
Thermal-wrap 4 in. x 6 in.	0.11	No movement
Thermal-wrap fragments	0.19	No further testing
Thermal-wrap 4 in. x 6 in.	0.19	Some movement
Thermal-wrap fragments	0.23	No further testing
Thermal-wrap 4 in. x 6 in.	0.23	100% moves

Inlet flow conditioning: Configuration C

Type of Insulation	Velocity (ft/s)	Observation
Thermal-wrap fragments	0.06	No movement
Thermal-wrap 4 in. x 6 in.	0.06	No movement
Thermal-wrap fragments	0.10	Some movement
Thermal-wrap 4 in. x 6 in.	0.10	Some movement
Thermal-wrap fragments	0.11	100% movement
Thermal-wrap 4 in. x 6 in.	0.11	No movement
Thermal-wrap fragments	0.17	50% moves
Thermal-wrap 4 in. x 6 in.	0.17	Some movement
Thermal-wrap fragments	0.20	100% moves
Thermal-wrap 4 in. x 6 in.	0.20	100% moves

Table C.7. Lift-at-Curbs for Thermal-Wrap.

Inlet flow conditioning: Configuration A

Type of Insulation	Velocity (ft/s)	2-in. Curb	6-in. Curb
Thermal Wrap fragments	0.22	Stayed at the curb	Stayed at the curb
Thermal Wrap 4 in. x 6 in.	0.22	Stayed at the curb	Stayed at the curb
Thermal Wrap fragments	0.25	Jumped over the curb	Stayed at the curb
Thermal Wrap 4 in. x 6 in.	0.25	Jumped over the curb	Stayed at the curb
Thermal Wrap fragments	0.28	No further testing	Some jumped over
Thermal Wrap 4 in. x 6 in.	0.28	No further testing	Stayed at the curb
Thermal Wrap fragments	0.30	No further testing	Some jumped over
Thermal Wrap 4 in. x 6 in.	0.30	No further testing	Some jumped over

Inlet flow conditioning: Configuration B

Type of Insulation	Velocity (ft/s)	2-in. Curb	6-in. Curb
Thermal Wrap fragments	0.19	Stayed at the curb	Stayed at the curb
Thermal Wrap 4 in. x 6 in.	0.19	Stayed at the curb	Stayed at the curb
Thermal Wrap fragments	0.25	Small fragments jumped over Most moved upstream	Moved upstream
Thermal Wrap 4 in. x 6 in.	0.25	Stayed at the curb	Moved upstream
Thermal Wrap fragments	0.28	No further testing	No further testing
Thermal Wrap 4 in. x 6 in.	0.28	Moved upstream	No further testing
Thermal Wrap fragments	0.30	No further testing	No further testing
Thermal Wrap 4 in. x 6 in.	0.30	No further testing	No further testing

Inlet flow conditioning: Configuration C

Type of Insulation	Velocity (ft/s)	2-in. Curb	6-in. Curb
Thermal Wrap fragments	0.20	Stayed at the curb	Stayed at the curb
Thermal Wrap 4 in. x 6 in.	0.20	Stayed at the curb	Stayed at the curb
Thermal Wrap fragments	0.22	Small fragments moved over	Stayed at the curb
Thermal Wrap 4 in. x 6 in.	0.22	Moved over	Stayed at the curb
Thermal Wrap fragments	0.28	No further testing	Stayed at the curb
Thermal Wrap 4 in. x 6 in.	0.28	No further testing	Stayed at the curb
Thermal Wrap fragments	0.30	No further testing	Moved over
Thermal Wrap 4 in. x 6 in.	0.30	No further testing	Moved over

Table C.8. Drop Tests with Thermal-Wrap Debris.

Inlet flow conditioning: Configuration B

	Trial 1		Trial 2		Trial 3		Trial 4		Trial 5	
Vel. (ft/s)	Time (s)	Dist. (in.)								
0.15	8	29	8	23	10	29	9	29	11	12
0.22	8	21	5	8	9	27	7	18	8	16
0.27	15	67	16	24	10	28	8	-10	28	80
0.36	8	35	10	68	6	15	5	6	14	58
0.42	18	66	10	45	14	75	3	2	8	44

Inlet flow conditioning: Configuration C

	Trial 1		Trial 2		Trial 3		Trial 4		Trial 5	
Vel. (ft/s)	Time (s)	Dist. (in.)								
0.31	10.4	31	10.4	58	18.0	88	8.7	46	25.2	29
0.33	9.6	28	15.7	77	21.7	79	7.6	36	17.9	91
0.45	4.9	61	7.0	19	10.3	*	17.4	-9	11.9	*
0.54	5.0	35	13.5	71	12.1	*	10.3	38	14.6	92
0.57	12.4	*	8.8	45	13.0	91	17.6	*	13.8	90

C.1.3 Kaowool Test Measurements

Measured settling velocities of shredded Kaowool material are listed in Table C.9. The average settling velocity was calculated.

Incipient and bulk tumbling velocities of the shredded material were measured in the large flume with all three methods of inlet flow conditioning. The results are listed in Table C.10. Velocities required to lift Thermal-Wrap fragments above a 2-in. and a 6-in. curb also were measured as shown in Table C.11.

Drop tests were conducted according to the procedure described in Appendix C. Results are shown in Table C.12 for Configurations B and C of inlet flow conditioning. Tests were not performed for Configuration A.

Table C.9. Kaowool Settling Velocity.

Test #	Velocity (ft/s)
1	0.15
2	0.19
3	0.25
4	0.23
5	0.19
6	0.19
7	0.19
8	0.30
9	0.19
10	0.22
Ave. Vel (ft/s)	0.21

Table C.10. Floor Transport of Kaowool.

Inlet flow conditioning: Configuration A

Type of Insulation	Velocity (ft/s)	Observation
Kaowool pieces	0.11	No movement
Kaowool 4 in. x 6 in.	0.11	No movement
Kaowool pieces	0.12	No movement
Kaowool 4 in. x 6 in.	0.12	50% moves
Kaowool pieces	0.16	Some movement
Kaowool 4 in. x 6 in.	0.16	50% moves
Kaowool pieces	0.19	50% moves
Kaowool 4 in. x 6 in.	0.19	50% moves

Inlet flow conditioning: Configuration B

Type of Insulation	Velocity (ft/s)	Observation
Kaowool fragments	0.07	No movement
Kaowool 4 in. x 6 in.	0.07	No movement
Kaowool fragments	0.09	Some movement
Kaowool 4 in. x 6 in.	0.09	No movement
Kaowool fragments	0.11	No further testing
Kaowool 4 in. x 6 in.	0.11	No movement
Kaowool fragments	0.23	No further testing
Kaowool 4 in. x 6 in.	0.23	no movement
Kaowool fragments	0.25	No further testing
Kaowool 4 in. x 6 in.	0.25	Moves to screen

Inlet flow conditioning: Configuration C

Type of Insulation	Velocity (ft/s)	Observation
Kaowool fragments	0.10	No movement
Kaowool 4 in. x 6 in.	0.10	No movement
Kaowool fragments	0.17	Some movement
Kaowool 4 in. x 6 in.	0.17	Some movement
Kaowool fragments	0.20	50% movement
Kaowool 4 in. x 6 in.	0.20	Some movement
Kaowool fragments	0.22	100% moves
Kaowool 4 in. x 6 in.	0.22	100% moves

**GSI-191: Separate Effects Characterization
of Debris Transport in Water**

Table C.11. Lift-at-Curbs Velocity - Kaowool

Inlet flow conditioning: Configuration A

Type of Insulation	Velocity (ft/s)	2-in. Curb	6-in. Curb
Kaowool fragments	0.22	Stayed at the curb	Stayed at the curb
Kaowool 4 in. x 6 in.	0.22	Stayed at the curb	Stayed at the curb
Kaowool fragments	0.25	Stayed at the curb	Stayed at the curb
Kaowool 4 in. x 6 in.	0.25	Jumped over the curb	Stayed at the curb
Kaowool fragments	0.28	Stayed at the curb	Stayed at the curb
Kaowool 4 in. x 6 in.	0.28	No further testing	Stayed at the curb
Kaowool fragments	0.30	Jumped over the curb	Stayed at the curb
Kaowool 4 in. x 6 in.	0.30	No further testing	Stayed at the curb
Kaowool fragments	0.37	No further testing	Stayed at the curb
Kaowool 4 in. x 6 in.	0.37	No further testing	Stayed at the curb
Kaowool fragments	0.41	No further testing	50% moved over
Kaowool 4 in. x 6 in.	0.41	No further testing	Stayed at the curb
Kaowool fragments	0.43	No further testing	No further testing
Kaowool 4 in. x 6 in.	0.43	No further testing	Stayed at the curb
Kaowool fragments	0.47	No further testing	No further testing
Kaowool 4 in. x 6 in.	0.47	No further testing	Moved over curb

Inlet flow conditioning: Configuration B

Type of Insulation	Velocity (ft/s)	2-in. Curb	6-in. Curb
Kaowool fragments	0.19	Stayed at the curb	Stayed at the curb
Kaowool 4 in. x 6 in.	0.19	Stayed at the curb	Stayed at the curb
Kaowool fragments	0.25	Small pieces jumped over Most moved upstream	Moved upstream
Kaowool 4 in. x 6 in.	0.25	Stayed at the curb	Moved upstream
Kaowool fragments	0.28	No further testing	No further testing
Kaowool 4 in. x 6 in.	0.28	Moved upstream	No further testing
Kaowool fragments	0.30	No further testing	No further testing
Kaowool 4 in. x 6 in.	0.30	No further testing	No further testing

Inlet flow conditioning: Configuration C

Type of Insulation	Velocity (ft/s)	2-in. Curb	6-in. Curb
Kaowool fragments	0.24	Stayed at the curb	Stayed at the curb
Kaowool 4 in. x 6 in.	0.24	Stayed at the curb	Stayed at the curb
Kaowool fragments	0.28	Small pieces moved over	Stayed at the curb
Kaowool 4 in. x 6 in.	0.28	Stayed at the curb	Stayed at the curb
Kaowool fragments	0.30	No further testing	Stayed at the curb
Kaowool 4 in. x 6 in.	0.30	Moved over	Stayed at the curb
Kaowool fragments	0.32	No further testing	Moved over
Kaowool 4 in. x 6 in.	0.32	No further testing	Stayed at the curb
Kaowool fragments	0.34	No further testing	No further testing
Kaowool 4 in. x 6 in.	0.34	No further testing	Stayed at the curb
Kaowool fragments	0.39	No further testing	No further testing
Kaowool 4 in. x 6 in.	0.39	No further testing	Moved over

Table C.12. Kaowool Drop Tests.

Inlet flow conditioning: Configuration B

	Trial 1		Trial 2		Trial 3		Trial 4		Trial 5	
Vel. (ft/s)	Time (s)	Dist. (s)								
0.15	5	17	6	20	8	4	4	14	6	15
0.22	4	19	5	13	7	17	4	9	7	7
0.27	6	6	5	17	5	3	8	16	7	-16
0.36	5	6	6	-10	7	-15	7	26	6	23
0.42	4	12	5	34	4	0	16	49	19	43

Inlet flow conditioning: Configuration C

	Trial 1		Trial 2		Trial 3		Trial 4		Trial 5	
Vel. (ft/s)	Time (s)	Dist. (s)								
0.31	7.8	36	5.9	36	6.8	47	7.3	42	5.6	26
0.33	4.3	33	3.2	16	8.3	45	5.1	22	10.5	59
0.45	10.3	87	12.3	90	3.0	42	7.0	51	8.2	70
0.54	17.2	89	4.2	33	5.6	46	6.0	56	4.5	14
0.57	4.7	59	12.7	91	5.4	49	7.7	73	41	25

C.2 Reflective Metal Insulation (RMI)

C.2.1 Aluminum RMI Test Measurements

The settling and tumbling characteristics of the aluminum RMI fragments are given in Tables C.13(a) and C.13(b), respectively.

Drop tests were conducted in the large flume according to the procedures described in Appendix D. The distance that each piece traveled before hitting the floor was recorded. In Table C.14, this measured distance has been compared with the distance calculated using classical expressions for particle trajectory [distance traveled = (average flow velocity x height of flow)/settling velocity]. Measured transport distances are quite close to calculated values for the flat and semi-crumpled RMI debris but differ substantially for crumpled debris.

**GSI-191: Separate Effects Characterization
of Debris Transport in Water**

Table C.13(a). Terminal Velocity Measurements for Al-RMI Fragments.

Run	Sample Shape	Drop Distance (in.)	Time (s)	Terminal Velocity (ft/s)
1	Flat (2-in. square)	20	12	0.14
2	Flat (2-in. square)	20	11	0.15
3	Flat (2-in. square)	20	12	0.14
4	Crumpled (2-in. square)	20	20	0.08
5	Crumpled (2-in. square)	20	19	0.09
6	Crumpled (2-in. square)	20	21	0.08
7	Semi-Crumpled (2-in. square)	20	16	0.10
8	Semi-Crumpled (2-in. square)	20	17	0.10
9	Semi-Crumpled (2-in. square)	20	14	0.12
Median Terminal Velocity (measured)				0.11 ft/s

Table C.13(b). Aluminum RMI Transport Data from Small Flume Tests (11/1999).
75 fragments consisting of flat, crumpled, semi-crumpled were placed on the flume floor.

Run	Debris Types	Flume Velocity (ft/s)	Observation
1	Aluminum RMI	0.05	No movement
2		0.10	No movement.
3		0.15	One piece out of approximately 25 transported. This also moved only few inches.
4		0.20	Several pieces traveled on the flume floor. Most of these pieces tended to be crumpled with large projected area facing the flow. Movement is sliding.
5		0.25	Almost all the pieces traveled to the screen. Few very flat pieces (3 out of 25) did not move.
6		0.30	All debris transported.
7		0.35	Another 25 pieces were added and all 25 pieces made it to the screen. Debris accumulated preferentially on the floor. But with arrival of newer debris the fragments moved upwards.

Table C.14. Drop Tests on Aluminum RMI with Inlet Flow Configuration A.

Type of Al RMI	Measured Distance (in.)	Calculated Distance (in.)
Crumpled	10–16	24–30
Semi Crumpled	16–28	17–21
Flat	15–20	14–15

C.2.2 Stainless-Steel RMI Test Measurements

Settling velocity tests were performed in a cylindrical tank filled with 30 in. of room-temperature water. Table C.15 lists the measured time (in seconds) that the debris took to travel from the initial height of 30 in. to a height of 18 in. (the height of water in the large flume), and from 30 in. to the bottom of the tank (0 in.). Two stopwatches were used to take these readings. The average settling velocity obtained for the various types of material is shown at the bottom of each table.

Incipient and bulk tumbling velocities were measured in the large flume with all three methods of inlet flow conditioning. Results are listed in Table C.16. Velocities required to lift SS RMI foils above a 2-in. and a 6-in. curb also were measured as shown in Table C.17.

Drop tests were performed with both sizes of SS RMI foil. The time required for foils to settle to the flume floor and the corresponding horizontal distance traveled were recorded as listed in Table C.18a and Table C.18b. Results in Table 3.18a were obtained using inlet flow conditioning Configuration B; results in Table C.18b were collected using Configuration C. No measurements were made with Configuration A.

Table C.15. SS RMI Settling Velocity.

Steel 1/2 in. x 1/2 in. semi-crumpled		
No.	18 in.	0 in.
1	NA	8.16
2	NA	9.25
3	2.97	8.00
4	3.29	8.15
5	4.06	10.91
6	2.50	7.50
7	2.75	7.84
8	NA	5.47
9	2.30	6.18
10	NA	6.53
Ave. Velocity (ft/s) =		0.32

Steel 1/2 in. x 1/2 in. crumpled		
No.	18 in.	0 in.
1	1.68	5.28
2	2.41	6.22
3	air bubble	
4	NA	6.32
5	NA	4.60
6	NA	7.62
7	1.97	6.10
8	2.19	6.53
9	1.87	5.87
10	2.69	6.75
Ave. Velocity (ft/s) =		0.41

Steel 2 in. x 2 in. semi-crumpled		
No.	18 in.	0 in.
1	1.90	5.46
2	2.21	5.78
3	NA	5.13
4	2.53	6.47
5	2.38	6.56
Ave. Velocity (ft/s) =		0.43

Steel 2 in. x 2 in. crumpled		
No.	18 in.	0 in.
1	1.84	4.28
2	1.59	4.65
3	1.66	4.44
4	1.53	NA
5	2.25	5.34
Ave. Velocity (ft/s) =		0.53

**GSI-191: Separate Effects Characterization
of Debris Transport in Water**

Table C.16. Floor Transport of SS RMI.

Inlet Flow Conditioning: Configuration A

5.1.1.1.1.1.1	Type of Insulation	Velocity (ft/s)	Observation
	SS RMI ½ in. x ½ in.	0.19	No movement
	SS RMI 2 in. x 2 in.	0.19	No movement
	SS RMI ½ in. x ½ in.	0.23	No movement
	SS RMI 2 in. x 2 in.	0.23	No movement
	SS RMI ½ in. x ½ in.	0.28	20% moves
	SS RMI 2 in. x 2 in.	0.28	20% moves
	SS RMI ½ in. x ½ in.	0.30	>50% moves
	SS RMI 2 in. x 2 in.	0.30	>50% moves
	SS RMI ½ in. x ½ in.	0.37	No further testing
	SS RMI 2 in. x 2 in.	0.37	No further testing
	SS RMI ½ in. x ½ in.	0.41	No further testing
	SS RMI 2 in. x 2 in.	0.41	No further testing

Inlet Flow Conditioning: Configuration B

Type of Insulation	Velocity (ft/s)	Observation
SS RMI ½ in. x ½ in.	0.23	No movement
SS RMI 2 in. x 2 in.	0.23	No movement
SS RMI ½ in. x ½ in.	0.28	No movement
SS RMI 2 in. x 2 in.	0.28	Moves a little
SS RMI ½ in. x ½ in.	0.30	No movement
SS RMI 2 in. x 2 in.	0.30	No movement
SS RMI ½ in. x ½ in.	0.37	No movement
SS RMI 2 in. x 2 in.	0.37	Moves to screen
SS RMI ½ in. x ½ in.	0.41	Moves to screen
SS RMI 2 in. x 2 in.	0.41	No further testing

Inlet Flow Conditioning: Configuration C

Type of Insulation	Velocity (ft/s)	Observation
SS RMI ½ in. x ½ in.	0.10	No movement
SS RMI 2 in. x 2 in.	0.10	No movement
SS RMI ½ in. x ½ in.	0.17	No movement
SS RMI 2 in. x 2 in.	0.17	No movement
SS RMI ½ in. x ½ in.	0.20	1/3 moves
SS RMI 2 in. x 2 in.	0.20	Scattered in flume
SS RMI ½ in. x ½ in.	0.22	Moves to screen
SS RMI 2 in. x 2 in.	0.22	Moves to screen
SS RMI ½ in. x ½ in.	0.25	No further testing
SS RMI 2 in. x 2 in.	0.25	No further testing

Table C.17. SS RMI Lift-at-Curb Velocity.

Inlet Flow Conditioning: Configuration A

Type of Insulation	Velocity (ft/s)	2-in. Curb	6-in. Curb
SS RMI	0.77	Stayed at the curb	Stayed at the curb
SS RMI	0.81	Stayed at the curb	Stayed at the curb
SS RMI	0.84	Some jumped over	Stayed at the curb
SS RMI	0.90	Most jumped over	Stayed at the curb
SS RMI	0.99	All jumped over	Stayed at the curb

Inlet Flow Conditioning: Configuration B

Type of Insulation	Velocity (ft/s)	2-in. Curb	6-in. Curb
SS RMI	0.12	Stayed at the curb	Stayed at the curb
SS RMI	0.19	Stayed at the curb	Stayed at the curb
SS RMI	0.25	Some pieces moved upstream. None jumped over the curb	Some ½-in. pieces moved upstream. None jumped over the curb
SS RMI	0.28	Most pieces moved upstream. None jumped over the curb	Most pieces moved upstream. None jumped over the curb
SS RMI	0.30	All jumped upstream	All moved upstream

Inlet Flow Conditioning: Configuration C

Type of Insulation	Velocity (ft/s)	2-in. Curb	6-in. Curb
SS RMI	0.50	Stayed at the curb	Stayed at the curb
SS RMI	0.73	Stayed at the curb	Stayed at the curb
SS RMI	1.0	Half of the 2-in. pieces jumped over. All ½-in. pieces stayed at the curb	Stayed at the curb

**GSI-191: Separate Effects Characterization
of Debris Transport in Water**

Table C.18a. SS RMI Drop Tests: Inlet Flow Conditioning Configuration B.

1/2 in. x 1/2 in. SS RMI

Vel. (ft/s)	Trial 1		Trial 2		Trial 3		Trial 4		Trial 5	
	Time (s)	Dist. (in.)								
0.15	3	1	4	10	6	17	5.4	16	5	17
0.22	9	-6	6	6	6	7	5	2	5	9
0.27	4	2	8	4	3	20	4	7	5	6
0.36	5	-10	4	15	3	21	5	16	5	15
0.42	3	3	3	7	7	21	5	14	6	11

2 in. x 2 in. SS RMI

Vel. (ft/s)	Trial 1		Trial 2		Trial 3		Trial 4		Trial 5	
	Time (s)	Dist. (in.)								
0.15	4	12	2.35	6	5	7	4.4	18	4.6	12
0.22	4	22	5	3	3	2	4	2	4	3
0.27	4	-6	4	12	5	6	4	-8	3	2
0.36	5	-10	4	15	3	21	5	16	5	15
0.42	4	7	12	50	7	15	3	5	8	-9

Table C.18b. SS RMI Drop Tests: Inlet Flow Conditioning Configuration C.

1/2 in. x 1/2 in. SS RMI

Vel. (ft/s)	Trial 1		Trial 2		Trial 3		Trial 4		Trial 5	
	Time (s)	Dist. (in.)								
0.31	5.8	47	6.2	36	7.5	51	4.8	23	7.8	46
0.33	5.0	43	5.0	6	5.1	16	9.0	78	7.4	69
0.45	6.5	62	4.1	39	3.2	31	7.3	84	7.7	77
0.54	7.4	57	4.4	33	5.3	29	6.0	71	7.0	66
0.57	4.9	46	6.6	68	3.4	29	5.5	44	3.7	30

2 in. x 2 in. SS RMI

Vel. (ft/s)	Trial 1		Trial 2		Trial 3		Trial 4		Trial 5	
	Time (s)	Dist. (in.)								
0.31	3.7	21	5.8	43	4.9	30	3.6	23	10.1	81
0.33	4.1	7	5.2	45	4.9	23	5.6	44	4.9	45
0.45	1.3	15	3.6	42	4.4	50	4.5	34	8.8	82
0.54	4.6	24	4.3	16	3.8	40	4.5	35	3.2	30
0.57	8.3	57	5.5	26	2.7	28	9.3	63	4.6	32

C.3 Cal-Sil Test Measurements

Table C.19(a). Cal-Sil Transport Data from Small-Flume Tests (11/1999).
Between 5–10 chunks (each about 1in. in size) were placed on the flume floor.

Run	Debris Types	Flume Velocity (ft/s)	Observation
1	Cal-Sil	0.05	No movement
2		0.10	No movement. Dust and fibers detached.
3		0.15	No movement. Dust and fibers move away
4		0.20	Slight movement
5		0.25	Slight movement of smaller chunks. Not significant movement.
6		0.30	Larger pieces are ready to move. But very hesitant. Movement can 'start' and 'stop.' Appears as though this is the threshold for bigger chunks.
7		0.35	All debris moved to the screen.

Table C.19(b). Cal-Sil Saturated Nukon Transport Data from Large-Flume Tests.

Debris Type	Q (gal/min)	Height (in.)	Velocity (ft/s)	Observation			
Nukon and cal-sil	1000 (1000-1025 gpm) 49 Hz	24	0.40	<i>Debris rolled on the floor and reached the screen. They moved over the curb.</i>			
				Drop Test #	<u>Horz. Dist.</u>	<u>Time (s)</u>	<u>V_{set} (ft/s)</u>
				1	53 in.	16.2	0.13
				2	57 in.	15.9	0.13
				3	43 in.	12.0	0.17
				4	47 in.	14.2	0.15
Nukon	1000	24	0.40	<i>All pieces rolled to the screen. None got over the curb.</i>			
				Drop Test #	<u>Horz. Dist.</u>	<u>Time (s)</u>	<u>V_{set} (ft/s)</u>
				1	40 in.	11.7	0.18
				2	61 in.	18.7	0.11
				3	67 in.	15.1	0.13
				4	71 in.	16.3	0.13
Nukon and cal-sil	500 (490-515 gpm) 41 Hz	24	0.20	<i>All pieces rolled to the screen. None got over the curb.</i>			
				Drop Test #	<u>Horz. Dist.</u>	<u>Time (s)</u>	<u>V_{set} (ft/s)</u>
				1	27 in.	12.6	0.16
				2	34 in.	15.6	0.13
				3	28 in.	15.6	0.13
				4	26 in.	12.7	0.15
Nukon	500 (490-515 gpm) 41 Hz	24	0.20	<i>Debris rolled on the floor and reached the screen. They moved over the curb.</i>			
				Drop Test #	<u>Horz. Dist.</u>	<u>Time (s)</u>	<u>V_{set} (ft/s)</u>
				1	20 in.	12.5	0.17
				2	28 in.	14.2	0.15
				3	26 in.	12.0	0.17
				4	31 in.	13.0	0.16
5	32 in.	15.4	0.14				

C.4 Paint-Chip Test Measurements

Table C.20 lists the settling velocity of the paint chips measured in ambient-temperature water.

Tables C.21 and C.22 summarize the observations made regarding transport of paint chips in these tests. As shown in the upper portion of Table C.21, the incipient tumbling velocity for paint chips (where slight movement was first observed) was found to be approximately 0.4 ft/s. Bulk motion occurred only when the flow velocities reached or exceeded 0.45 ft/s. At a flow velocity of 0.5 ft/s, movement is almost instantaneous, and the debris is capable of being transported several feet. One could also see that the debris is intermittently lifted off the floor and resettles.

The settling and tumbling properties of paint chips also were measured in the large flume to examine the effects of turbulent flow patterns. Data were collected using inlet flow conditioning Configuration A (diffusers on) and Configuration B (diffusers off). The results are summarized in Table C.22.

Lift-at-the-curb velocity measurements were also carried out in the large flume using a 2-in.-high curb. Results are indicated in Table C.22. The water height was maintained between 18 and 19 in.

Table C.20. Terminal Velocity Measurements for Epoxy Paint Chips.

ID	Sample Size	Drop Distance (in.)	Time (s)	Terminal Velocity (ft/s)
1	Large (1-in. x ½-in.)	10	6	0.14
2	Medium (¼-in. – ¾ in.)	20	15	0.11
3	Small (1/8-in. – ¼-in.)	20	9	0.19
4	Small (1/8-in. – ¼-in.)	20	11	0.15
5	Small (1/8-in. – ¼-in.)	10	5	0.17
6	Small (1/8-in. – ¼-in.)	10	10	0.08
7	Large (1-in. x ½-in.)	20	13	0.13
8	Medium (¼-in. – ¾ in.)	20	10	0.17
Median Terminal Velocity				0.15 ft/s

**GSI-191: Separate Effects Characterization
of Debris Transport in Water**

Table C.21. Paint Chips Transport Data from Small Flume Tests (November 24, 1999).

*Chips used ranged from 1/8 in. to 1 in. with few larger than 1 in.
Between 20 and 25 chips or 50 ml in volume were placed on the flume floor.*

Run	Debris Types	Flume Velocity (ft/s)	Observation
<i>Paint Chip Transport</i>			
1	Paint-Chips	0.10	No movement
2		0.15	No movement
3		0.20	No movement
4		0.25	No movement
5		0.30	Slight movement of particles
6		0.35	Still no movement (flutter)
7		0.40	1 piece moved
8		0.45	All pieces started to move
9		0.50	All pieces moved immediately to screen
<i>Paint Chip and Nukon Debris Transport</i>			
10	Paint + Nukon	0.05	No transport/movement
		0.10	Some fluttering (Nukon fines move)
		0.15	≈10% Nukon transport/no paint movement
		0.20	≈50-75% Nukon transport/no paint movement
		0.25	100% Nukon transport/no paint movement
		0.45	Paint-chips move slowly; may go to screen
		0.50	All pieces reached screen instantaneously

Table C.22. Paint Chips Transport Data from Large-Flume Tests.

*Chips used ranged from 1/8-in. to 1-in. with few larger than 1-in.
Between 20 and 25 chips or 50 ml in volume were placed on the flume floor.*

Diffuser Status	Q (gal./min)	Height (in.)	Velocity (ft/s)	Observation			
Diffuser on Calm flow. No eddies.	1000 (1000–1025 gpm)	24	0.40	Paint chips dropped at the top surface settled down to floor. No movement thereafter. Debris added on the floor did not move. Occasional fluttering did not result in movement.			
				Drop Test #	Horz. Dist.	Time (s)	V_{set} (ft/s)
				1	37.5 in.	13	0.16
				2	30 in.	12.5	0.17
				3	29 in.	13.2	0.16
				4	38 in.	11.5	0.18
			5	25 in.	12.9	0.16	
Diffuser on	1150	24	0.45	About 10–15% traveled to the curb, but none went over. The rest moved from initial location. But in about 20 min they did not reach the curb.			
Diffuser on	1150	19	0.55	All debris reached the curb, all most instantaneously. Only very curled up ones and larger debris made it over the curb. The rest stayed put on the floor.			
Diffuser off	1150	19	0.55	All pieces moved to the curb and more go over it, but not all.			
Diffuser off	1000	24	0.40	All most all pieces moved to curb. None over it.			
Diffuser off	850	24	0.31	Several pieces moved towards the curb. Not all reached the curb. Significant hesitance during movement.			

C.5 Marinite Test Measurements

Table C.23. Marinite Settling Velocity.

Curved 4 in. x 4 in.		Flat 4 in. x 4 in.		Flat 1 in. x 1 in.	
Sample	V (ft/s)	Sample	V (ft/s)	Sample	V (ft/s)
1	0.45	1	0.60	1	0.63
2	0.44	2	0.60	2	0.54
3	0.48	3	0.57	3	0.60
4	0.42	4	0.55	4	0.59
5	0.47	5	0.49	5	0.59

Table C.24 Marinite Floor Transport.

Velocity (ft/s)	4 in. x 4 in. Curved	4 in. x 4 in. Flat	1 in. x 1 in. Flat
0.66	Rocked but did not travel	No movement	No movement
0.70	Moved a small distance	No movement	No movement
0.73	No movement	No movement	Move 2–4 in. over 5 min
0.77	Moves slowly toward screen	No movement	Moves slowly toward screen
0.99	Traveled easily to screen	No movement	Traveled easily to screen

APPENDIX D TEST PROCEDURES

D.1. Introduction

Based on findings of the exploratory testing and conduct of several final tests, UNM has developed procedures for conducting each type of test. This section provides a list of test procedures used in these tests.

D.2. Terminal Velocity Tests

To develop a procedure for determining terminal velocity, debris was dropped into the column of water immediately below the water surface, and the time taken to travel 10 in., 20 in., and 30 in. from the water surface was measured. The objective was to see if the particles take a certain time to accelerate before they reach a steady-state velocity.

Table D.1 shows the time in seconds taken for 3/4-in. flat aluminum RMI pieces to fall a certain distance. For all terminal velocity studies reported in this document, any particle that touched the side of the cylinder during the fall was discarded from the data automatically.

It was observed that the settling velocity depends on the orientation of the piece as it falls (H - horizontal, V - vertical), with the horizontally falling pieces being slower. As can be expected, the pieces can flip-flop and change orientation as they fall, thereby slowing down during the fall. The time taken to travel the first 10 in. is statistically no different than the time to travel the next 10 in. Therefore, settling velocity can be measured for the entire 30-in. drop.

Table D.2 shows the corresponding data for approximately 1-in. pieces of cal-sil. It can be observed that the cal-sil has a faster terminal velocity. Also, there is a general tendency for it to take longer to fall the first 10 in. compared with the next 10 in. This is because the dry cal-sil loses a lot of the loosely held powdery particles as it falls, thereby changing its morphology during the descent. Therefore, the terminal velocity measurements need to be conducted between 10 and 30 in. of drop.

Table D.1. Initial Measurement of Terminal Velocity of Aluminum RMI.

Distance Traveled (in.)	Sample #1 (s)	Sample #2 (s)	Sample #3 (s)	Sample #4 (s)	Sample #5 (s)
10	6	8	6	6	6
20	14	16	10	11	15
30	23	27	13	13	26
	H	H	V	V	H

Table D.2. Initial Measurement of Terminal Velocity of Cal-Sil.

Distance Traveled (in.)	Sample #1 (s)	Sample #2 (s)	Sample #3 (s)	Sample #4 (s)	Sample #5 (s)
10 in.	9	4	5	4	5
20 in.	13	7	9	7	8
30 in.	15	10	12	12	12

D.3. Drop Tests

The pump speed is set to the desired frequency (to obtain the target average flow velocity). Water height is maintained at 18 in. by adjusting the 12-in. outflow valve. A period of 5 min is allowed for the flow pattern to settle down and to make sure that the water height remains at 18 in. \pm 1 in. One person drops the treated debris just under the water surface with a pair of tongs at a location 4 ft from the end of the flow straightener. A second person uses a stopwatch to time the debris falling to the floor of the flume.

The location of the fall is noted, and the distance is measured with a ruler (1/16-in. accuracy). A graduated ruler is placed on the side of the flume and the person noting the drop point moves with the falling debris to minimize parallax error. After a set of 5 drops is completed, the frequency of the pump is increased to the next desired level and the process is repeated.

D.4. Floor Transport Tests

The purpose of these tests is to observe at which flow rates the debris starts to move. This is also referred to as the 'incipient motion.' The procedure for running the test and the pump is as described above. The treated debris is introduced to the bottom of the flume inside a 6-in.-diam PVC tube. The debris is allowed to settle down at the bottom, and the tube is slowly lifted up to minimize perturbation of the flow field.

Tests are started at low average flow velocities, and the pump outflow is gradually increased (increments of 1 Hz. on the pump dial). Each time the pump output is increased, the outflow valve is adjusted to keep the height of water at 18 in.

Tests were run in three different configurations that are discussed below. Configuration A is the uniform flow condition used for most of the data presented in this report. Test configurations B and C provided progressively more turbulence and nonuniformity in the flow conditions.

Configuration A

Specifications for test:

- Diffuser in
- 10-in.-diam inflow pipe positioned above water surface
- No curb
- Debris settled to the bottom of the flume (via pipe) 4 ft 7 in. from screen
- 18-in. depth (\pm 1 in.)

Configuration B

Specifications for test:

- Diffuser out
- 10-in.-diam inflow pipe positioned above water surface
- No curb
- Debris settled to the bottom of the flume (via pipe) 4 ft 7 in. from screen
- 18-in. depth (\pm 1 in.)

Configuration C

Specifications for test:

- Diffuser out
- 6-in.-diam inflow pipe positioned low (submerged about 1 ft above flume floor)
- No curb
- Debris settled to the bottom of the flume (via pipe) 4 ft 7 in. from screen
- 18-in. depth (\pm 1 in.)

D.5. Lift Tests

These tests were conducted to study whether the debris is able to climb over 2-in.- and 6-in.-high curbs (2 in. wide, made of plywood) placed adjacent to the screen at the downstream end of the large flume. The debris was introduced at the same location as for the floor transport tests discussed in the previous section. The debris moved to the curb and remained on the floor. The pump flow rate was gradually increased, and the average velocities at which the debris managed to climb over the curb were noted. The tests were repeated for each of the three flume entrance flow configurations (A, B and C).

D.6. Screen Attachment Velocity

The objective of these tests was to determine the minimum velocity at which debris of different types would adhere to the screen instead of dropping to the bottom of the flume. These tests were only done under test configuration A because it was believed that the Configurations B and C were not relevant at the downstream end and their effect will be minimal.

For each flow rate below, debris was placed approximately 2 in. to 3 in. away from the screen and released into the stream 3 in. below the surface. The debris then moved to the screen. The average flow velocity at which each type of debris remained stuck to the screen and did not settle was recorded.

APPENDIX E CALIBRATION OF TEST INSTRUMENTATION

E.1. Introduction

The velocity of the water flow through the flume was measured indirectly by measuring the net volumetric flow and dividing it by the flow cross-sectional area. Because the flow velocity is a critical experimental parameter, extensive efforts were devoted to routinely calibrate the flow meter used to measure the volumetric flow rate. It should be noted that flow meter calibration was undertaken several times throughout the test program to ensure that flow meters provided accurate readouts of the actual flow.

E.2. Calibration of Flow Meter on the Large Flume

The large flume is equipped with a turbine flow meter with a digital read-out. The meter displayed both the instantaneous flow (in gallons per minute) and cumulative flow (in gallons). Because of fluctuations in the instantaneous flow, it was decided to use the cumulative flow read out to average the fluctuations.

This flow meter was calibrated by measuring the volume pumped into the flume over a 2-min time frame with the indicators attached to the pump. The purpose of this experiment was to validate the measurements of the flow meter attached to the new pump serving the large flume. The comparison test checked the accuracy of the indicators by measuring the time taken for water level to rise 5 in.. Test data are provided in Table E.1. The flow meter readings were recorded by noting the difference in the total volume of water (gallons) that flows through the meter over a 2-min interval (measured with a stopwatch). The actual flow was calculated from the test performed by timing the 5-in. rise in the water level. The calibration of the flow meter was achieved using the following procedure.

- Selecting a pump frequency and throttling the pump discharge valve as needed to set the water flow through the flume. The frequency is listed in column 2 below.
- The flow meter readout for the cumulative flow through the pump was recorded initially and 2 min after that. The difference is divided by 2 to obtain the flow meter reading in gallons per minute. These values were listed in columns three through six below.
- This value was compared with the ‘instantaneous’ meter readout (which usually fluctuates by $\pm 10\%$).
- The flume discharge valve was closed, and the water was allowed to buildup in the flume.
- The time taken for water level to rise by 5 in. was measured. This value was used to determine actual gallons per minute discharged into the flume. These values were listed in columns 7 and 8.

Table E.1. Flow Measurements from the Flow Meter vs Volumetric Measurements.

Test	Pump Freq. (Hz)	5.1.1.1.2 Flow Meter Reading Measured				Time for 5 in. (s)	Actual Flow (gpm)
		start	stop	difference	flow(gpm)		
1	33	N/A	N/A	N/A	120	94.12	119
2	36	381765	382184	419	210	53.94	208
3	38	383880	384505	625	312	34.65	324
4	40	386398	387280	882	441	25.19	445
5	42	388769	389927	1158	579	20.13	557
6	46	391911	393578	1667	833	13.72	818

Figure E-1 shows the data, along with 5%-error bars. From this figure, it is clear that the flow meter performs its intended function adequately.

The calibration process was repeated several times throughout the test program.

E.3. Calibration of Flow Meter on the Small Flume

The small flume is equipped with an orifice flow meter based analog readout. This flow meter was also calibrated first by measuring the time taken to fill the flume to 3.5 in. with the outflow completely shut down. The procedures used are very similar to those described in Sec. E.2. The result of the comparison between the meter read-out and the volumetrically measured flow rate is shown in Table E.2. This calibration was repeated several times over the duration of test program. At all times, the measured flow was within +10% of the meter read-out.

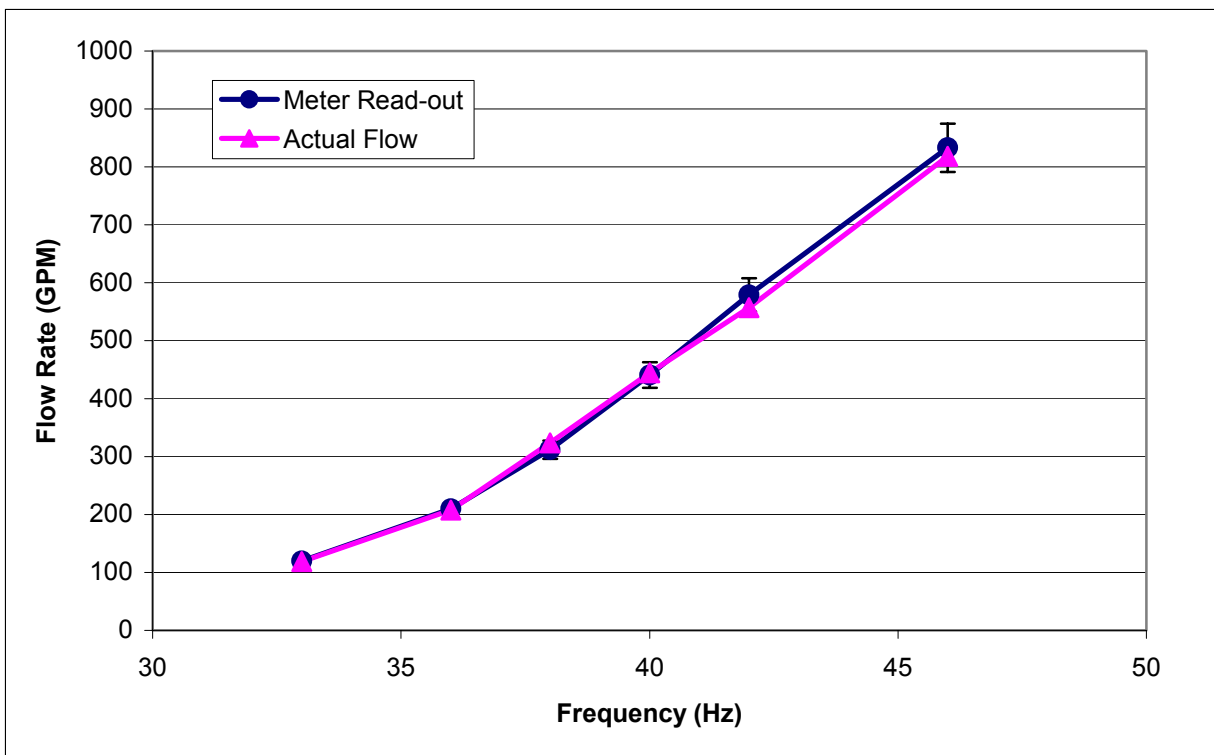


Fig. E-1. Comparison of meter readout with actual flow measurements.

Table E.2. Calibration of Flow Meter on Small Flume.

Q from Flow meter (gpm)	Q from volumetric measurement (gpm)
20	17.7
30	30.0
40	37.9

APPENDIX F SUPPORTING CFD CALCULATIONS

F.1 Scope of UNM Flume CFD Calculations

CFD calculations were performed of flow through the flume built by UNM to investigate the transportability of various types of insulation debris that might be generated in a high-pressure LOCA event at a PWR nuclear power plant. The goal of the calculations was to provide insight as to how flow develops in the flume under various configurations.

F.2 FLOW-3D

The flume CFD calculations were performed with the FLOW-3D computer program. FLOW-3D is a general-purpose software package for modeling the dynamic behavior of liquids and gases influenced by a wide variety of physical processes. The program is based on the fundamental laws of mass, momentum, and energy conservation and has been constructed for the treatment of time-dependent, multidimensional problems. FLOW-3D is applicable to almost any flow process.

F.3 Flume Model

A description of different aspects of the FLOW-3D model built of the UNM flume is given below.

Computational Domain

A computational domain was defined with extents based on the physical dimensions of the UNM flume. The flume is 20 ft long, 3 ft wide, and 4 ft high. The extents of the FLOW-3D computational grid match these dimensions. FLOW-3D grids normally are constructed in rectangular coordinates (cylindrical coordinates are also an option), and the cells of the flume model are rectangular. The typical cell was defined square with a length of 3 in. The cells along the bottom and sides of the model were defined thinner than the typical cell to better resolve velocities at the walls. These cells are 1 in. thick in their dimension normal to the wall.

Internal Structure

The UNM flume has a bank of cooler pads and a grid of flow-straightening plates just downstream of where water is introduced to smooth the flow before it enters the test region. The cooler pads (diffuser) and straightening plates (straighteners) are represented in the CFD model with a three-dimensional porous obstacle and with two-dimensional baffles, respectively.

The porous obstacle representing the diffuser is 6 in. long, begins 18 in. from the inlet end of the flume, and extends across the full width and height of the flume. This is very similar to the size and placement of the actual diffuser. The flow resistance characteristics of the model diffuser have been defined so as to give 4-in. H₂O pressure drop at 0.25 ft/s in the flume test section, consistent with measurements made in the UNM flume. The flow resistance traits of the porous obstacle are defined homogeneously, i.e., equivalently in all directions. This is thought to be consistent with the traits of the actual diffuser.

The baffles representing flow straighteners are oriented in the model as they are in the flume. There are a number of horizontal and vertical baffles that intersect to form 3-in.-square horizontal flow passages very similar to the passages in the UNM flume. Consistent with the flume, the baffles are 1 ft long. Their leading edge is 2 ft from the inlet end of the flume. The physical straighteners are made of thin sheet steel. FLOW-3D baffles consistently are two-dimensional and so have no thickness.

The UNM flume has a small angle bracket attached to the floor to keep the straighteners in place. The downstream end of the straighteners bumps up against the bracket. The bracket protrudes up from the floor approximately ½ in. and spans the width of the flume. This bracket is represented in the FLOW-3D model by a ½-ft tall, ½-in. wide object 3 ft long.

A debris-catching screen is positioned in the UNM flume to catch insulation debris. (The screen is multi-purpose in the flume testing, but one of its important functions is to stop debris from recirculating or settling in the trench system of the laboratory.) The model debris-catching screen is located 3 ft from the outlet end of the flume. The flow-loss characteristics of the screen baffle are defined to give a 3-in. H₂O pressure drop at 0.75 ft/s (at the screen). These traits are consistent with the physical screen.

Flow Source/Sink

A fluid source was specified to FLOW-3D, which added water to the calculation at a location above the water level, centered in the width of the flume 9 in. from the inlet end. The water from the source was routed downward through a hollow object of revolution (inlet pipe) to a point either 27 in. or 12 in. above the floor of the flume, depending on the particular calculation. The inlet pipe was defined with an inside diameter of 6 in. These traits are similar to the orientation and size of the physical flow supply to the UNM flume. The 27-in. or 12-in. inlet pipe exit elevations correspond to the exit being above the water surface or submerged, respectively.

A fluid sink was specified that removed water from the calculation at the identical rate at which the source added water. The sink was placed on the floor centered in the width of the flume 9 in. from the end. The sink was circular, 10 in. in diameter, and 1½-in. high. These traits fairly represent the drain in the UNM flume.

Mass flow rates for the flow source and sink were specified at 202 gal./min. This flow relates to a uniform velocity in the body of flume of 0.1 ft/s—a velocity of particular interest in the debris transport tests.

Solution Options

Default solution schemes and convergence criteria were used in the FLOW-3D calculations. The free-surface logic was enabled to capture surface effects at the water/air interface. The fluid was treated as viscous.

Boundary Conditions

No-slip, zero-velocity boundary conditions were defined on the bottom, ends, and sides of the model flume. A stagnant ambient pressure condition was defined at the top boundary.

Initial Conditions

An 18-in. water depth was defined for all calculations presented here. Velocity was initialized uniformly in the flume at 0.1 ft/s in the axial (lengthwise) direction. Pressure was initialized as hydrostatic.

F.4 UNM Flume Configurations

CFD calculations were made for various flume configurations. Results for four configurations are presented here. They are characterized by the following.

- All flow smoothing structures near the inlet of the flume (diffuser and straighteners) being in place and by the exit of the flow inlet pipe being above the water surface.
- The diffuser having been removed from the flume. The flow inlet pipe is elevated here also.
- The diffuser being removed and the inlet pipe being submerged.
- All flow smoothing structure being in place and a 3-in.-high curb being placed just in front of the debris catching screen.

Each of the calculations was run for 15 min of real time. Typical CPU time for a calculation was 24+ h on a 450-MHz PC. Fifteen real-time minutes showed to be largely sufficient in establishing steady-state conditions as indicated by unchanging average kinetic energy in the flow field and unvarying velocity distributions.

F.5 Results

A collection of figures for each of the flume configurations identified above follows. The figures show velocity as a function of location. In most cases, three-dimensional (3-D) velocity magnitude is presented. A few of the figures present specific components of overall velocity.

The coordinate system of the CFD model aligns the X-axis along the length of the flume, the Y-axis aligns along the width of the flume, and the Z-axis aligns along the height of the flume. The origin is at a lower corner of the end of the flume where water is introduced. The positive directions of X and Z are down the flume and up, respectively. The positive direction of the Y-axis is consistent with the right-hand rule.

The CFD model of the UNM flume was built in SI units. Velocity units in the figures are m/s. Length units are m.

A few different types of figures are included. Below is a description of each type.

Full Flume Color-Scaled Figures

(The extents in these figures are full extents of the flume.)

- 3-D velocity magnitude in a vertical length-height (X-Z) section located at mid width (mid Y) in the flume.
- 3-D velocity magnitude in a horizontal length-width (X-Y) section located just above the floor of the flume.

Test Region Color-Scaled Figures

(The 10-ft length of the flume beginning where the flow straighteners end is referred to here as the test region.)

- 3-D velocity magnitude in a vertical length-height (X-Z) section located at mid width (mid Y) in the flume.
- 3-D velocity magnitude in a horizontal length-width (X-Y) section located just above the floor of the flume. This section extends the full width of the flume.
- 3-D velocity magnitude in a vertical width-height (Y-Z) section located centrally in the test region. This section extends the full width and height of the flume.

Axial (X) velocity in a vertical length-height (X-Z) section located at mid width (mid Y) in the flume with superimposed velocity vectors. X velocity is colored scaled in these figures with an upper bound of zero imposed on the scaling to illustrate negative velocities. Colors other than red in these figures identify backward flow in the flume. The velocity vectors reflect X and Z velocity components, i.e., the projection of the 3-D velocity vector onto the X-Z section. Figures F-2.6 and F-3.6 are of this description.

Test Region Line Charts

- X-velocity near the flume floor as a function of position along the width of the flume at various locations along the length of the test region (Figs. F-1.6 and F-3.8).
- X-velocity as a function of height at various locations along the length of the test region and centered in the width of the flume (Fig. F-1.7).
- Transverse (Y) and vertical (Z) velocities near the floor of the flume versus position along the width of the flume (Figure F-3.9).

Miscellaneous Figures

For the flume calculation with a curb, Fig. F-4.2 is included showing velocity vectors in a vertical section located at mid width in the vicinity of the curb. The vectors are color-scaled by velocity magnitude.

For the calculation without a diffuser and with the inlet pipe submerged, a velocity vector plot for a vertical full-length section mid-width in the flume is included (Fig. F-3.7). The vectors are color-scaled by axial (X) velocity magnitude.

F.6 Observations

Several observations were made over the course of performing the CFD calculations for the varying flume configurations. The observations are presented below by configuration.

Flume With Diffuser

Results of the CFD calculation of the UNM flume with all inlet flow smoothing structures (diffuser and straighteners) in place show a nicely uniform fully axial flow where insulation debris was placed in the transport experiments (many feet downstream of the straighteners).

Flume Without Diffuser but With Elevated Inlet Pipe

CFD results for the flume with the diffuser removed and with the inlet pipe elevated show the existence of large-scale recirculative flow structure throughout the test region. Strong asymmetries are also shown. In considering the asymmetries, it was noticed that the water spilling from the elevated inlet pipe does not fill the cross section of the pipe and does not fall from the pipe centrally. This is reasoned to be the driver behind the asymmetries.

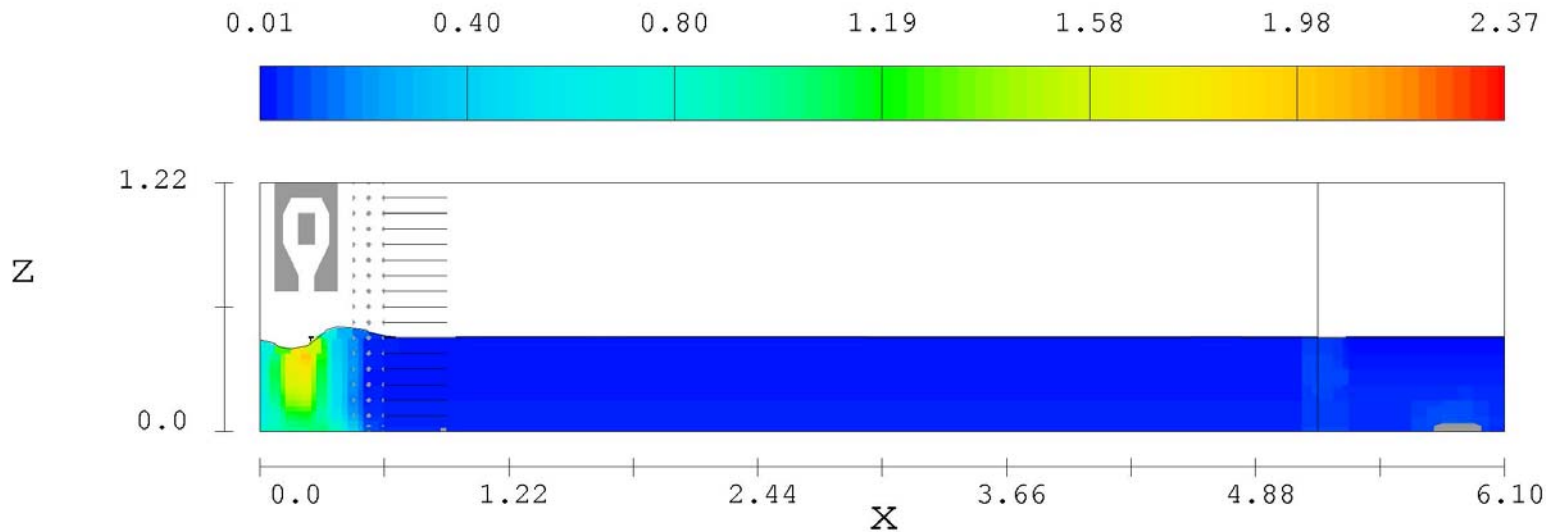
Flume Without Diffuser and With Submerged Inlet Pipe

The CFD results here differ dramatically from the results of the flume without the diffuser and with the inlet pipe elevated. Submerging the inlet pipe greatly mutes the asymmetries thought to be associated with water falling noncentrally from the inlet pipe. The asymmetries are small here, and the recirculative flow structure in the test region is localized near the flow straighteners. However, velocities across the flume are not especially uniform. This is the case even many feet downstream of the straighteners.

Flume With 3-In. Curb at Debris Catching Screen

The CFD analysis here shows no sizeable influence on flume test region flow introduced by a 3-in. curb placed against the base of the debris catching screen.

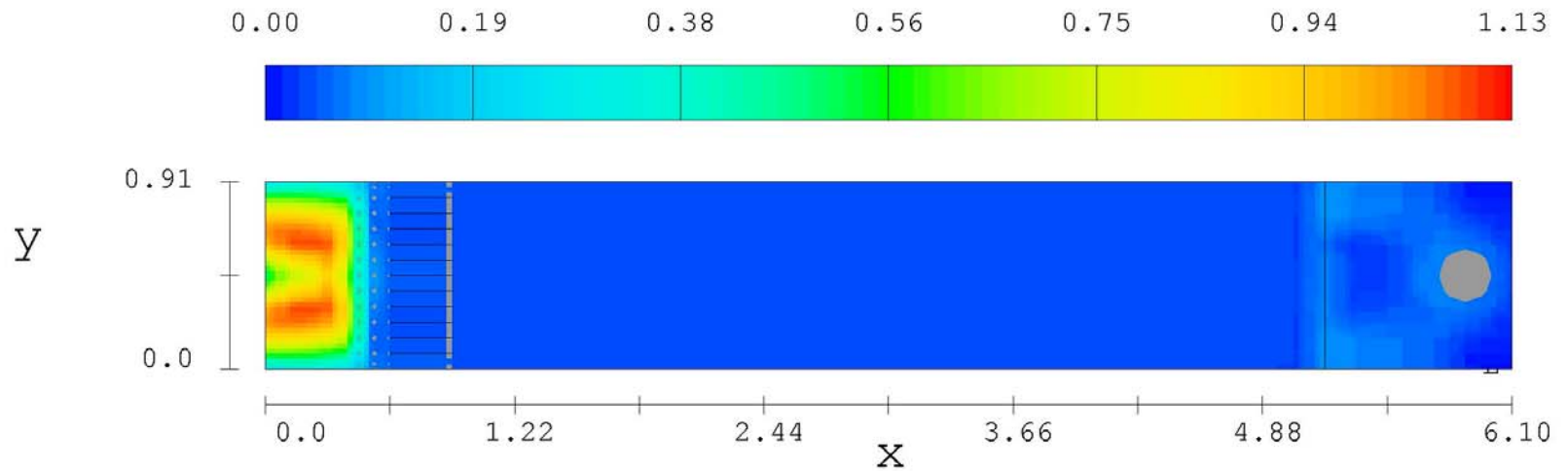
velocity magnitude contours



FLOW-3D® t=900.0 y=4.953E-01 (ix=2 to 82 kz=2 to 18)
09:36:04 8-25-2000eifd hydr3d: version 7.6 win32 1999
UNM flume

Fig. F-1.1. UNM Flume With diffuser - Velocity Magnitudes (Length-Height Section at Mid Width).

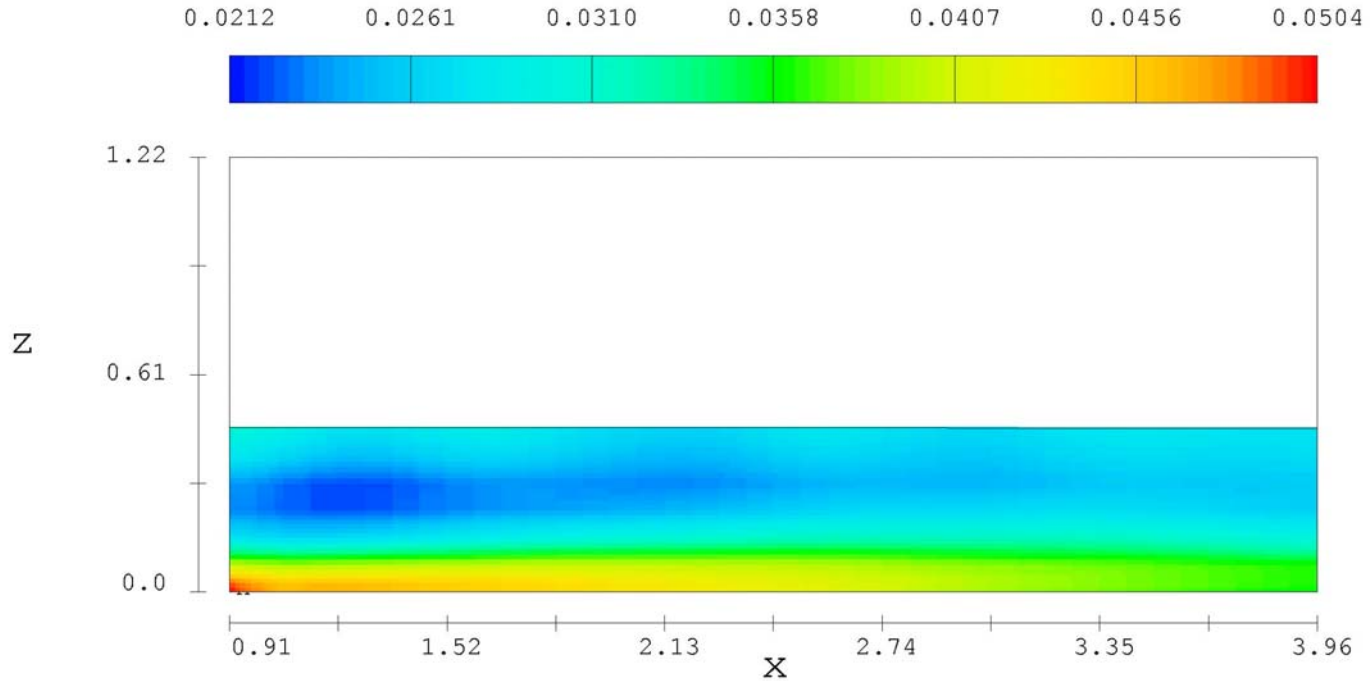
velocity magnitude contours



FLOW-3D[®] t=900.0 z=1.270E-02 (ix=2 to 82 jy=2 to 15)
09:36:04 8-25-2000eifd hydr3d: version 7.6 win32 1999
UNM flume

Fig. F-1.2. UNM Flume With Diffuser - Velocity Magnitudes (Length-Width Section Just Above the Floor).

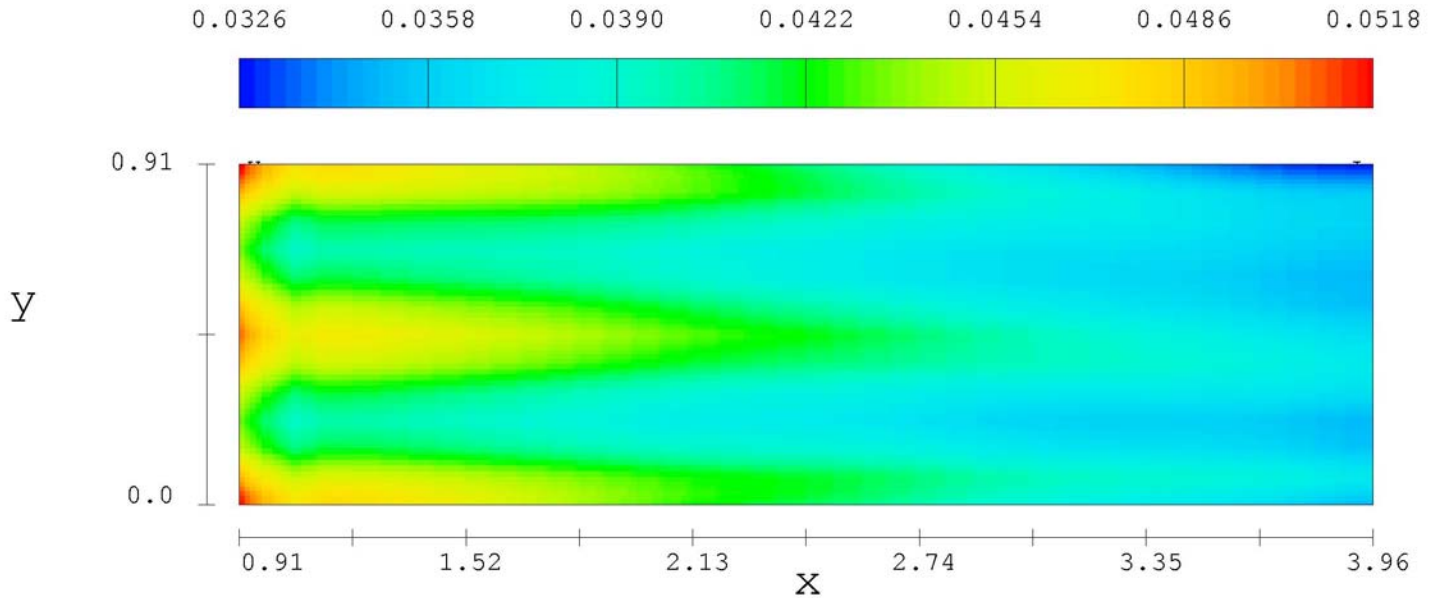
velocity magnitude contours



FLOW-3D® t=900.0 y=4.953E-01 (ix=15 to 54 kz=2 to 18)
09:36:04 8-25-2000eifd hydr3d: version 7.6 win32 1999
UNM flume

Fig. F-1.3. UNM Flume With Diffuser - Test Region Velocity Magnitudes (Length-Height Section at Mid Width).

velocity magnitude contours



FLOW-3D[®] t=900.0 z=1.270E-02 (ix=15 to 54 jy=2 to 15)
09:36:04 8-25-2000eifd hydr3d: version 7.6 win32 1999
UNM flume

Fig. F-1.4. UNM Flume With Diffuser - Test Region Velocity Magnitudes (Length-Width Section Just Above the Floor).

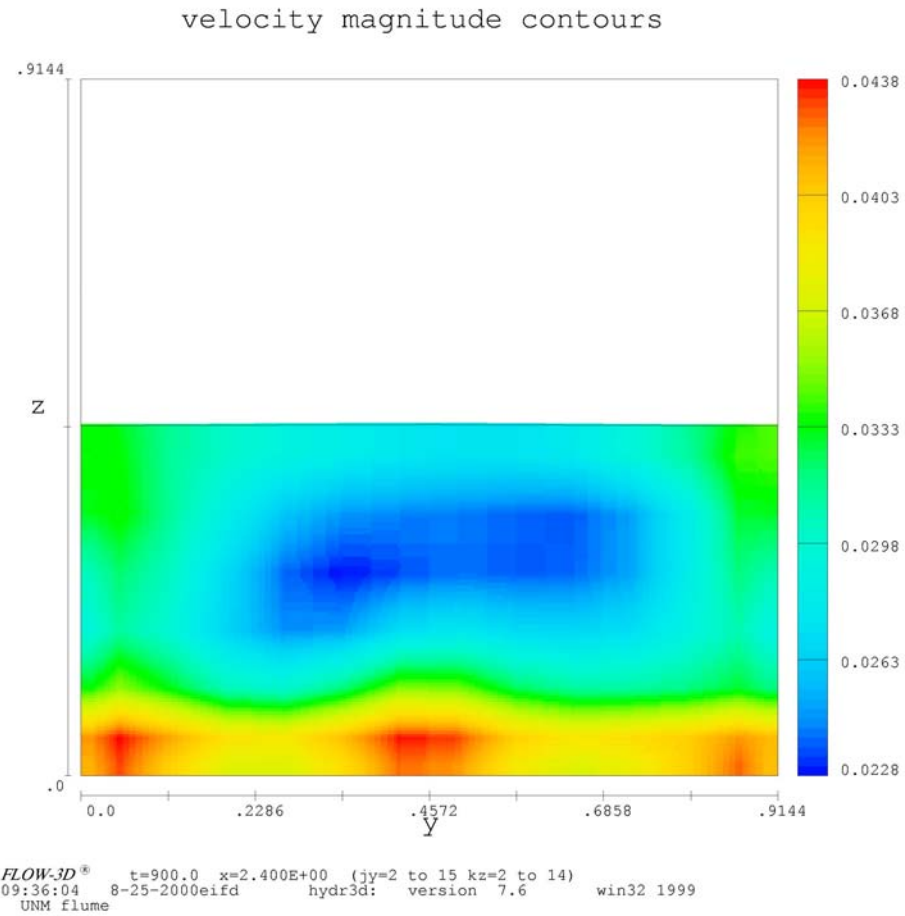


Fig. F-1.5. UNM Flume With Diffuser - Test Region Velocity Magnitudes (Width-Height Section).

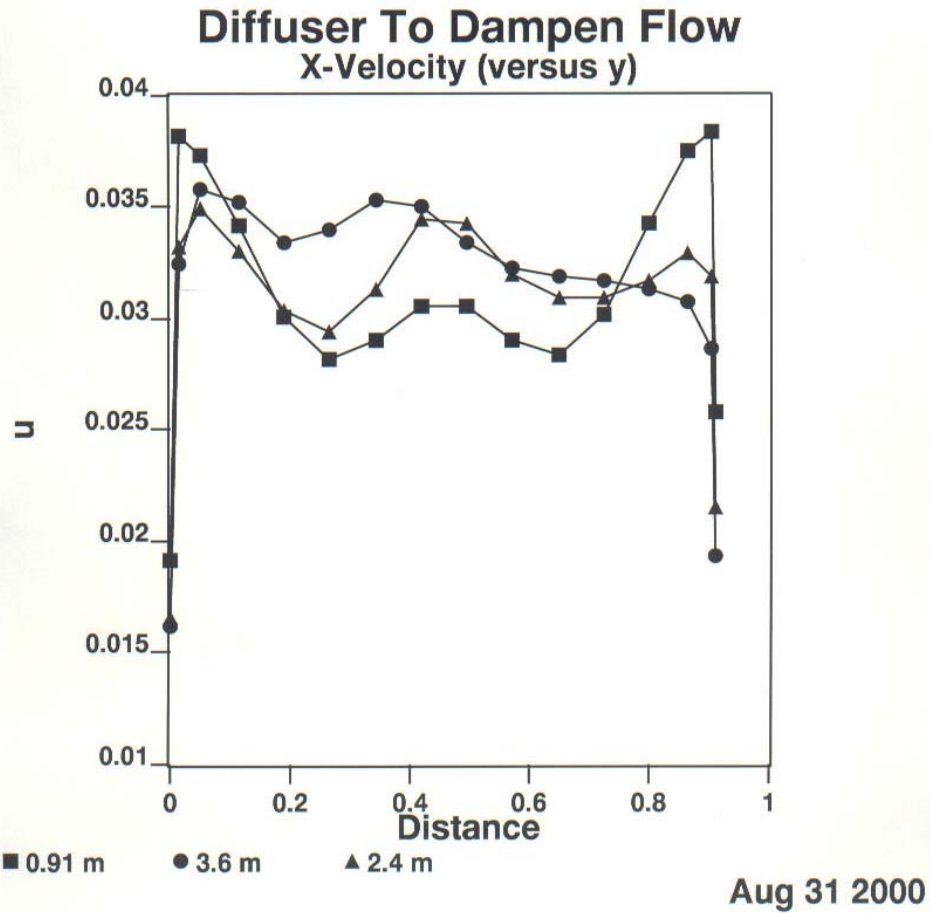


Fig. F-1.6. UNM Flume With Diffuser - Axial Velocity Just Up from the Floor of the Flume Versus Width at Different Axial Locations.

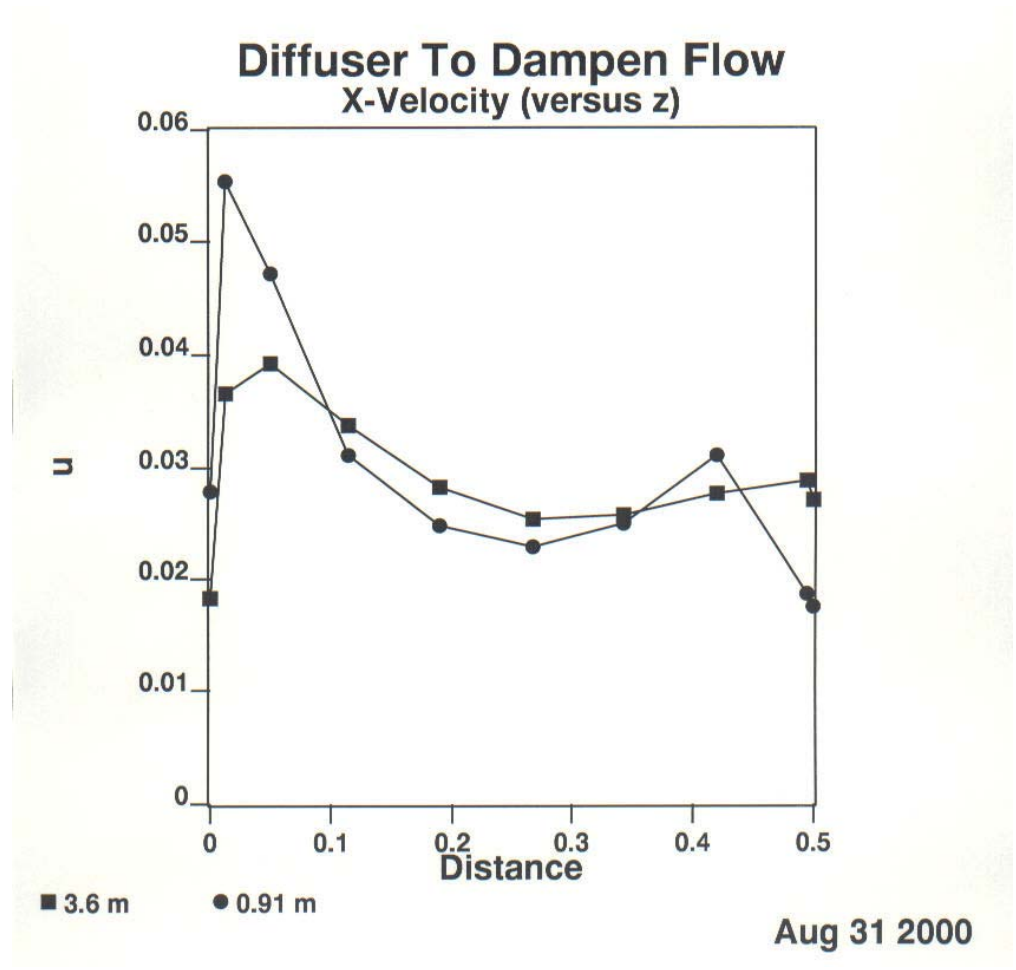
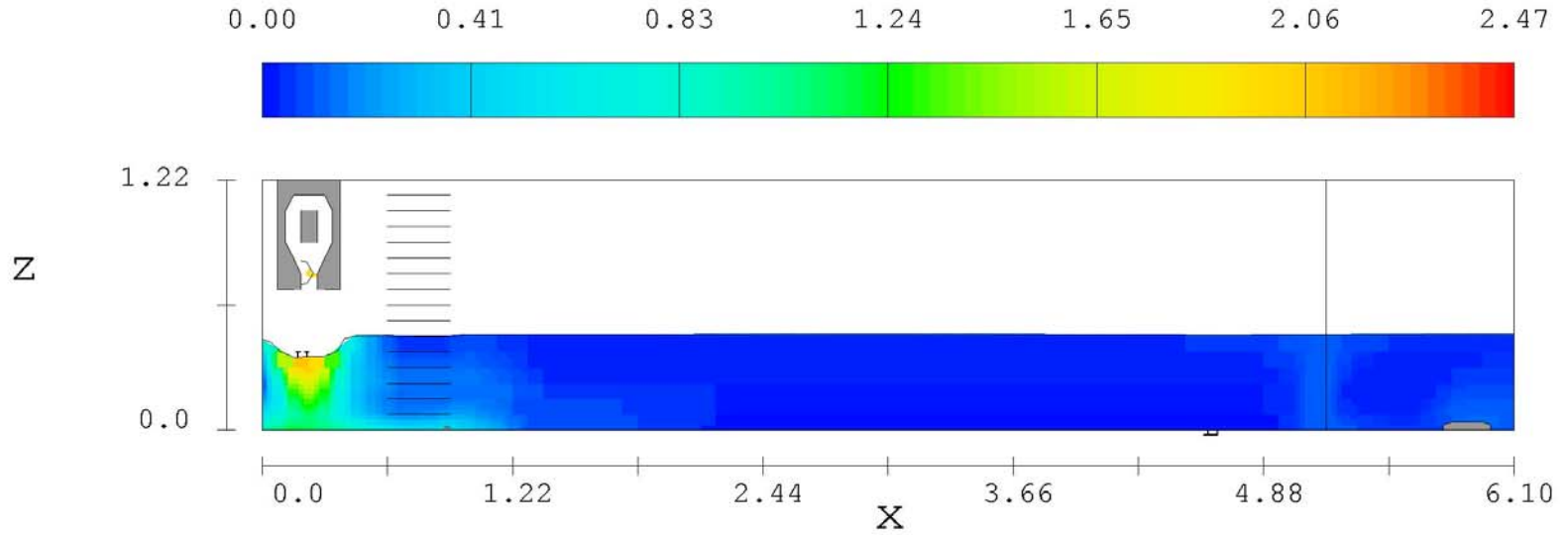


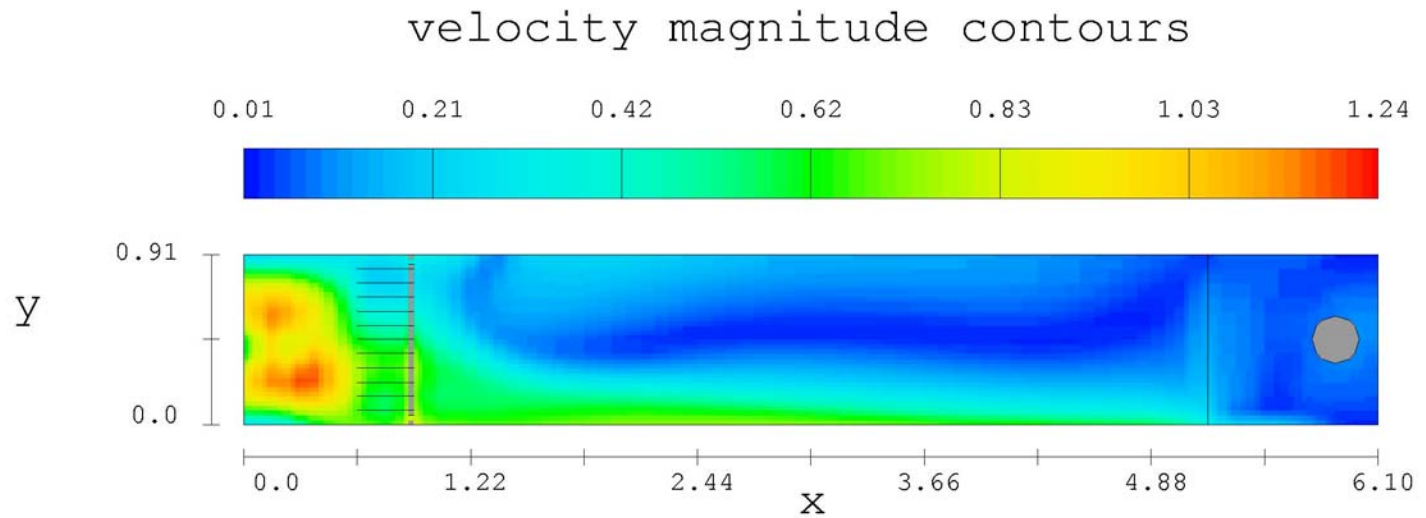
Fig. F-1.7. UNM Flume With Diffuser - Axial Velocity Versus Height at Different Axial Locations and Mid Width in the Flume.

velocity magnitude contours



FLOW-3D[®] t=900.0 y=4.953E-01 (ix=2 to 82 kz=2 to 18)
08:38:22 8-26-2000kqln hydr3d: version 7.6 win32 1999
UNM flume

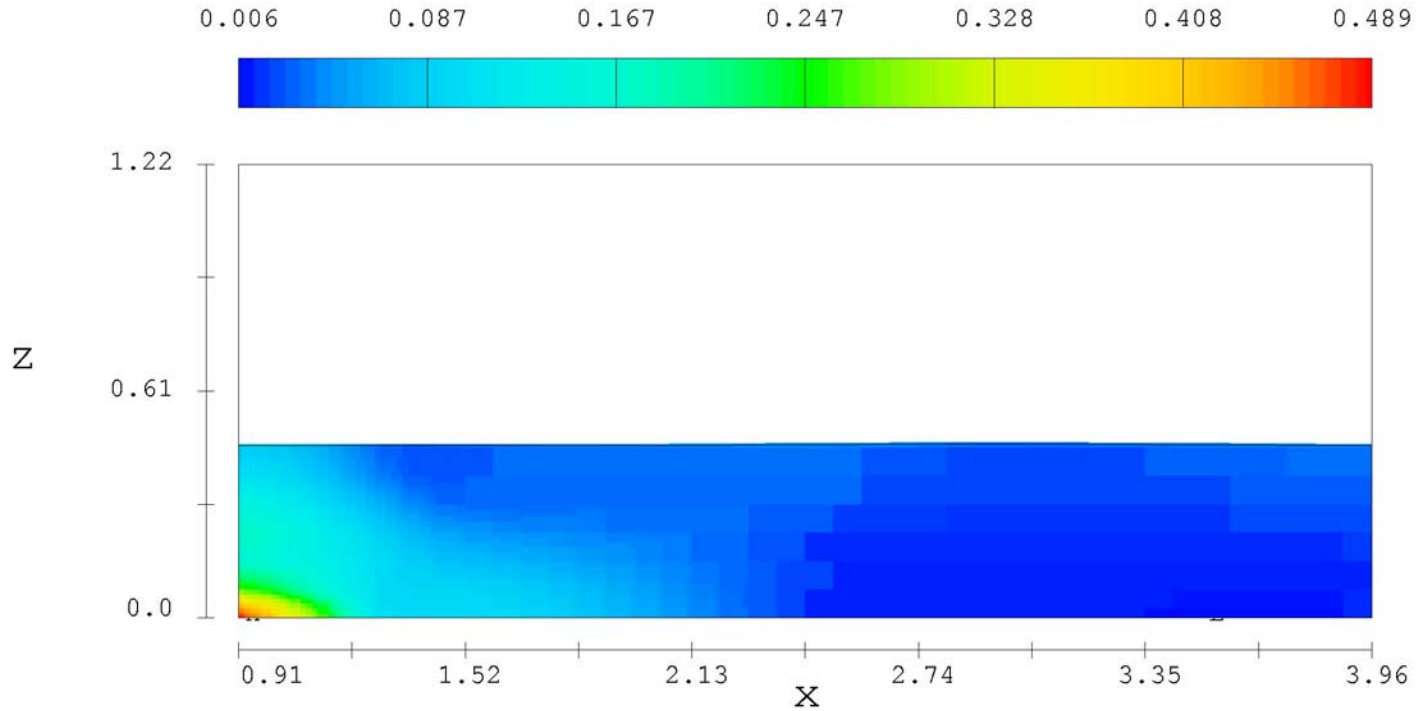
Fig. F-2.1. UNM Flume Without Diffuser - Velocity Magnitudes (Length-Height Section at Mid Width).



FLOW-3D[®] t=900.0 z=1.270E-02 (ix=2 to 82 jy=2 to 15)
 08:38:22 8-26-2000kqln hydr3d: version 7.6 win32 1999
 UNM flume

Fig. F-2.2. UNM Flume Without Diffuser - Velocity Magnitudes (Length-Width Section Just Above the Floor).

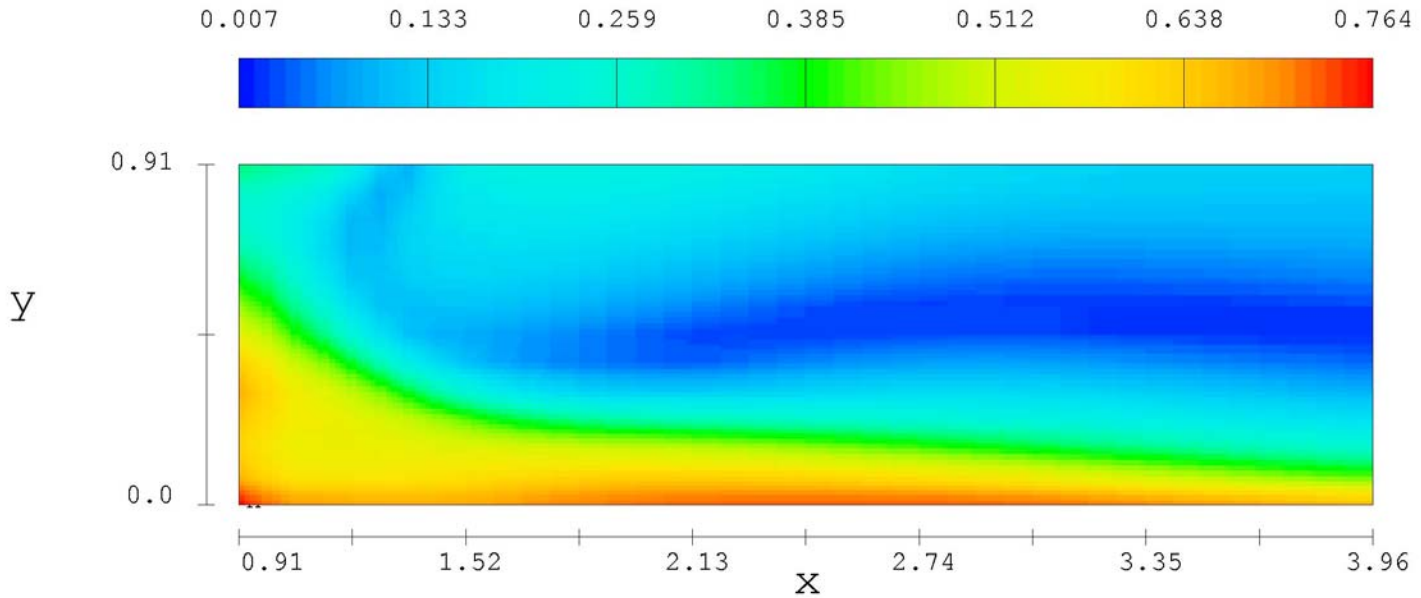
velocity magnitude contours



FLOW-3D[®] t=900.0 y=4.953E-01 (ix=15 to 54 kz=2 to 18)
08:38:22 8-26-2000kqln hydr3d: version 7.6 win32 1999
UNM flume

Fig. F-2.3. UNM Flume Without Diffuser - Test Region Velocity Magnitudes (Length-Height Section at Mid Width).

velocity magnitude contours



FLOW-3D[®] t=900.0 z=1.270E-02 (ix=15 to 54 jy=2 to 15)
08:38:22 8-26-2000kqln hydr3d: version 7.6 win32 1999
UNM flume

Fig. F-2.4. UNM Flume Without Diffuser - Test Region Velocity Magnitudes (Length-Width Section Just Above the Floor).

velocity magnitude contours

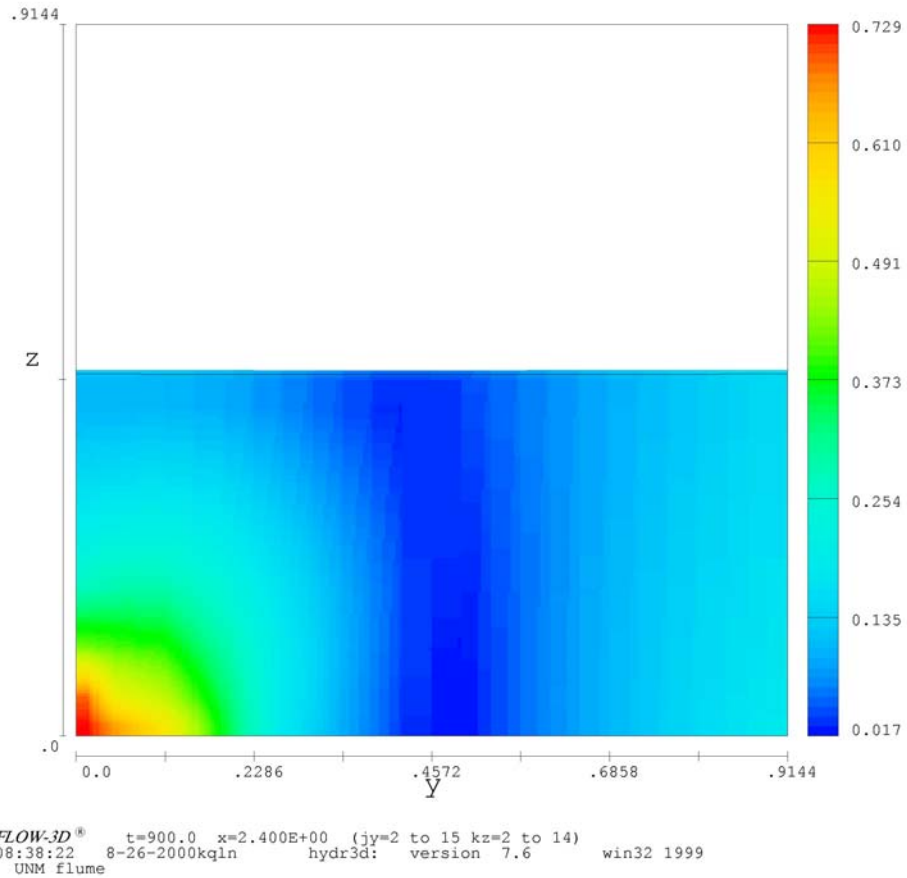
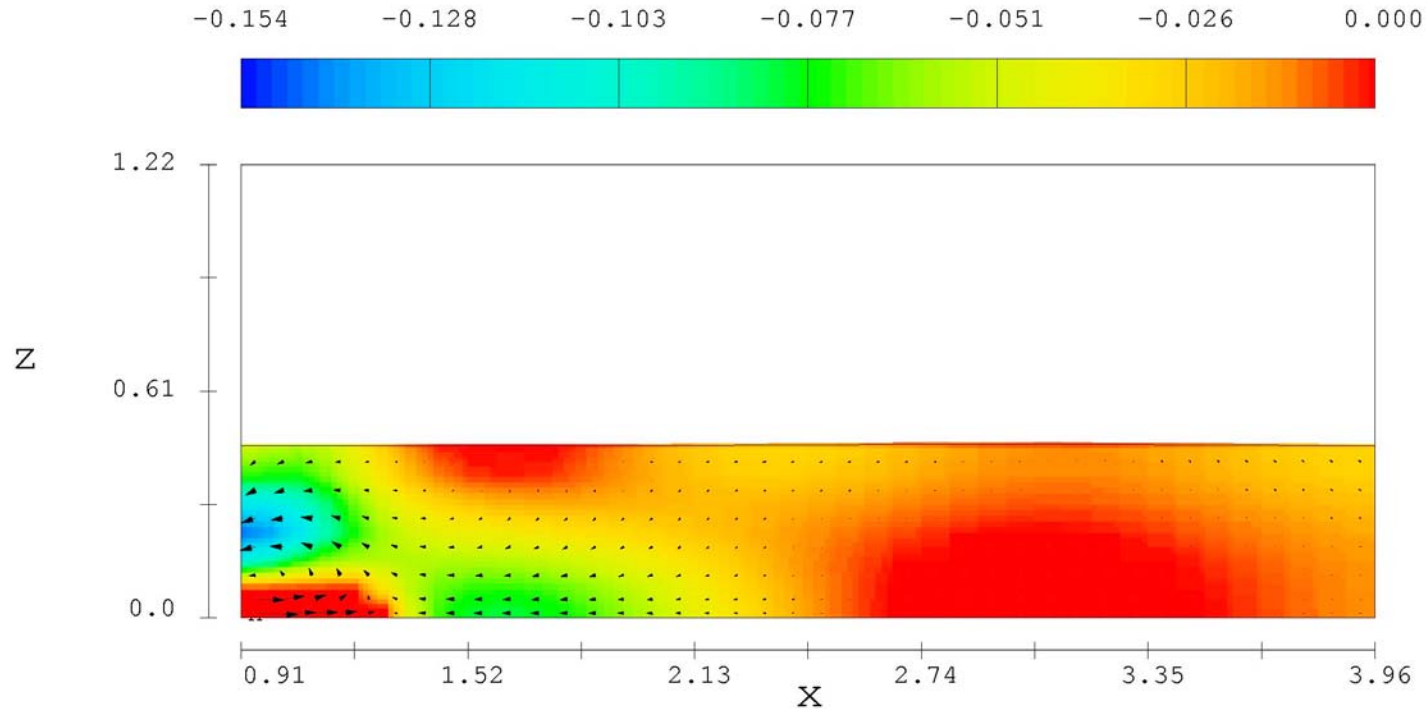


Fig. F-2.5. UNM Flume Without Diffuser - Test Region Velocity Magnitudes (Width-Height Section).

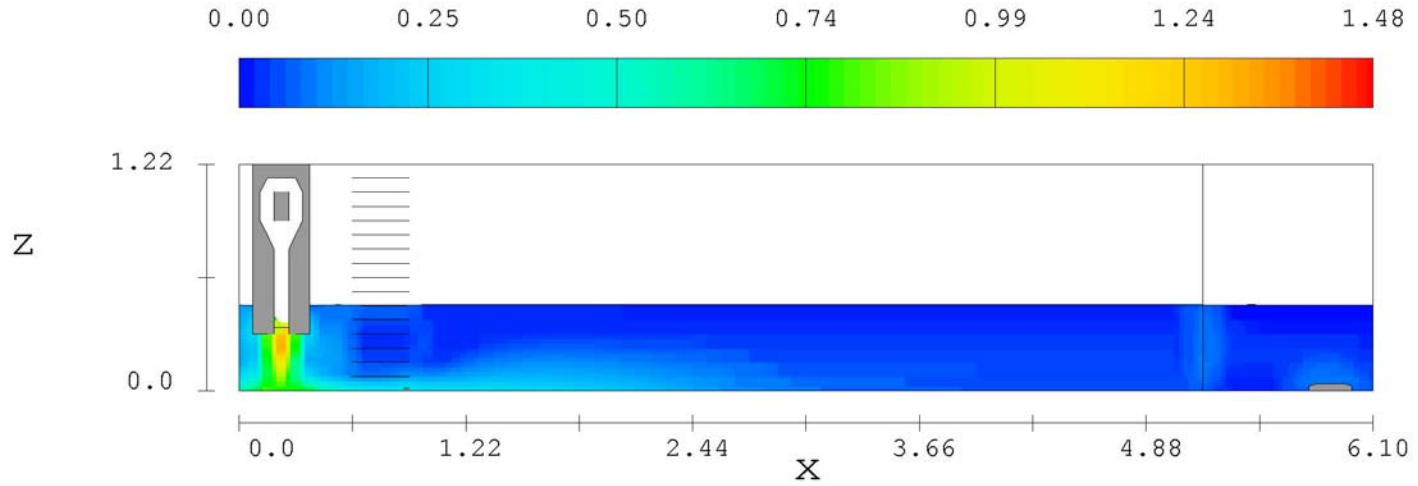
x velocity and vectors (vmax=4.47E-01)



FLOW-3D® t=900.0 y=4.953E-01 (ix=15 to 54 kz=2 to 18)
08:38:22 8-26-2000kqln hydr3d: version 7.6 win32 1999
UNM flume

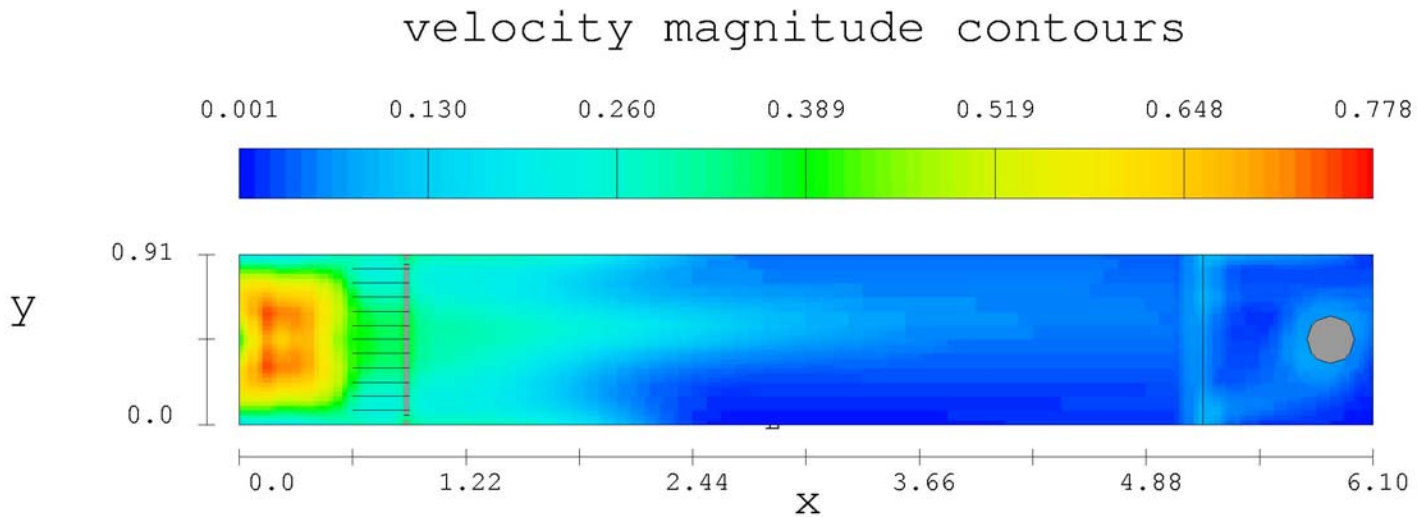
Fig. F-2.6. UNM Flume Without Diffuser - Test Region Axial Velocity and Velocity Vectors (Length-Height Section at Mid Width with Zero Upper Bound on Color).

velocity magnitude contours



FLOW-3D[®] t=900.0 y=4.953E-01 (ix=2 to 82 kz=2 to 18)
11:39:22 8-28-2000kqln hydr3d: version 7.6 win32 1999
UNM flume

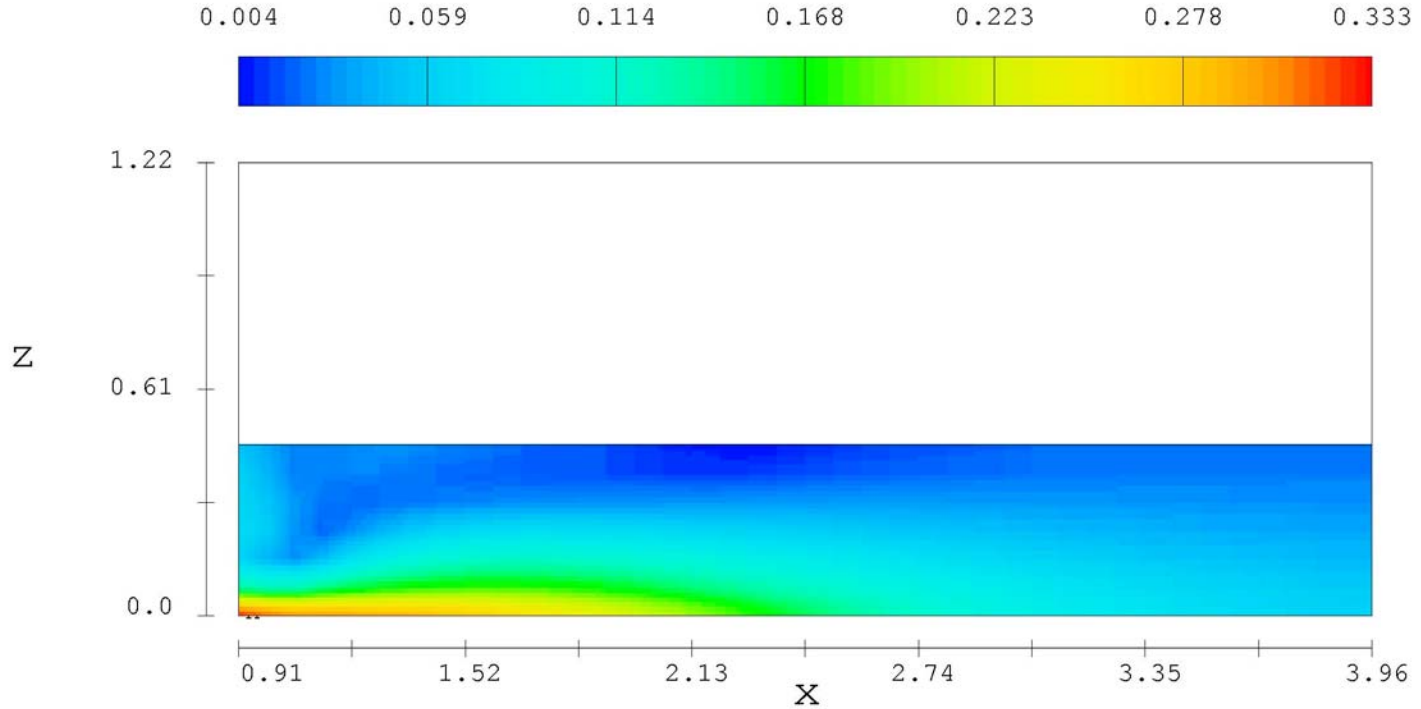
Fig. F-3.1. UNM Flume Without Diffuser/With Inlet Submerged - Velocity Magnitudes (Length-Height Section at Mid Width).



FLOW-3D[®] t=900.0 z=1.270E-02 (ix=2 to 82 jy=2 to 15)
 11:39:22 8-28-2000kqln hydr3d: version 7.6 win32 1999
 UNM flume

Fig. F-3.2. UNM Flume Without Diffuser/With Inlet Submerged - Velocity Magnitudes (Length-Width Section Just Above the Floor).

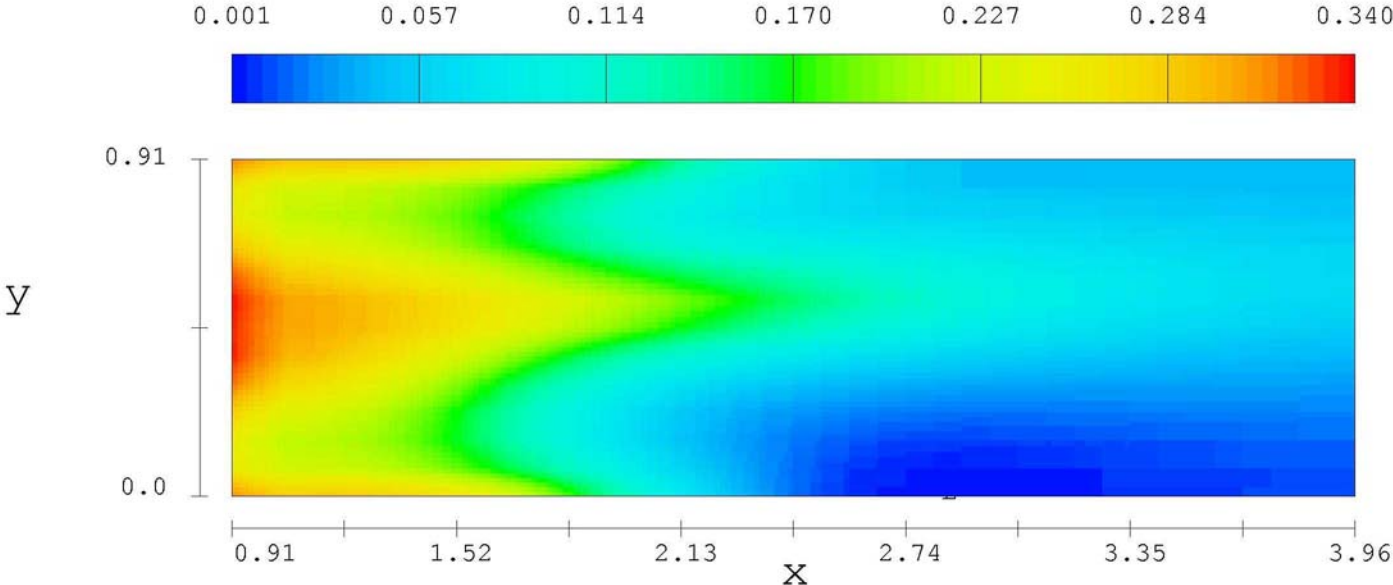
velocity magnitude contours



FLOW-3D[®] t=900.0 y=4.953E-01 (ix=15 to 54 kz=2 to 18)
11:39:22 8-28-2000kqln hydr3d: version 7.6 win32 1999
UNM flume

Fig. F-3.3. UNM Flume Without Diffuser/With Inlet Submerged - Test Region Velocity Magnitudes (Length-Height Section at Mid Width).

velocity magnitude contours



FLOW-3D® t=900.0 z=1.270E-02 (ix=15 to 54 jy=2 to 15)
11:39:22 8-28-2000kqln hydr3d: version 7.6 win32 1999
UNM flume

Fig. F-3.4. UNM Flume Without Diffuser/With Inlet Submerged - Test Region Velocity Magnitudes (Length-Width Section Just Above the Floor).

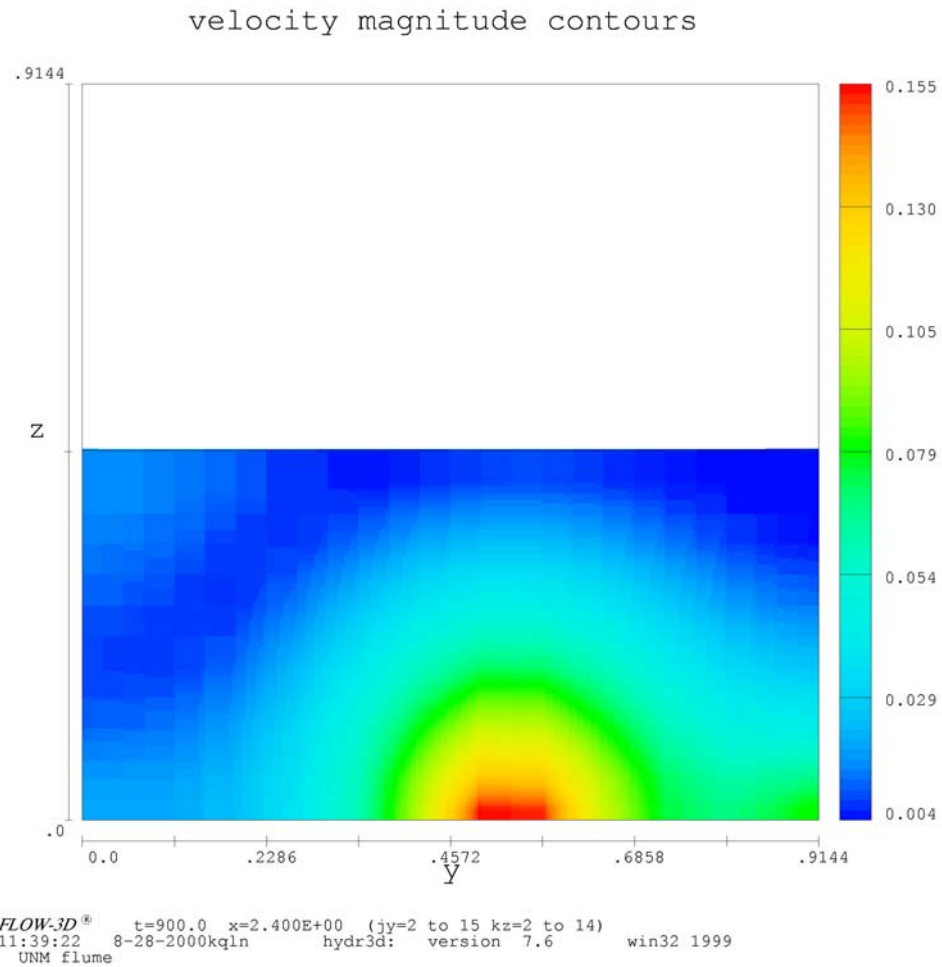
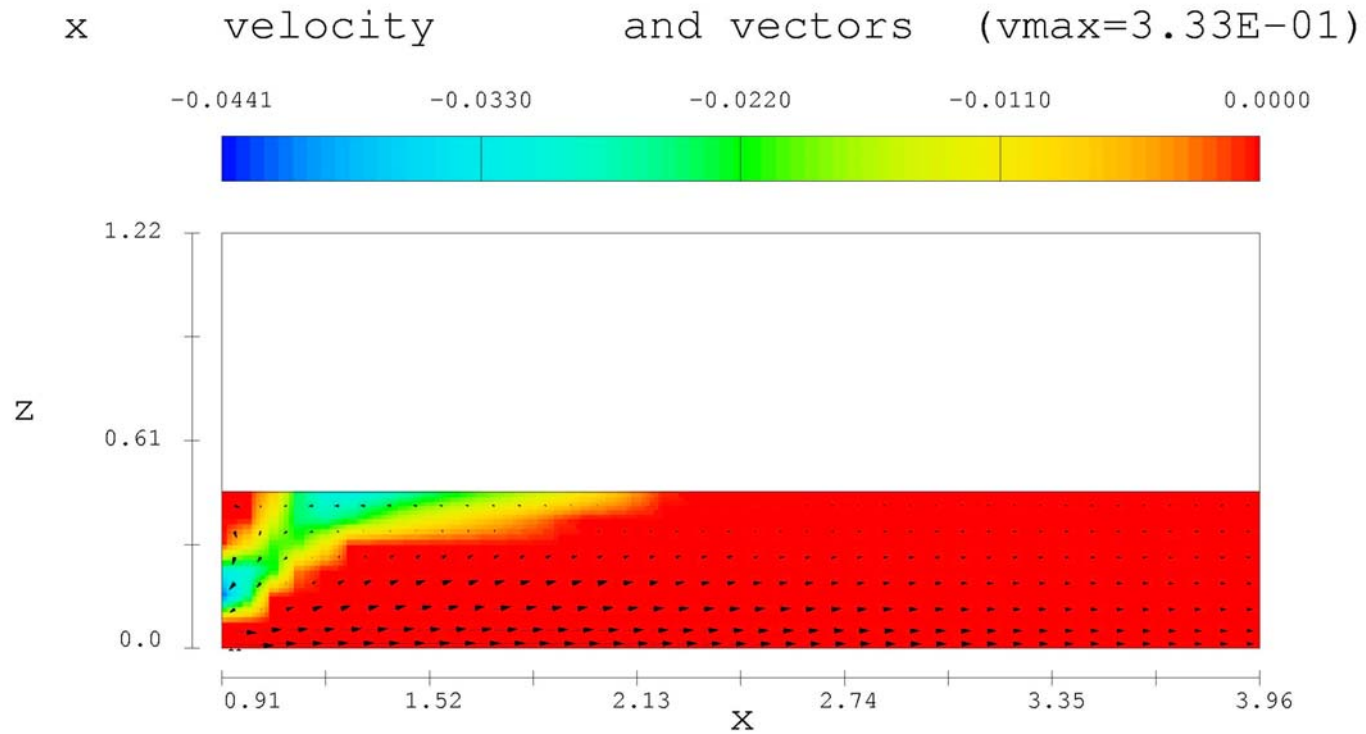


Fig. F-3.5. UNM Flume Without Diffuser/With Inlet Submerged - Test Region Velocity Magnitudes (Width-Height Section).



FLOW-3D® t=900.0 y=4.953E-01 (ix=15 to 54 kz=2 to 18)
 11:39:22 8-28-2000kq1n hydr3d: version 7.6 win32 1999
 UNM flume

Fig. F-3.6. UNM Flume Without Diffuser/With Inlet Submerged - Test Region Axial Velocity and Velocity Vectors (Length-Height Section at Mid Width with Zero Upper Bound on Color).

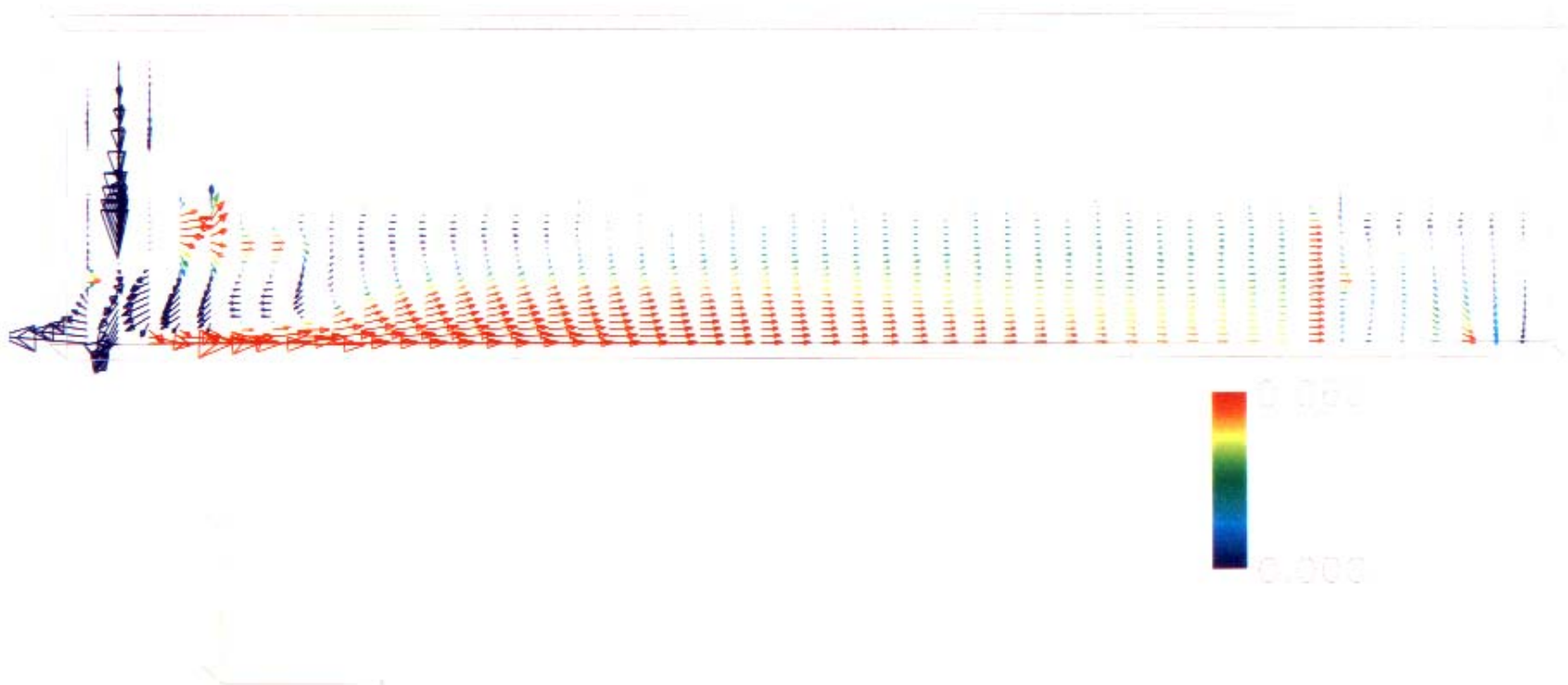


Fig. F-3.7. UNM Flume Without Diffuser/With Inlet Submerged - Velocity Vectors Colored By Axial Velocity Magnitude.

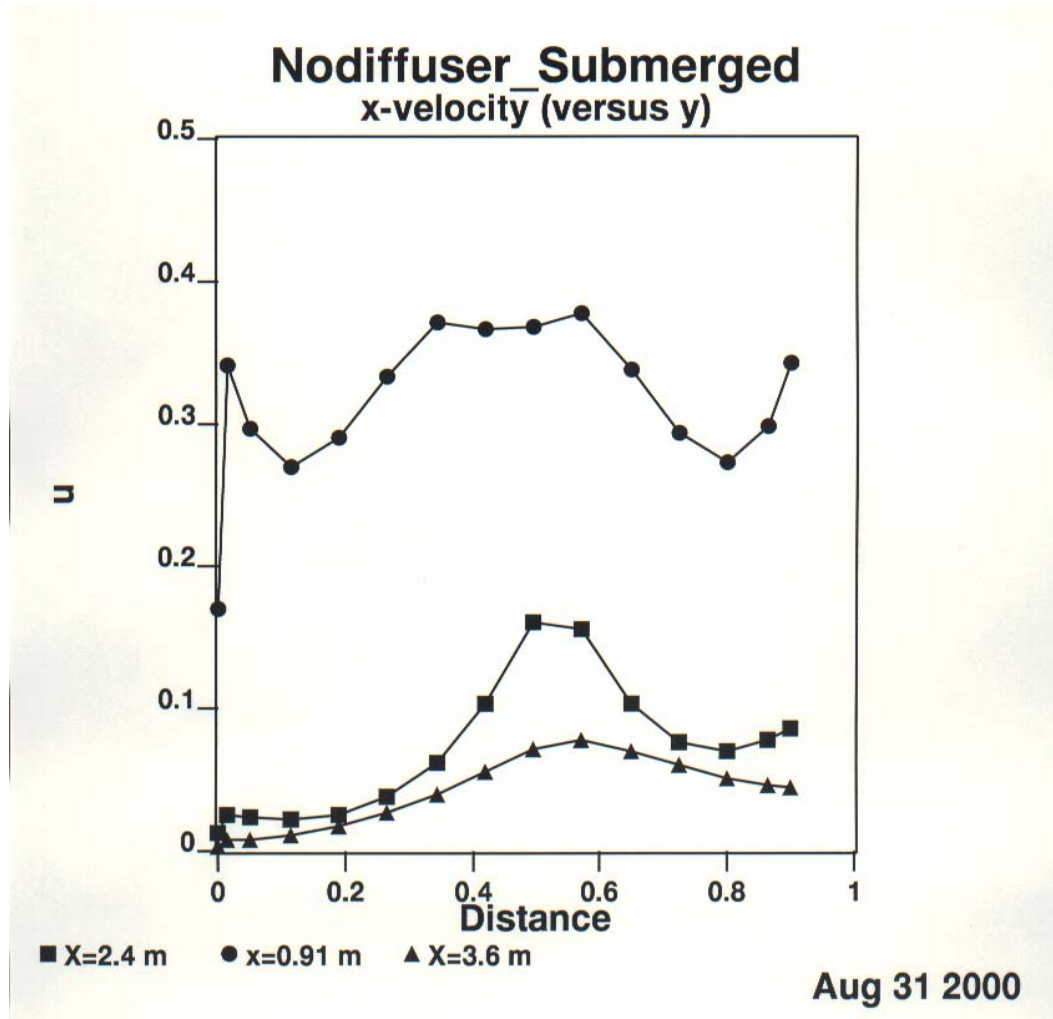


Fig. F-3.8. UNM Flume Without Diffuser/With Inlet Submerged - Axial Velocity Just Up from the Floor of the Flume Versus Width at Different Axial Locations.

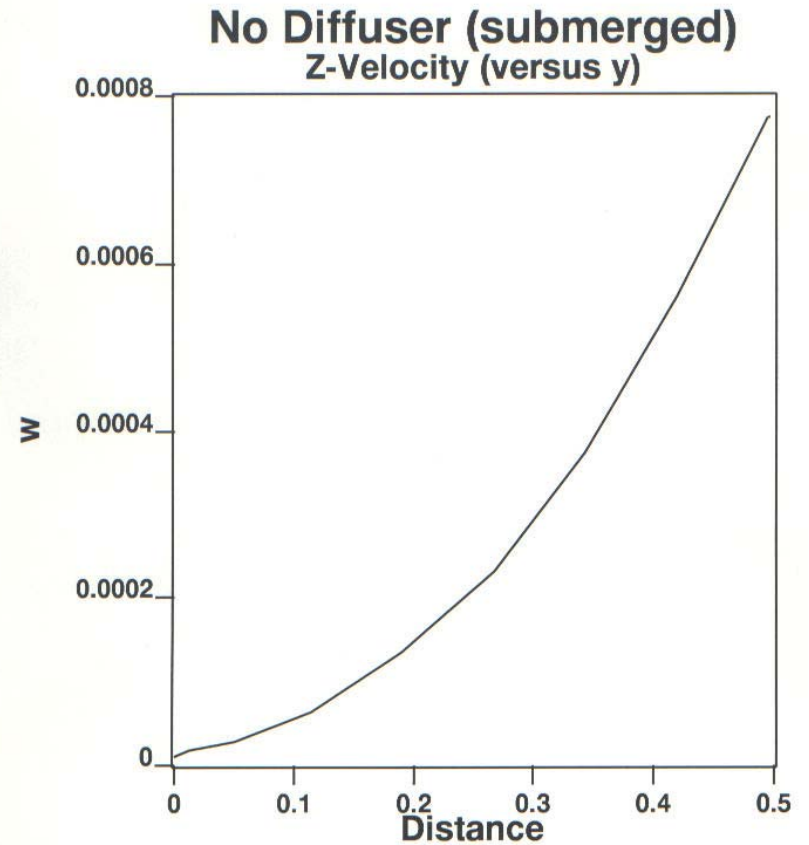
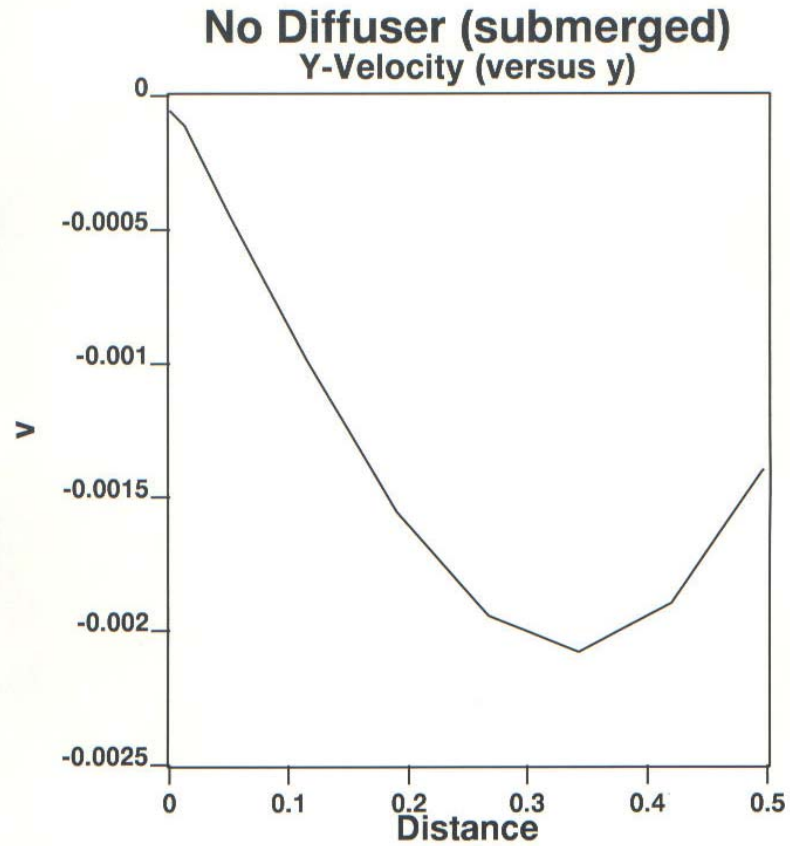
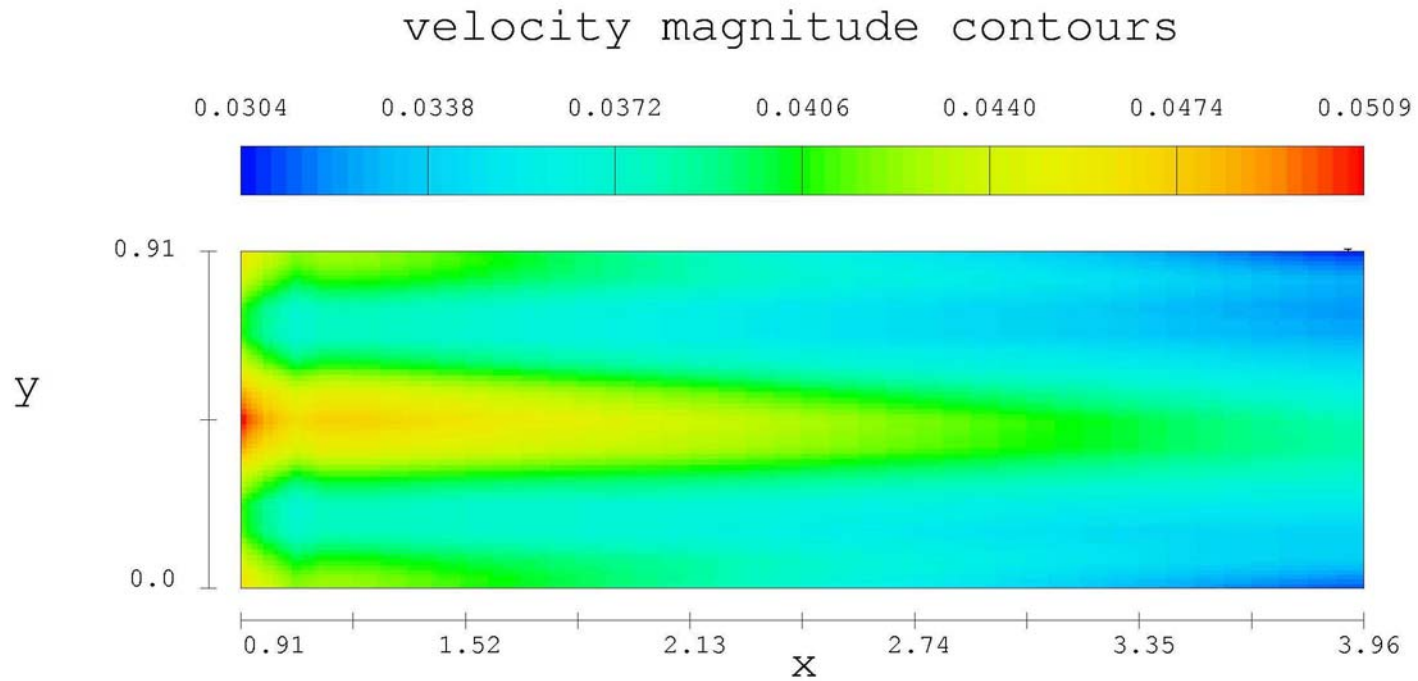


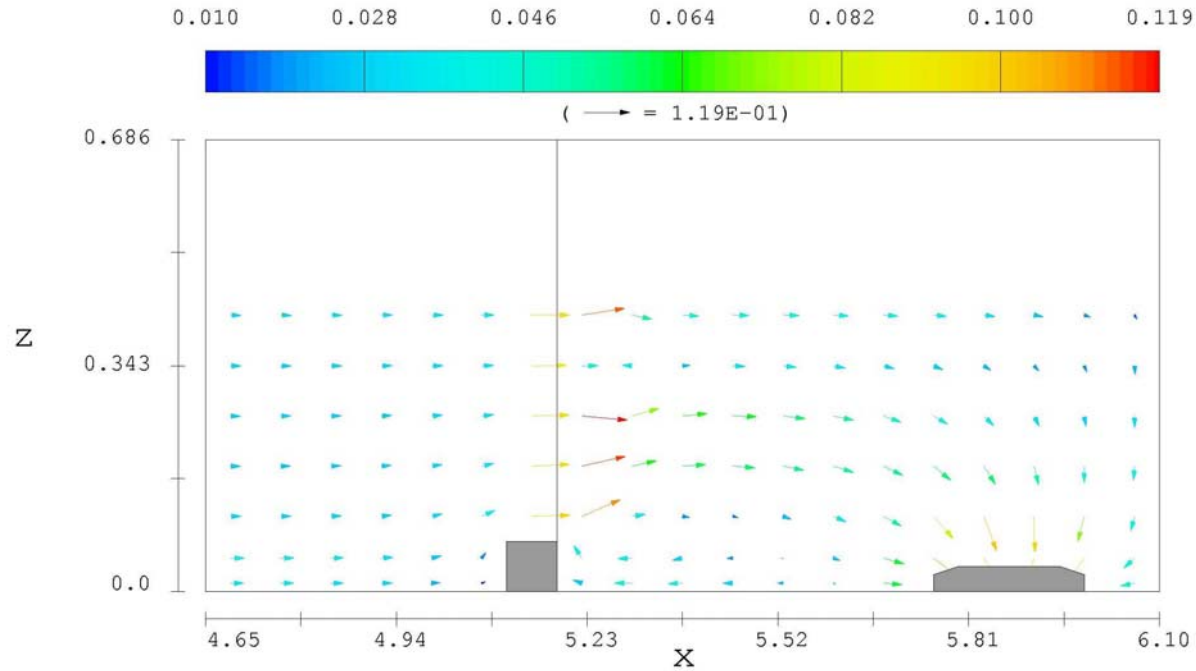
Fig. F-3.9. UNM Flume Without Diffuser/With Inlet Submerged - Transverse (Y) and Vertical (Z) Velocities Near the Floor of the Flume Versus Width in Test Region.



FLOW-3D[®] t=900.0 z=1.270E-02 (ix=15 to 54 jy=2 to 15)
 16:52:07 9- 1-2000dtpo hydr3d: version 7.6 win32 1999
 UNM flume

Fig. F-4.1. UNM Flume With Diffuser and Curb - Test Region Velocity Magnitudes (Length-Width Section Just Above the Floor).

velocity vectors: colored by 3d velocity magnitude



FLOW-3D® t=900.0 y=4.953E-01 (ix=64 to 82 kz=2 to 11)
16:52:07 9- 1-2000dtpo hydr3d: version 7.6 win32 1999
UNM flume

Fig. F-4.2. UNM Flume With Diffuse and Curb - Velocity Vectors Near the Curb Colored by 3-D Velocity Magnitude (Length-Height Section at Mid Width).